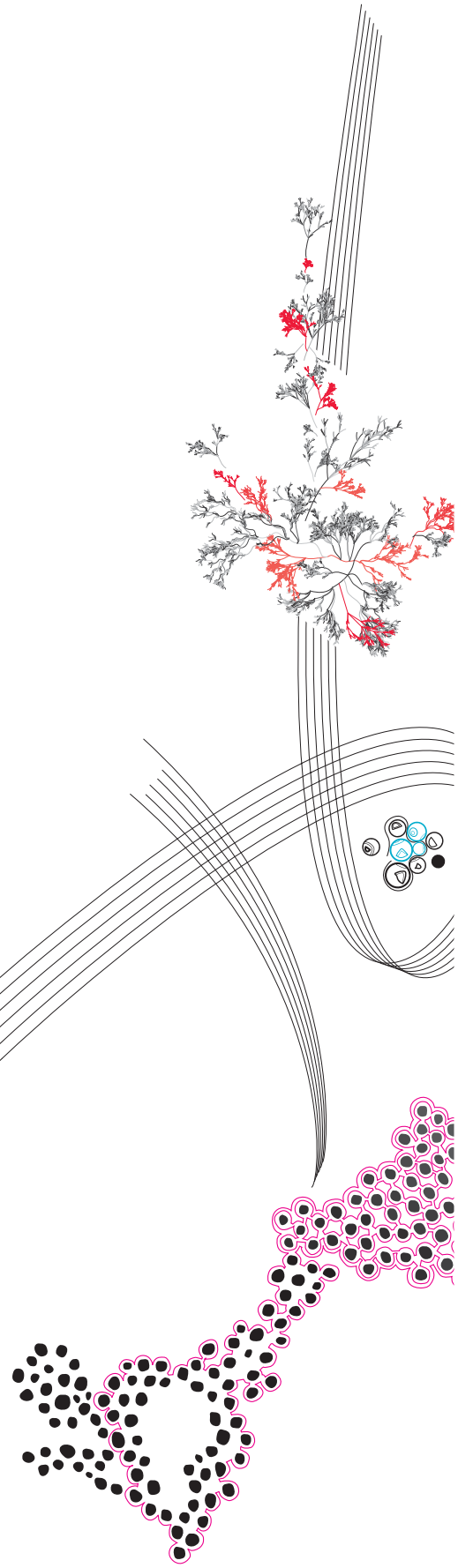

MSc Biomedical Engineering
MSc Electrical Engineering

Combined Master Thesis Project

Proteome secretion analysis from PCa cell lines using optical and electrochemical measuring methods

BSc Diana Susanne Andreoli

May 13, 2024

Supervisors
Assoc.Prof.Dr.Ir. Ruchi Bansal
Prof.Dr.Ir. L.W.M.M. Terstappen
Ir. E. Dathathri

Prof.Dr.Ir. L.I. Segerink
Dr. S. Sahin MSc
Dr.Ir. E. Tanumihardja

External Evaluators
Prof.Dr.Ir. L.I. Segerink

Dr.Ir. C. Salm

Department
Translational Liver Research group and
Medical Cell BioPhysics group
Faculty of Science & Technology
University of Twente

Department
BIOS Lab-on-a-chip group
Faculty of Electrical Engineering, Mathematics & Computer Science
University of Twente

UNIVERSITY OF TWENTE.

Acknowledgements

I would like to express my deepest and most sincere gratitude to my main supervisors, Assoc. Prof. Dr. Ir. R. Bansal, Prof. Dr. Ir. L.W.M.M. Terstappen, and Prof. Dr. Ir. L.I. Segerink, for their unwavering guidance and endless feedback throughout this project. Their availability for discussions and support has been invaluable. I especially want to thank Prof. Dr. Ir. R. Bansal and Prof. Dr. Ir. L.I. Segerink for their understanding and encouragement during challenging times. I feel honoured to have had the opportunity to carry out my project with the TLR / MCBP and BIOS groups.

Simultaneously, I wish to extend my gratitude to my daily supervisors, Ir. E. Dathathri, Dr. S. Sahin MSc, and Dr. Ir. E. Tanumihardja, for guiding me in the lab and imparting invaluable knowledge. Their willingness to answer my questions and provide support was crucial to my progress.

Furthermore, I am grateful to the technical staff, Ing. C. Breukers, A. Mentink-Leusink MSc, and Y. Kraan MSc, as well as the other members of the MCBP and BIOS groups, including PhD students and postdocs, for their assistance with experiments and willingness to help whenever needed.

I extend my deepest thanks to my family for their unwavering support and encouragement throughout this journey. Additionally, I owe a special thank you to my friends for their essential technical advice, and whose encouragement and companionship were a beacon of light during this journey.

Finally, I would like to thank my exam committee, which consists of Assoc. Prof. Dr. Ir. R. Bansal, Prof. Dr. Ir. L.W.M.M. Terstappen, Prof. Dr. Ir. L.I. Segerink, Dr. Ir. C. Salm, Ir. E. Dathathri and Dr. S. Sahin MSc, for their time and effort in evaluating this work.

Thank you all for your guidance, support, and encouragement. Your contributions have made this project an immensely learnful and rewarding journey.

Abstract

Prostate Cancer is a leading malignancy affecting men worldwide, necessitating accurate diagnosis and effective treatment strategies. This study aims to evaluate the proteome secretion of PCa cells based on their cell cycle phases and to develop a multiplexing platform for identifying potential biomarkers. Moreover, it compares the efficacy of optical and electrochemical measurement setups in analyzing proteome secretion.

A comprehensive methodology was employed, starting with the identification of potential biomarkers using proteome profiling arrays. PCa cell lines (LnCAP, PC-3, and 22Rv1) were cultured, and their supernatants analyzed to identify distinct protein secretion profiles. Immunocytochemistry (ICC) staining was used to validate intracellular protein levels and visualize PSA secretion. Fluorescence-Activated Cell Sorting (FACS) was utilized to sort cells into G1, and G2/M phases, followed by analysis of PSA secretion using the ELISpot assay and staining of PVDF membranes. A spotting device was further developed to multiplex multiple antibodies onto a single membrane.

In parallel, Poly-L-Lysine (PLL) derivatives were synthesized and characterized using Nuclear Magnetic Resonance (NMR) spectroscopy. Their functionality was validated through Quartz Crystal Microbalance with Dissipation Monitoring (QCM-D) measurements. Electrochemical sensing using Cyclic Voltammetry (CV) was performed to detect the attachment of EpCAM proteins on functionalized Pt-plated electrodes, with Methylene Blue as a redox mediator.

The results revealed significant heterogeneity in PSA secretion across different cell cycle phases, with only the G1 phase secreting PSA. The proteome array identified multiple potential biomarkers, including PSA, suggesting that multiplexing provides a comprehensive understanding of PCa proteome secretion. The spotting device concept was proven feasible, though further optimization is required. Synchronization of cells to the G1 phase remains a challenge needing refinement.

Comparing optical and electrochemical methods, optical measurement provides a comprehensive and sensitive multiplexing platform but is complex and time-consuming. Electrochemical measurement offers real-time monitoring of binding events and requires less preparation but is limited to single biomarker detection.

The societal impact of this research lies in its potential to improve early detection and personalized treatment of PCa. By identifying heterogeneity in PSA secretion across different cell cycle phases, the findings underscore the need for accurate diagnostic tools that consider this variability. The development of a multiplexing platform to identify multiple potential biomarkers could pave the way for better understanding tumor heterogeneity, leading to more effective and personalized therapeutic strategies. Additionally, liquid biopsy, being less invasive and easier to perform, may enhance patient compliance and outcomes.

Keywords: Prostate Cancer, Biomarkers, Proteome Secretion, Multiplexing, Optical Measurement, Electrochemical Measurement, PSA, Cell Cycle Phases.

Contents

Acknowledgements 1

Abstract 2

List of Acronyms 5

1 Introduction 7
- 1.1 Prostate cancer . . . 7
- 1.2 Technologies for Secretion Measurement: Exploring Sensing Methodologies . 8
- 1.3 Research gap . . . 11
- 1.4 Aim, objectives and goals . . . 11
- 1.5 Biomarkers in Prostate cancer . . . 12
- 1.6 Heterogeneity in PSA Secretion from Prostate Cancer Cells . . . 13

2 Materials and Methods 16
- 2.1 Cell lines, culturing, and drug treatment . . . 16
- 2.2 Identification of potential PCa biomarkers using proteome array . . . 18
- 2.3 Optical measurement setup and methods . . . 20
  - 2.3.1 Intracellular PSA of PCa's cell lines . . . 20
  - 2.3.2 Measuring PSA secretion from PCa's cell lines . . . 22
  - 2.3.3 Identification and sorting of cells in different cell cycle phases . . . 25
  - 2.3.4 Membranes and secretion detection . . . 25
- 2.4 Electrochemical measurement setup and methods . . . 26
  - 2.4.1 Poly-L-Lysine synthesis . . . 26
  - 2.4.2 Nuclear Magnetic Resonance spectroscopy . . . 27
  - 2.4.3 Quartz Crystal Microbalance with dissipation . . . 27
  - 2.4.4 Cyclic Voltammetry . . . 28

3 Results and Discussion 30
- 3.1 Identification of potential PCa biomarkers using Proteome array . . . 30
- 3.2 Intracellular PSA of PCa's cell lines . . . 34
- 3.3 Visualisation of the cells using cytospin . . . 35
- 3.4 Spotting device for multiplexing . . . 37
- 3.5 Measuring PSA secretion from PCa's cell lines . . . 37
- 3.6 Identification and sorting of cells in different cell cycle phases . . . 39
- 3.7 Evaluation of Pharmacological Agents for Synchronization of Cells into the G1 Phase . . . 42
- 3.8 PLL synthesis and NMR . . . 43
- 3.9 QCM-D experiments . . . 48
- 3.10 Cyclic Voltammetry validation . . . 53

3.11 Conclusion 55
3.12 Future recommendations 57

A Identification of potential PCa biomarkers using Proteome array 62

B Intracellular PSA of PCa's cell lines 64

C Measuring PSA secretion from PCa's cell lines 66

D Identification and sorting of cells in different cell cycle phases 69

E Membranes and secretion detection 71

F Poly-L-Lysine synthesis 73

G Nuclear Magnetic Resonance spectroscopy 75

H Quartz Crystal Microbalance 77

I Cyclic Voltammetry 79

J Protein Analyzer Software 81

K QCM-D experiments 85

List of Acronyms

A2M Alpha-2-Macroglobulin.

ACT Alpha-1-Antichymotrypsin.

API Alpha-1-Protease Inhibitor.

BPSA Benign Prostate-Specific Antigen.

BSA Bovine Serum Albumin.

cfDNA Cell-free DNA.

cPSA Complexed Prostate-Specific Antigen.

CTCs Circulating Tumor Cells.

CV Cyclic Voltammetry.

D_2O Deuterium Oxide (Heavy Water).

DMSO Dimethyl Sulfoxide.

ELISpot Enzyme-Linked ImmunoSpot.

EpCAM Epithelial Cell Adhesion Molecule.

FACS Fluorescence-Activated Cell Sorting.

fPSA Free Prostate-Specific Antigen.

FSC Forward Scatter.

G0 Resting Phase of the Cell Cycle.

G1 Gap 1.

G2/M Gap 2/Mitosis.

GAPDH Glyceraldehyde-3-Phosphate Dehydrogenase.

ICC Immunocytochemistry.

IL-8 Interleukin-8.

iPSA Intact Prostate-Specific Antigen.

MMP-3 Matrix Metallopeptidase 3.

MWCO Molecular Weight Cut Off.

NHS N-Hydroxysuccinimide.

NMR Nuclear Magnetic Resonance.

PBS Phosphate-Buffered Saline.

PCa Prostate Cancer.

phi Prostate Health Index.

PLL Poly-L-Lysine.

PLL-OEG Poly-L-Lysine-Oligo(ethylene glycol).

PLL-OEG-Biotin Poly-L-Lysine-Oligo(ethylene glycol)-Biotin.

PSA Prostate-Specific Antigen.

PSMA Prostate-specific membrane antigen.

PVDF Polyvinylidene Fluoride.

QCM-D Quartz Crystal Microbalance with Dissipation Monitoring.

S Synthesis.

SSC Side Scatter.

Chapter 1

Introduction

1.1 Prostate cancer

Prostate Cancer (PCa) is one of the most common malignancies affecting the male population worldwide. While many cases of PCa are characterized by slow progression and low risk, a subset exhibits aggressive behavior that necessitates early detection and intervention. The five-year relative survival rate for PCa stands at an average of 83%, but this rate climbs to 90% among men aged 55 to 64, underlining the critical role of timely and effective treatment strategies [1].

Diagnosis and Treatment of prostate cancer

PCa diagnosis typically involves several key assessments including the measurement of biomarkers such as the Prostate Health Index (phi) and Prostate-Specific Antigen (PSA). Elevated levels of PSA, while indicative of potential PCa, can also be influenced by age, prostate size, and other non-cancerous conditions. Further diagnostic steps may include digital rectal examinations and imaging tests such as ultrasound or MRI, followed by a prostate biopsy to confirm the presence of cancer cells. Depending on the tumor's characteristics—size, location, and growth rate—treatment options may vary from active surveillance for less aggressive cancers to surgery, radiation, hormone therapy, or chemotherapy for more advanced stages [20].

The Role of Biomarkers in Prostate Cancer

The lack of reliable biomarkers that can predict therapeutic efficacy represents a significant gap in PCa management. In this context, liquid biopsy has emerged as a groundbreaking approach, offering a minimally invasive means to detect and analyze Circulating Tumor Cells (CTCs), Cell-free DNA (cfDNA), and other biomarkers in blood samples. This method not only provides insights into tumor heterogeneity but also enables real-time monitoring of treatment responses [16].

Heterogeneity in Prostate Cancer and Biomarker Utility

Tumor heterogeneity in PCa poses unique challenges in treatment decisions, as it can affect the efficacy of therapeutic interventions. Understanding this heterogeneity through biomarkers like PSA is essential, as it may influence the secretion patterns and levels of biomarkers depending on the cell cycle phase of the tumor cells. Assessing these variations at a single-cell level is crucial for a more accurate evaluation of the disease state and the selection of appropriate therapeutic strategies [11]. Figure 1.1 provides a schematic representation of PSA secretion in both normal and cancerous tissues.

Methodological Approach to Biomarker Analysis

To explore the secretion dynamics of PSA and its correlation with cell cycle phases, this study employs both optical and electrochemical measurement techniques. These method-

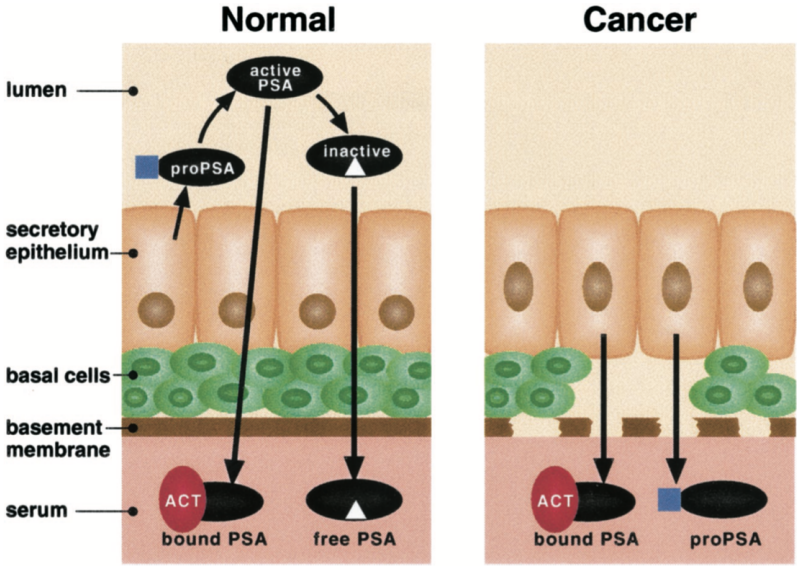

FIGURE 1.1: This image compares the secretion of Prostate-Specific Antigen (PSA) between normal and cancerous prostate tissues. In normal tissues, PSA is actively secreted by the epithelial cells, with proPSA converted into its active form and secreted as bound or free PSA. In cancerous tissues, secretion is altered, with higher levels of bound PSA and proPSA present in the serum, and a reduction in free PSA. The image illustrates the changes in PSA secretion patterns due to prostate cancer, highlighting the heterogeneity in protein expression central to this thesis. [18]

ologies allow for precise quantification and comparison of protein secretions from PCa cells, providing deeper insights into the cellular behaviors that underpin biomarker variability and tumor heterogeneity. By integrating these advanced analytical techniques, the research aims to enhance the diagnostic accuracy and prognostic evaluation of PCa, paving the way for more personalized and effective treatment plans. This project specifically focuses on key biomarkers such as PSA and other relevant biomarkers, the impact of cell cycle phases on the secretome, and the emerging field of single-cell analysis. These areas of investigation offer valuable insights into the complexities of PCa progression and are central to advancing our understanding of the disease.

1.2 Technologies for Secretion Measurement: Exploring Sensing Methodologies

Various technologies are available for measuring protein secretion, each with its advantages and limitations. In this study, we aim to utilize optical and electrochemical measurement methods for their suitability in detecting PCa biomarkers. Below we outline some of the main methodologies used in various measuring methods.

- **Optical measurement method**
  - **Enzyme-Linked Immunosorbent Assay (ELISA):** A widely used technique for detecting and quantifying proteins based on antigen-antibody interactions. It offers high sensitivity but is limited to detecting one protein at a time.

- **ELISpot:** ELISpot is a variant of ELISA that is used to detect the secretion of cytokines or other proteins from individual cells. It offers high sensitivity and the ability to detect secreted proteins at the single-cell level. Multiplexing is also possible, although due to the antibodies species origin not that simple.
- **Bio-barcode Assay (BCA):** BCA is a highly sensitive method that allows for the detection of multiple proteins simultaneously. It utilizes gold nanoparticles functionalized with DNA barcodes that bind to target proteins.
- **Fluorescence-Based Assays:** These methods utilize fluorescent probes to detect proteins, offering high sensitivity and the potential for multiplexing. However, they require specialized equipment and reagents.
- **Fluorescence-Activated Cell Sorting:** FACS is a powerful technique used to analyze and sort cells based on their fluorescent properties. It can be used to detect and quantify specific biomarkers on individual cells, providing high-throughput analysis and the ability to isolate cells of interest for further study.

- **Electrochemical measurement method**
  - **Macro-electrodes:** Macro-electrodes are relatively large electrodes used in electrochemical measurements. They are typically made of conductive materials such as metals and are used for detecting and quantifying analytes in solution.
  - **Nanowires:** Nanowires are nanostructured materials with diameters on the order of nanometers. They have unique electronic and electrochemical properties that make them useful for sensing applications. Nanowires can be functionalized with specific receptors to detect target analytes with high sensitivity.
  - **Nanocapacitor array:** A nanocapacitor array consists of a series of nanoscale capacitors arranged in an array format. These arrays can be used for sensing applications by measuring changes in capacitance caused by the adsorption of analytes onto the capacitor surface.
  - **Nanopipette array:** A nanopipette array is an array of nanoscale pipettes that can be used for electrochemical measurements. Nanopipettes can be used to deliver or aspirate small volumes of liquid and can be functionalized for sensing applications.
  - **Electrochemical Impedance Spectroscopy:** EIS is a technique used to study the electrical properties of materials and interfaces. It involves applying a small AC voltage to a system and measuring the resulting AC current. EIS can provide information about the resistance, capacitance, and impedance of a system, which can be used to study processes such as adsorption, desorption, and electron transfer.
  - **Cyclic Voltammetry:** CV is an electrochemical technique used to study redox reactions. It involves sweeping the potential of an electrode and measuring the resulting current. CV can provide information about the kinetics and thermodynamics of redox reactions, as well as the concentration of electroactive species in solution.

- **Microfluidic platform**
  - **Micro- and nanowell systems:** Micro- and nanowell systems consist of arrays of wells or chambers with dimensions at the micro- and nanoscale. These systems are used for high-throughput screening and analysis of biomolecules.

They offer the advantage of miniaturization, allowing for the analysis of small sample volumes. However, they may suffer from issues such as crosstalk between wells and limited dynamic range.

- **Microchamber system:** Microchamber systems consist of microscale chambers used for various biological and chemical analyses. These systems offer advantages such as high sensitivity, low sample consumption, and rapid analysis times. However, they may be limited by the complexity of fabrication and potential issues with sample handling.
- **Flow-based droplet microfluidics:** Flow-based droplet microfluidics involves the generation and manipulation of droplets in microfluidic channels. This technique offers advantages such as high throughput, precise control over droplet size, and the ability to encapsulate single cells or molecules in droplets. However, it may be limited by the complexity of droplet generation and the need for specialized equipment.
- **Microfluidic devices** can be used for multiplexed protein analysis by integrating various assay components into a single device. They offer advantages such as low sample volumes, rapid analysis, and potential for automation.

The chosen methodologies for this study include ELISpot and FACS for their ability to detect and quantify protein secretion at the single-cell level, providing insights into the heterogeneity of secretion across different cell cycle phases. Additionally, Cyclic Voltammetry (CV) was selected for its capacity to study biomolecular interactions and redox processes, respectively. These methods offer complementary approaches, collectively providing a comprehensive analysis of the secretion patterns of PCa biomarkers. ELISpot and FACS allow for high sensitivity and quantification of protein secretion, while EIS and CV offer label-free detection and sensitivity to changes in impedance and redox potentials. Together, these techniques will offer valuable insights into the secretion dynamics of PCa cells in various cell cycle phases and disease stages. We will also be looking into multiplexing possibilities within these methodologies.

Multiplexing methods in both ELISpot and FACS technologies for PCa markers offer the potential for simultaneous detection of multiple biomarkers, providing a more comprehensive analysis in a single assay. However, the application of multiplexing in these technologies for secretome markers in PCa appears to be limited in current literature, presenting a significant gap in research.

For ELISpot, multiplexing capabilities have been explored in the context of cytokine detection, where multiple cytokines can be detected simultaneously in a single assay [17]. However, multiplexing for secretome markers in PCa, particularly for proteins such as PSA and other potential biomarkers, has not been extensively reported.

Similarly, while FACS allows for the analysis of multiple biomarkers simultaneously on a single-cell level, its application for secretome markers in PCa is not well-documented. Most studies focus on cell surface markers rather than secreted proteins [13]).

Therefore, the lack of established multiplexing methods for secretome markers in PCa presents a motivation for further research in this area. Developing multiplexing techniques for these technologies could significantly enhance our ability to understand the complex secretome profiles of PCa cells, potentially leading to improved diagnostic and therapeutic strategies [31].

1.3 Research gap

The current landscape of prostate cancer biomarker analysis lacks studies that specifically investigate the secretion of Prostate-Specific Antigen (PSA) in different cell cycle phases. This gap raises critical questions about potential heterogeneity in PSA secretion dependent on the cell cycle phase and whether such variations might also manifest differently in various disease stages, especially when looking at single-cell analysis. To address this gap, the research hypothesis posits that the secretion patterns of proteins, including PSA, can indeed differ according to the cell cycle phase, which we can see when analyzing at the single-cell level. Additionally, an exploration into whether there is any possible relevance to disease stages in this context becomes essential. This entails investigating if secretion in different cell cycle phases may vary in distinct disease stages. A comprehensive review of existing literature is crucial to shed light on the presence of any prior research regarding these aspects, providing valuable insights into potential correlations between cell cycle phases, disease progression, and protein secretion patterns in the realm of PCa.

1.4 Aim, objectives and goals

The aim of the study is to evaluate proteome secretions of the PCa cells based on the cell cycle phases and develop a multiplexing platform for measuring potential biomarkers to improve the understanding of tumor heterogeneity, as well as evaluating optical measurement setup versus electrochemical measurement setup in order to measure proteome secretions.

Biomedical Engineering – Bioengineering Technologies

Objective 1: Investigate Heterogeneity in Protein Secretion of Prostate Cancer (PCa) Cells Based on Cell Cycle Phase

- Use ELISpot assay to measure PSA secretion in PCa cells.
- Sort cells into G1 phase, S phase, and G2/M phase using flow cytometry and Hoechst staining.
- Measure and compare PSA secretion levels in each cell cycle phase.
- Prove real heterogeneity in proteome secretion of PCa cells.

Objective 2: Multiplex Protein Analysis on PVDF Membrane

- Identify potential biomarkers and use this for further multiplexing on the PVDF membrane using the proteome array.
- Use a spotting device to multiplex 11 antibodies onto the membrane.
- Include a housekeeping gene (GAPDH) and 10 target proteins (including PSA) for normalization and analysis.

Objective 3: Synchronize PCa Cells in G1 Phase

- Establish a protocol to synchronize PCa cells specifically in the G1 phase of the cell cycle.
- Ensure synchronization is effective and reproducible for further analysis.

Objective 4: Implement Multiplexing of 4 Antibodies on a Single PVDF Membrane

- Develop a protocol for multiplexing 4 antibodies on one PVDF membrane.
- Ensure the method is reliable and allows for accurate detection and quantification of target proteins.

Electrical Engineering – Lab On A Chip

Objective 1: Demonstrate Feasibility of Detection with Electrochemical Sensing

- Synthesize PLL derivatives and biotinylate them for surface functionalization.
- Characterize the degree of modification of the PLL derivatives via NMR spectroscopy.
- Use Quartz Crystal Microbalance with Dissipation Monitoring (QCM-D) as a proof of concept to determine saturation limits for the detection of biomarkers.

Objective 2: Develop Electrochemical Sensing Methods for Real Measurements

- Use Cyclic Voltammetry to perform proteome secretion detection on functionalized Pt-plated electrodes.
- Utilize cell supernatant for initial tests and validation of the concept.
- Establish a method to analyze cells on top of the chip for real-time analysis.

1.5 Biomarkers in Prostate cancer

Prostate cancer biomarkers include those that are expressed and those that are secreted or shed by PCa cells. These biomarkers play crucial roles in the diagnosis, prognosis, and monitoring of PCa. The expression of certain antigens in PCa cells, such as Prostate-specific membrane antigen (PSMA) and prostate-specific antigen (PSA), can be used as indicators of disease progression and response to treatment [28].

In addition to PSA and PSMA, several other biomarkers have been identified as potentially valuable in the clinical management of PCa. Caveolin-1, a protein involved in cellular signaling and cholesterol management, has been noted for its overexpression in PCa cells and its potential as a prognostic marker for aggressive disease [7]. Similarly, STEAP2, a six-transmembrane epithelial antigen of the prostate, and Prostein, a marker expressed in normal and malignant prostate tissues, are gaining attention for their diagnostic and prognostic capabilities [22][12].

Despite the array of available biomarkers, the challenge remains to find reliable markers that can predict the efficacy of various therapies. In response to this, liquid biopsy has emerged as a promising diagnostic approach. Liquid biopsy, a minimally invasive method, involves the analysis of Circulating Tumor Cells (CTCs), Cell-free DNA (cfDNA), and other biomarkers present in a patient's blood sample to detect PCa [16]. This technique offers advantages over traditional tissue biopsy, including its less invasive nature, ability to capture tumor heterogeneity, and potential for real-time monitoring of treatment response.

This project specifically focuses on the secretion of Prostate-Specific Antigen (PSA). PSA is a serine protease produced by prostate epithelial cells and is traditionally used in screening for PCa. Elevated levels of PSA in blood can indicate the presence of the disease, although factors such as age and prostate size can also influence PSA levels [9]. By studying

the secretion dynamics of PSA at a cellular level, we aim to enhance the understanding of its role in PCa progression and response to therapy, thus providing deeper insights into the disease's heterogeneity and improving the precision of diagnostics and treatment strategies.

PSA

Prostate-specific antigen, abbreviated as PSA, is also known as gamma seminoprotein or kallikrein-3 (KLK3). This glycoprotein, with a molecular mass of approximately 34 kDa, serves as a serine protease produced by the prostate gland. Immunologically and biochemically, PSA is distinct from prostate acid phosphatase (PAP), which can also be used as a PCa biomarker but has no added value from PSA [4].

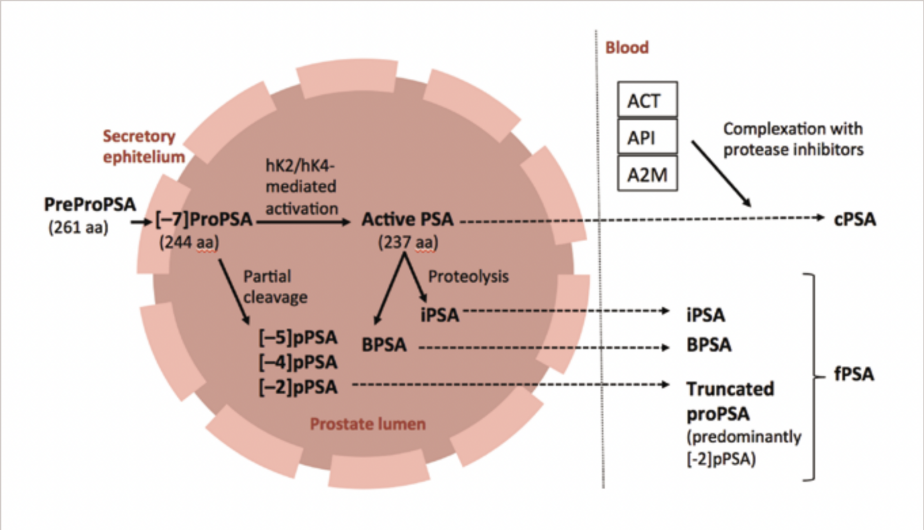

FIGURE 1.2: This figure illustrates the molecular pathway of Prostate-Specific Antigen (PSA). PreProPSA (261 aa) converts to ProPSA (244 aa) in the secretory epithelium and undergoes further cleavage to active PSA (237 aa) via hK2/hK4-mediated activation. Active PSA is then processed into Complexed Prostate-Specific Antigen (cPSA) by binding to protease inhibitors (ACT, API, A2M) or remains as Free Prostate-Specific Antigen (fPSA), including iPSA, BPSA, and truncated proPSA. [31]

Prostate Health Index (phi)

The Prostate Health Index (phi) incorporates various biomarkers, including [-2] proPSA (p2PSA), Free Prostate-Specific Antigen (fPSA), and total PSA (tPSA). The ratio between free PSA and total PSA is utilized to assess prostate health. Notably, if the free PSA falls below 10% while the total PSA exceeds the established cut-off, it raises the risk of PCa significantly [6]. Figure 1.2 depicts the molecular pathway of PSA cellular processes.

1.6 Heterogeneity in PSA Secretion from Prostate Cancer Cells

PCa is characterized by significant heterogeneity, which is evident not only in the genetic and morphological differences across tumors but also in the variability of biomarker expression, such as PSA. This heterogeneity complicates the management of the disease, often resulting in varied responses to treatment among patients and affecting overall outcomes [27].

Understanding Tumor Heterogeneity

Tumor heterogeneity in PCa can manifest as diverse patterns of PSA secretion, which in turn may influence the effectiveness of diagnostic markers and treatment modalities. Differences in tumor cell expression and the microenvironment contribute to the complexity of the disease, necessitating advanced diagnostic strategies to improve patient management. For example, while elevated PSA levels are commonly associated with PCa, variations in secretion levels can lead to challenges in accurately gauging disease severity or progression [24].

Molecular and Biological Mechanisms

The molecular mechanisms underpinning this heterogeneity are complex, yet a significant factor is the variability in cell cycle phases among cancer cells. The cell cycle consists of four distinct phases: Gap 1 (G1), Gap 1 (G1), G2 (Gap 2), and M (Mitosis). Each phase has a specific set of events and checkpoints to ensure proper cell division and function, which is often disrupted in tumor tissues. Understanding these cell cycle phases is essential in the context of PCa secretome and the mechanisms underlying its development [8]. The cell cycle phase can influence not only the growth and replication behaviors of cells but also their biochemical properties, including the secretion of proteins like PSA. Understanding how the cell cycle affects PSA secretion is crucial for developing more nuanced diagnostic and therapeutic approaches that account for the heterogeneity of the tumor.

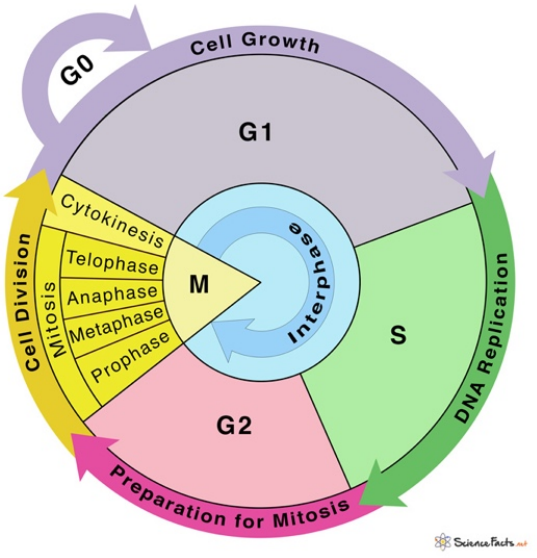

FIGURE 1.3: The diagram depicts the stages of the cell cycle, including the G0 phase (resting), G1 phase (cell growth), S phase (DNA replication), G2 phase (preparation for mitosis), and M phase (mitosis), which is further divided into prophase, metaphase, anaphase, telophase, and cytokinesis. [23].

Single-Cell Analysis

There is a growing body of literature that focuses on single-cell analysis of PCa, particularly through the examination of the proteome and secretome. These studies aim to elucidate the heterogeneity of PCa cells and identify novel biomarkers for early detection and personalized treatment strategies [29]. By examining the behavior of individual cells, researchers can gain insights into the diverse pathways through which PCa develops and responds to treatments.

Context for Cell Cycle Investigation

Given the heterogeneity in PCa, a detailed understanding of what makes each cell and

tumor unique is vital. One approach to understanding this is by studying how the cell cycle influences PSA secretion, which in turn contributes to the heterogeneity observed in tumor behavior. This approach can help predict which patients may not respond well to conventional treatments and aid in developing more targeted therapies that can manage or mitigate the disease more effectively.

Electrochemical sensing

Electrochemical sensing is a technique that utilizes the principles of electrochemistry to detect and quantify analytes in a sample. It involves the measurement of electrical signals produced by redox reactions between the analyte and an electrode surface. This method is widely used in biomedical engineering (BME) applications due to its sensitivity, selectivity, and ease of miniaturization.

Electrochemical sensors can be used for various purposes, such as monitoring biomolecules, detecting pathogens, and measuring biochemical parameters in biological fluids. These sensors are particularly useful in medical diagnostics, drug development, and environmental monitoring. For example, in cancer research, electrochemical sensors can be used to detect cancer biomarkers in blood samples, providing a non-invasive and rapid method for cancer diagnosis.

One of the key advantages of electrochemical sensing in BME is its ability to perform real-time measurements. This allows for continuous monitoring of biological processes, such as cell signaling or drug interactions, providing valuable insights into complex biological systems. Additionally, electrochemical sensors are relatively simple to fabricate and can be integrated into portable devices, making them suitable for point-of-care applications.

Overall, electrochemical sensing is a powerful tool, offering high sensitivity, selectivity, and versatility for a wide range of applications. Its integration into BME devices has the potential to revolutionize medical diagnostics and healthcare by providing rapid and accurate measurements of biological parameters [30].

Chapter 2

Materials and Methods

2.1 Cell lines, culturing, and drug treatment

The PCa cell lines used in this study, namely LnCAP, PC-3, and 22Rv1, were cultured to investigate their proteome secretion profiles. These cell lines were chosen for their relevance to different stages and characteristics of PCa. All cell lines were acquired from the American Tissue Culture Collection (ATCC, USA) to ensure the authenticity and reliability of the experimental models.

Culturing and Passaging

The cell lines were cultured in appropriate growth media, as detailed in Table 2.1, and maintained in a humidified atmosphere of 5% CO_2 at 37°C. The LnCAP, PC-3, and 22Rv1 cells were grown in T25 flasks and monitored until they reached approximately 70% confluency. At this stage, they were washed with Phosphate-Buffered Saline (PBS) and detached using a solution of 0.05% trypsin-EDTA. All solutions used were prewarmed at 37°C. The reaction was neutralized with a complete medium containing 10% Fetal Bovine Serum (FBS), and the cells were subsequently counted with an automated cell counter (Luna-FLTM, Westburg B.V., The Netherlands).

For passaging, cells were seeded at 5,000 cells/cm^2 densities to promote optimal growth, into new flasks with fresh media to continue cultivation.

Reagent	Concentration in media	Stock concentration	Catalogue number	Supplier
Roswell Park Memorial Institute (RPMI 1640)	-	500 mL	BE12-702F	Lonza
Fetal Bovine Serum (FBS)	10%	-	F7524	
Penicillin/streptomycin	100 u and 100 µg/mL	10.000 u and 10.000 µg/mL	Cat. DE17602E	Lonza
L-Glutamine	2 mM	200 mM	Cat. Be17605E	Lonza

Table 2.1: Cell culture medium components of LnCAP, 22Rv1 and PC-3 cells.

Treating the Cells with Synchronization Drugs

In the process of cell cycle synchronization, three pharmacological agents – Ciclopirox olamine, Aphidicolin, and Palbociclib – were utilized. The synchronization primarily tar-

geted the G1 phase of the cell cycle to standardize the cellular environment for subsequent analyses. The schematic of the workflow of this experiment can be found in Figure 2.1.

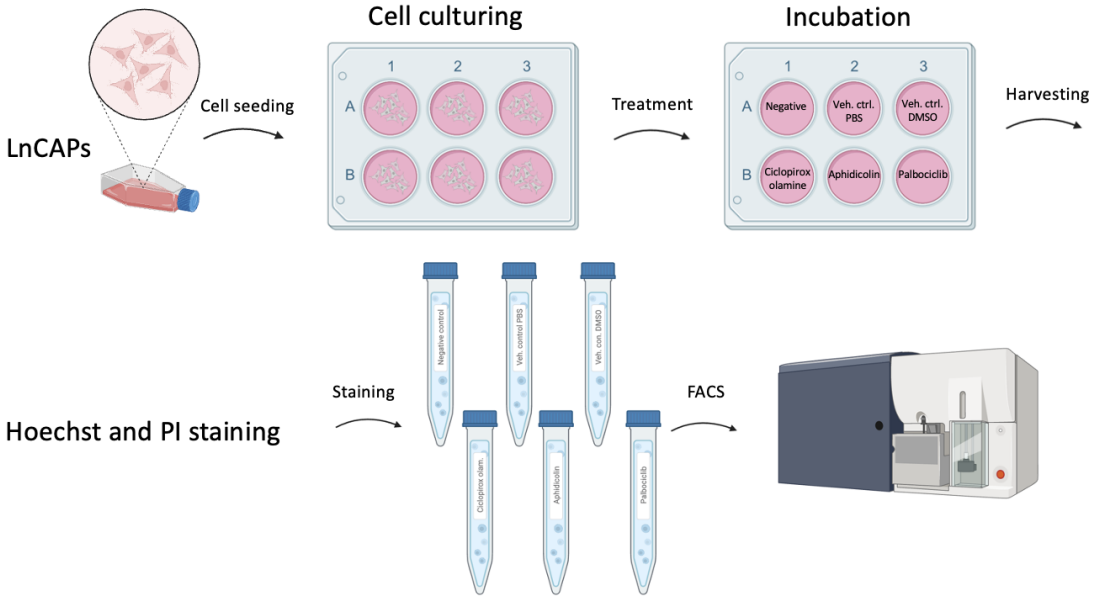

FIGURE 2.1: Workflow for cell cycle synchronization and analysis in LnCAPs cell lines. The process begins with cell seeding, followed by treatment with specific compounds (Ciclopirox olamine, Aphidicolin, Palbociclib) and respective vehicle controls (PBS, DMSO). After incubation, cells are harvested and stained with Hoechst and propidium iodide (PI) for cell cycle analysis via Fluorescence-Activated Cell Sorting (FACS).

Drug Preparation and Treatment Conditions

Ciclopirox olamine was prepared at a stock concentration of 1 mg/mL in PBS, Aphidicolin was solubilized in DMSO to a final concentration of 10 mg/mL, and Palbociclib was dissolved in PBS at 0.1 mg/mL using ultrasonication for enhanced solubility. From these stock solutions, the working concentrations were derived as follows: Ciclopirox olamine at a working concentration of 10 µM, achieved by diluting the stock solution to 2 µL/mL. Aphidicolin at a working concentration of 2 µg/mL, using a direct dilution from the stock. Palbociclib at a working concentration of 0.25 µmol/L, with precise dilution to 1.12 µL/mL from the stock.

Experimental Setup

PCa cells were harvested and seeded in 6-well plates at a density of 5×10^5 cells per well. The cells were allowed to adhere and recover for a period of 24 hours, and subsequently treated with the addition of synchronization drugs. Separate well plates were designated for each drug to assess the efficacy and potential cytotoxic effects. This can be found in the Table 2.2. The experimental conditions were as follows:

For FACS Analysis: To evaluate whether cells had been synchronized in the G1 phase, drug treatments were administered accordingly.

For Cytotoxicity Analysis: The AlamarBlue assay was employed, with cells treated with the respective drugs. Controls:

Negative Control for FACS: Untreated cells were included to establish a baseline for cell cycle distribution.

Vehicle Controls: For Ciclopirox olamine, a vehicle control with PBS and DMSO was included to account for any effects of the solvent.

Control for AlamarBlue: To ensure the accuracy of cytotoxicity readings, an untreated control was also included.

All drugs were stored at -20°C to maintain stability and potency. For the application of drugs to the cell cultures, aliquots were thawed and diluted to the desired concentration immediately before use to ensure consistency of treatment.

6-well plate	LnCAPs – $5x10^5$ cells in each well		
FACS	Ciclopirox olamine 2 µg/ml	Aphidicolin 2 µg/ml	Palbociclib 0.112 µg/ml
Control	Negative control	Vehicle control (PBS)	Vehicle control (DMSO)

TABLE 2.2: Experimental setup for the evaluation of cell cycle synchronization in LnCAPs cell lines.

2.2 Identification of potential PCa biomarkers using proteome array

To identify potential PCa biomarkers, we employed the Proteome Profiler™ Array Human XL Oncology Array Kit (Catalog Number ARY026). This kit enabled us to detect and quantify multiple biomarkers simultaneously across different PCa cell lines, providing insights into proteomic variations.

Cell Culture and Sample Collection

The LnCAP, PC-3, and 22Rv1 PCa cell lines were maintained at 37°C in a humidified atmosphere containing 5% CO_2. Cells were cultured in T25-treated culture flasks (VWR international B.V., Amsterdam, The Netherlands) and harvested at approximately 80% confluency.

- Medium Composition:
  - LnCAP: RPMI-1640 medium supplemented with 10% fetal bovine serum (FBS) and 1% penicillin-streptomycin.
  - PC-3: RPMI-1640 medium supplemented with 10% FBS and 1% penicillin-streptomycin.
  - 22Rv1: RPMI-1640 medium supplemented with 10% FBS and 1% penicillin-streptomycin.

The cell culture medium was replaced every 2-3 days for all cell lines. Once the cells reached around 80% confluency, they were harvested using 0.05% trypsin-EDTA (Gibco, ThermoFisher Scientific, Waltham, USA) and counted using the Luna-FL™ automated cell counter (Westburg B.V., Leusden, The Netherlands). Cells were seeded in 6-well plates at a density of 1×10^6 cells per well and cultured for two days. After this period, 2 mL of supernatant was collected from each well, centrifuged to remove particulates, aliquoted, and stored at ≤ -20°C to avoid repeated freeze-thaw cycles. Control samples containing only culture medium were also included to account for proteins present in the medium.

Proteome Array Assay Setup and Execution

The Proteome Profiler™ Array Human XL Oncology Array Kit includes nitrocellulose membranes printed with 84 different capture antibodies in duplicate, along with a comprehensive set of reagents:

- **Array Buffers 4 and 6:** Served as blocking and dilution buffers.
- **Wash Buffer Concentrate:** A 25-fold concentrated wash solution diluted before use.
- **Detection Antibody Cocktail:** A biotinylated antibody cocktail reconstituted in deionized water.
- **Streptavidin-HRP:** Streptavidin conjugated to horseradish peroxidase.
- **Chemi Reagents:** Solutions mixed equally to prepare a luminescent solution.
- **4-Well Multi-Dish:** A clear rectangular dish for incubation steps.
- **Transparency Overlay Template:** For coordinate reference during analysis.

Before starting the assay, all reagents were brought to room temperature. Each membrane was placed in a 4-Well Multi-Dish and blocked with Array Buffer 6 for 1 hour. Supernatant samples were diluted with Array Buffer 4 and adjusted to 1.5 mL with Array Buffer 6. The membranes were incubated overnight with the samples at 2-8°C. Following incubation, the membranes were washed with 1X Wash Buffer, incubated with the Detection Antibody Cocktail, and then incubated with Streptavidin-HRP. Chemi Reagents 1 and 2 were mixed and spread over the membranes to produce a luminescent solution for development. Finally, the membranes were exposed to X-ray film for 1-10 minutes for visualization. The steps can be found in the schematic of Figure 2.2

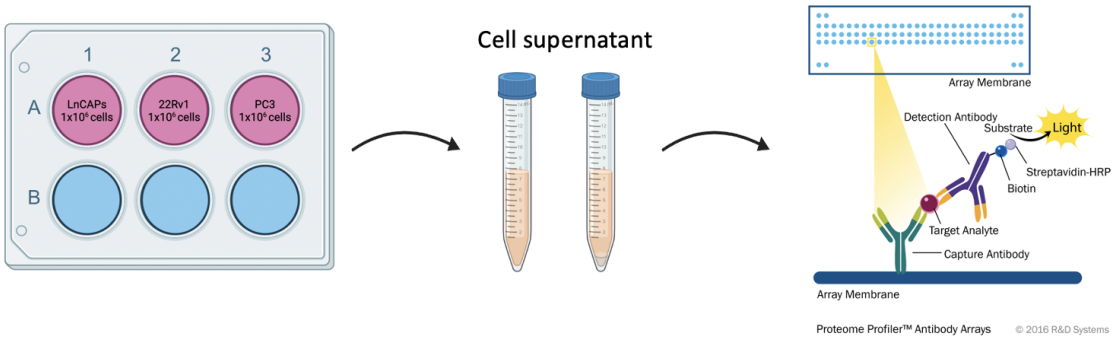

FIGURE 2.2: Proteome Profiler Array – Human XL Oncology Array Kit. This figure illustrates the workflow for the Proteome Array Assay. Prostate cancer cell lines (LnCAP, 22Rv1, and PC-3) are cultured in a 6-well plate. After two days, the cell supernatant is collected and analyzed using the Proteome Profiler™ Antibody Array to detect specific biomarkers. The array uses capture and detection antibodies, along with a chemiluminescent substrate, to identify and visualize proteins of interest.

Data Analysis and Interpretation:

The resulting membranes were analyzed using Proteome Analyzer Software, see Appendix J, to measure the intensity of each protein spots. The spots were compared against control samples, allowing the identification of potential PCa biomarkers secreted by LnCAP, PC-3, and 22Rv1 cell lines. The comprehensive analysis provided a foundation for understanding biomarker profiles across different PCa cell lines and further characterizing their proteomic signatures. This data can help identify potential biomarkers for early diagnosis, prognosis, and therapeutic targets in PCa.

2.3 Optical measurement setup and methods

2.3.1 Intracellular PSA of PCa's cell lines

To analyze the cellular characteristics and detect specific proteins within the PCa cell lines, we employed several staining techniques. This section details the methods utilized, starting with immunocytochemistry and immunofluorescence staining. The workflow of ICC staining for cell protein content analysis is depicted in Figure 2.3.

Immunofluorescence Staining of Cells

To visualize and quantify specific antigens within PCa cell lines, an immunofluorescence staining protocol was employed, primarily focusing on detecting Prostate-Specific Antigen (PSA).

Sample Preparation and Fixation

Cultured cells were first seeded on glass coverslips and grown to the desired confluency. They were fixed in 1% formalin in 1X PBS for 15 minutes at room temperature. This fixation step stabilized cellular structures and preserved proteins for analysis.

Permeabilization and Blocking

After fixation, the cells were washed twice with 1X PBS to remove residual formalin. They were then permeabilized with 0.1% Triton X-100 in 1X PBS for 15 minutes at room temperature, allowing antibodies to access intracellular targets. Following permeabilization, the cells were gently washed three times with PBS. To reduce nonspecific binding of antibodies, the cells were blocked with 1% Bovine Serum Albumin (BSA) in PBS for 60 minutes at room temperature.

Primary and Secondary Antibody Incubation

A primary antibody, rabbit anti-PSA, was diluted to 10 µg/mL in 0.1% BSA/PBS and incubated with the cells for 1 hour at room temperature. After incubation, the cells were washed three times (5-10 minutes each) with 1X wash buffer. A secondary antibody, anti-rabbit PE-conjugated (1:1000 v/v in PBS), was incubated with the cells for 60 minutes at room temperature. The cells were washed three times with 1X wash buffer to remove unbound antibodies.

Counterstaining and Visualization

For nuclear visualization, cells were counterstained with DAPI or Hoechst by incubating with the dye for 15 minutes at room temperature. After counterstaining, the cells were washed three times with 1X wash buffer. Cells stained in a 24-well plate were covered with 1X PBS to prevent drying. For cells on coverslips, they were mounted onto slides using antifade mounting solution.

Fluorescence Imaging

Fluorescent images of stained cells were captured using a fluorescence microscope, ensuring appropriate filters for detecting specific fluorescent signals. The PSA signal was

observed in the PE channel, and nuclear staining was visualized using the DAPI or Hoechst channels.

Conclusion

This immunofluorescence staining technique enabled the detection and quantification of PSA expression in PCa cell lines, providing valuable insights into their proteomic profiles. Additional staining methods, including cytospin, membrane staining, and spotting device-based approaches, were also employed to comprehensively characterize PSA and other biomarkers, as detailed in subsequent sections.

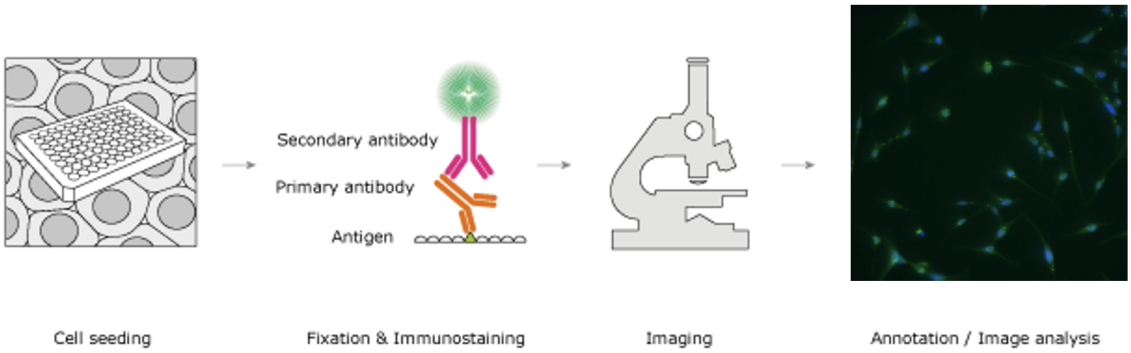

FIGURE 2.3: Workflow of ICC staining for immunocytochemistry analysis. The figure presents the workflow for Immunocytochemistry (ICC) staining. Initially, PCa cells are seeded onto a multi-well plate and subsequently fixed. The primary antibody binds to the target antigen, followed by a secondary antibody conjugated to a fluorescent dye. After staining, the samples are imaged using a fluorescence microscope, and the annotated images are analyzed to identify and quantify the expression of specific proteins.

Visualisation of the stained cell on a cover slip using the cytospin

To further examine the cellular structures and cycle phases of LnCAP cells, cytospin staining was employed following flow cytometric sorting. This methodology provided insights into the cellular distribution across different cell cycle phases, see Figure 2.4 for the schematic.

Sample Preparation and Hoechst Staining

LnCAP cells were first harvested from culture and stained with Hoechst, a fluorescent dye that binds to DNA, highlighting the nuclei.

FACS Analysis and Sorting

The stained cells were analyzed using Fluorescence-Activated Cell Sorting (FACS), where they were categorized according to their cell cycle phase. The cells were sorted into three groups: G1, and G2/M phases.

Cell Counting and Selection

After sorting, the cells were counted, and 10,000 cells from each cell cycle phase group were selected for cytospin analysis.

Cytospin Technique

The selected cells were spun down onto coverslips using the cytospin technique. This involved placing the cells into a specialized chamber, where they were centrifuged, spreading them evenly across the surface of the coverslip.

Mounting and Visualization

The coverslips with spun-down cells were mounted onto microscope slides using antifade mounting solution, preserving the fluorescent signal for extended analysis. The slides were

then examined under a fluorescence microscope using appropriate filters to visualize the Hoechst-stained nuclei. This allowed for a detailed examination of each cell cycle phase and comparison of cellular characteristics between the different phases.

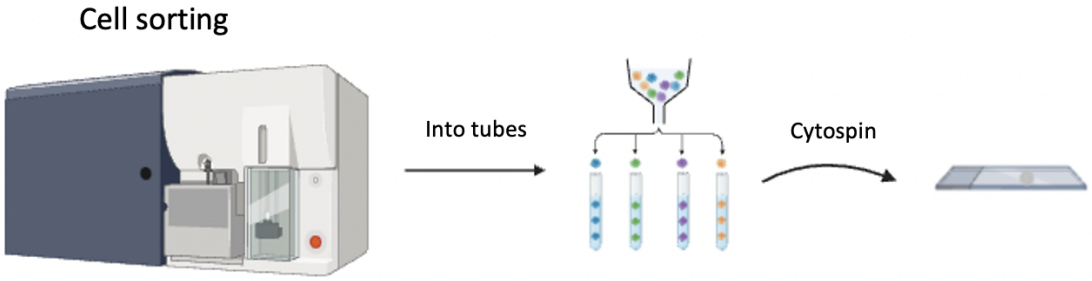

FIGURE 2.4: Workflow of Cell Sorting and Cytospin for Cell Cycle Phase Analysis. The figure illustrates the workflow for cell sorting and cytospin. PCa cells are sorted using Fluorescence-Activated Cell Sorting (FACS) based on their DNA content, allowing separation into different cell cycle phases (G1, S and G2/M). After sorting, the cells are collected into tubes and subjected to the cytospin method to deposit them onto glass slides for subsequent microscopic analysis. This technique allows for visual confirmation of sorted cell cycle phases using nuclear staining.

Conclusion

By incorporating FACS sorting and cytospin staining, this approach provided a comprehensive analysis of LnCAP cells, offering insights into their cell cycle dynamics and biological profiles. The visualization confirmed the presence of distinct nuclear features associated with each cell cycle phase, confirming that the cells were sorted by their cell cycle phase.

2.3.2 Measuring PSA secretion from PCa's cell lines

Staining PVDF Membranes to Visualize PSA Secretion

To investigate the secretion of Prostate-Specific Antigen (PSA), LnCAP, PC-3, and 22Rv1 cells were seeded onto PVDF membranes and stained using a specific protocol. This approach allowed for the visualization of PSA secretion using ELISpot assay and the VyCAP spot software system, see Figure 2.5 for the schematic.

Membrane Preparation and Activation

PVDF membranes were cut into circles to fit into a 24-well plate. Under sterile conditions, the membranes were placed into the wells and incubated with 500 µL of 100% methanol, ensuring complete coverage for 5-10 seconds. After activation, the membranes were washed twice with 500 µL of 1X PBS. Anti-PSA (capture) antibody solutions were prepared at a concentration of 25 µg/mL. The membranes were coated with 200 µL of this antibody solution, ensuring complete surface coverage, and incubated at 4°C overnight to allow effective antibody binding.

Membrane Blocking

After overnight incubation, the antibody solution was aspirated, and the membranes were blocked with 200-300 µL of a 3% BSA in 1X PBS solution for 1 hour at 4°C or room temperature. Once blocked, the membranes were washed with 1X PBS and left in the solution if not immediately used.

Cell Seeding on Membranes

The PBS was aspirated from the wells, and 500 µL of cell culture medium was added to each well. 5,000 cells from each cell line (LnCAP, PC-3, and 22Rv1) were suspended and added to each membrane. The 24-well plate was then incubated at 37°C overnight to allow the cells to adhere and grow.

Antibody Staining: The plate was removed from the incubator, and the membranes were washed with 0.1% Tween 20 (in 1% BSA PBS) for 15 minutes on a rocker shaker at 300 rpm. Subsequently, the membranes were washed with 1% BSA in PBS for 15 minutes on a rocker shaker at 300 rpm. A Rabbit anti-PSA antibody was prepared at 2 µg/mL in 1X PBS, and 200 µL of this solution was added to each membrane. The membranes were incubated for 1 hour on a shaker at 300 rpm with the lid closed. Following incubation, the membranes were washed three times with 1% BSA in PBS for 5 minutes each. A Goat anti-Rabbit antibody was then prepared at 2 µg/mL in 1X PBS, and 200 µL of this solution was added to each membrane. The membranes were incubated for 1 hour on a shaker at 300 rpm, covered with aluminum foil. After the secondary antibody incubation, the membranes were washed three times with 1% BSA in PBS for 5 minutes each.

Storage and Visualization: The membranes were stored in PBS, covered in aluminum foil, and placed at 4°C for further use. For long-term storage, the membranes were kept in Milli-Q water, sealed with parafilm, and covered in foil at 4°C. For imaging, the membranes were dried completely and placed on glass slides. The VyCAP spot software system is used to visualize the PSA secretion on the membranes.

Conclusion: This staining protocol allows for the clear visualization of PSA secretion from LnCAP, PC-3, and 22Rv1 cells using the VyCAP spot software, providing crucial data on the secretion profiles of each cell line. The method provides effective analysis of PSA secretion, offering a valuable tool for understanding tumor heterogeneity.

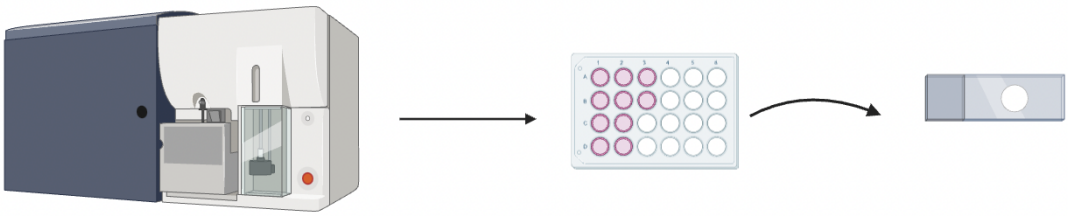

FIGURE 2.5: Workflow of Cell Sorting and Cell seeding for Cell Cycle Phase dependent proteome secretion analysis. The figure illustrates the workflow for cell sorting into a 24-well plate and the subsequent membrane processing for visualization. PCa cells are sorted using Fluorescence-Activated Cell Sorting (FACS) based on their DNA content, allowing separation into different cell cycle phases (G1, and G2/M). The cells are directly sorted onto the membranes and subsequently incubated. They are further analyzed according to the workflow in subsection 2.3.4.

Spotting device for multiplexing

To analyze cellular characteristics and detect specific proteins, a novel approach was implemented using a spotting device to perform multiplex staining on PVDF membranes. This method allowed for the simultaneous analysis of multiple antibodies on a single membrane.

Staining Membranes Using the Spotting Device:

Membrane Preparation and Activation: The PVDF membranes were prepared and activated using the protocol outlined in subsection 2.3.2, involving cutting, activating with methanol, and blocking the membrane to prepare it for antibody application. The device setup and assembly can be seen in Figure 2.6.

Insertion into the Spotting Device: The prepared and activated membranes were then placed into the spotting device, ensuring correct positioning to align with the wells of the device.

Antibody Application: Antibody solutions were prepared at a dilution of 1:1000 from the stock. Approximately 4 µL of the prepared antibody solution was added to each well of the spotting device. Each well could contain a different antibody, but for proof of concept, Anti-IgG PE was used in each well.

Assembly and Spotting: The spotting device was assembled to ensure that the filled well chambers aligned correctly with the membrane below. The device was then left to deposit spots of the antibody solution onto the membrane.

Incubation: The membrane was incubated with the spotted antibodies for varying durations: one hour, two hours, overnight, and up to 24 hours to assess different binding dynamics and staining intensities.

Washing: After incubation, the spotting device was removed, and the membrane was thoroughly washed with PBS to remove any unbound antibodies.

Visualization and Storage: The membrane could be visualized immediately using the VyCAP system to analyze the spots. Alternatively, the membrane was stored in Milli-Q water until ready for visualization, preserving the integrity of the antibody spots.

Conclusion: Using the spotting device proved to be a promising method for multiplex staining of PVDF membranes, allowing simultaneous detection of multiple antibodies. However, further optimization is required to improve the consistency of the results.

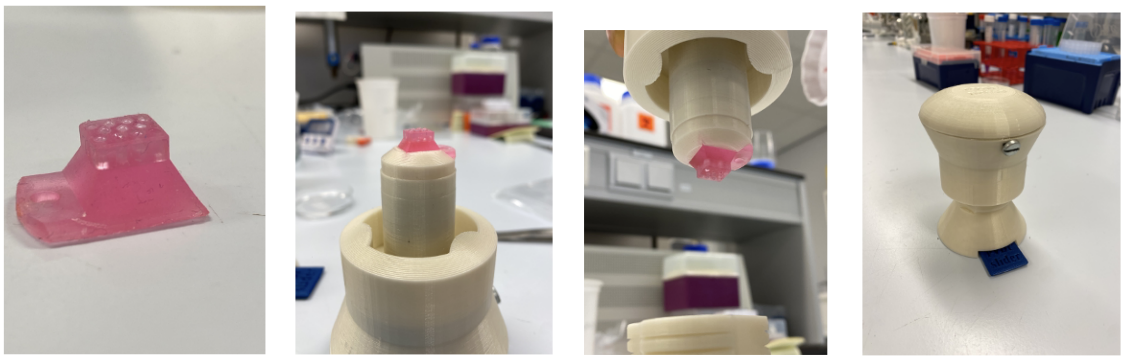

(A) (B) (C) (D)

FIGURE 2.6: The images illustrate the design and assembly of the spotting device used to imprint antibody solutions onto activated PVDF membranes: A) The first image shows the 11-well chamber where antibody solutions are loaded. Each well is capable of holding a different antibody solution for multiplexing purposes.; B) The second image depicts the top part of the spotting device, where the well chamber is inserted to hold it in place during the spotting process.; C) The third image demonstrates how the top part with the loaded well chamber is aligned and inserted into the bottom part, where the activated PVDF membrane is positioned.; D) The final image displays the fully assembled spotting device, where the well chamber is placed on the membrane, allowing the antibody spots to be imprinted precisely onto the surface.

2.3.3 Identification and sorting of cells in different cell cycle phases

The ability to identify and sort cells based on their cell cycle phase is crucial for numerous biological investigations. This was achieved using Fluorescence-Activated Cell Sorting (FACS), incorporating Hoechst 33342 staining to differentiate cells in various phases of the cell cycle.

FACS Staining Protocol

Cell Preparation: Cells were harvested when they reached approximately 80% confluency to ensure a high viability and representative population distribution. The cells were then counted and centrifuged at 3000 x G for 5 minutes to pellet them.

Resuspension and Staining: The supernatant was carefully removed, and the cells were resuspended in a solution of 2% FBS in PBS to a concentration aimed at reaching 300,000 cells per 200 µL in each FACS tube. Hoechst 33342 was added to each sample at a concentration of 1 µL per 100 µL of cell suspension. The cells were incubated with the dye for 30 minutes on ice to allow adequate staining while minimizing cell stress and dye toxicity.

Washing: After staining, the cells were washed by adding an additional 300 µL of 2% FBS in PBS to bring the total volume to 500 µL. The cells were then centrifuged to remove excess dye, and the supernatant was discarded.

FACS Analysis and Sorting:

Setup and Calibration: The flow cytometer was set up and calibrated for UV excitation (340 to 380 nm) and detection of Hoechst 33342 fluorescence at blue wavelengths. Adjustments were made to accurately gate single cells and exclude doublets using pulse-width/pulse-area analysis. A negative control (non-stained cells) was used to set the baseline fluorescence and adjust the sensitivity of the flow cytometer.

Measurement and Data Collection: The stained cells were analyzed by flow cytometry. Hoechst 33342 fluorescence was measured to determine the DNA content of the cells, allowing the identification of cells in G1, S and G2/M phases. Settings were adjusted as necessary based on the intensity of cell fluorescence and resolution of cells in different cell cycle phases.

Sorting: Cells were sorted based on their DNA content into different collection tubes for further experiments. Parameters such as Forward Scatter (FSC) and Side Scatter (SSC) were used alongside Hoechst fluorescence to refine the sorting accuracy.

Post-Sorting Processing: Sorted cells were collected and either cultured further or used immediately for downstream analyses.

Considerations and Precautions: The viability and cell cycle progression of sorted cells could be influenced by the staining procedure due to the potential light sensitivity induced by Hoechst 33342. Appropriate controls and replicates were included to ensure the reliability of the sorting process.

2.3.4 Membranes and secretion detection

To investigate the secretion dynamics of Prostate-Specific Antigen (PSA) across different cell cycle phases, a detailed analysis was performed using PVDF membranes and the VyCAP imaging system. This method allowed for the quantitative assessment of PSA secretion from cells sorted into G1, and G2/M phases.

Protocol for PSA and GAPDH Detection on PVDF Membranes

Membrane Preparation: The protocol for preparing and activating PVDF membranes, as described in "Staining PVDF Membranes to Visualize PSA Secretion," was followed to ensure that the membranes were properly conditioned for cell seeding and subsequent protein detection.

Cell Seeding on Membranes: Cells sorted into different cell cycle phases (G1, and G2/M) using FACS were seeded onto the prepared PVDF membranes. Seeding sorted cells enabled the investigation of phase-specific PSA secretion.

Overnight Incubation: The seeded membranes were incubated overnight under optimal cell culture conditions to facilitate cell attachment and secretion. Overnight incubation is crucial as it allows sufficient time for cells to recover from the sorting process and begin secreting PSA.

Washing of Membranes: Post-incubation, the membranes were washed with PBS containing 0.1% Tween-20 to remove and reduce background staining in subsequent steps. This step is crucial for removing cellular debris and any unattached cells, ensuring that subsequent antibody staining reflects PSA secreted from the cells.

Antibody Staining for PSA and GAPDH:

- **PSA Detection:** The antibody staining steps detailed in subsection 2.3.4 were followed. A primary antibody specific to PSA was applied, followed by a compatible secondary antibody to visualize the protein.
- **GAPDH Detection:** Concurrently, GAPDH was detected using a specific antibody. As a housekeeping protein, GAPDH serves to normalize the data, providing a baseline that compensates for variations in cell density and antibody application across the membrane.

Imaging Using the VyCAP System: After staining, the membranes were imaged using the VyCAP imaging system. This technology allows for detailed quantification of the fluorescent or chemiluminescent signals emitted by the labeled antibodies, enabling accurate measurement of both PSA and GAPDH levels.

Data Analysis and Normalization: The intensity of the signals from both PSA and GAPDH was quantified using image analysis software. Normalizing PSA signal intensity against GAPDH is critical as it ensures that the measured differences in PSA secretion are due to biological factors rather than technical variables like cell number or uneven distribution on the membrane.

2.4 Electrochemical measurement setup and methods

2.4.1 Poly-L-Lysine synthesis

To prepare Poly-L-Lysine (PLL) derivatives, including PLL modified with ethylene glycol groups (PLL-OEG) and PLL-OEG-Biotin, a series of synthesis, dialysis, and freeze-drying steps were performed. The chemical structure of the PLL-OEG molecule can be found in Figure 3.18.

Synthesis of PLL-OEG and PLL-OEG-Biotin: The materials, such as micropipettes, 1X PBS (filtered, pH 7.4), dry DMSO for stock solutions, and clean, dry vials, were taken out of the freezer (-30°C) at least 30 minutes before starting. A 10 mg/mL solution PLL was prepared by dissolving 100 mg of PLL in 10 mL of PBS (pH 7.4, filtered). To synthesize the other stock solutions, a 0.25 M solution of OEG NHS ester was prepared by

dissolving 100 mg of the ester in 1.2 mL of dry DMSO. Additionally, a 0.25 M solution of Biotin-OEG NHS ester was prepared by dissolving 50 mg of Biotin-OEG in 339.7 µL of DMSO. In a clean and dry vial, 1 mL of PLL.HBr (10 mg/mL) and 1 mL of PBS (pH 7.4) were mixed with the appropriate amounts of OEG NHS ester and Biotin-OEG NHS ester solutions, depending on the desired final product:

- For PLL-OEG, a 30% OEG concentration was achieved by adding 57.4 µL of the OEG NHS solution.
- For PLL-OEG-Biotin, a 4% Biotin concentration was achieved by adding 9.6 µL of the Biotin-OEG NHS solution.

The mixture was stirred vigorously for 4 hours on a shaker to ensure complete reaction.

Dialysis: After synthesis, the resulting solutions were dialyzed using SpectraPor dialysis tubing with a 6-8 kDa molecular weight cut-off and a diameter of 6.4 mm. The solutions were dialyzed against progressively diluted PBS solutions (70%, 50%, and 30%) followed by Milli-Q water. Each solution change was performed two to three times for thorough purification, and the dialysis solution was replaced twice daily.

Freeze-Drying and Storage: After dialysis, the purified solutions were freeze-dried to obtain a powdered form of the final compounds. The resulting product was then stored in the freezer for future use.

2.4.2 Nuclear Magnetic Resonance spectroscopy

Nuclear Magnetic Resonance (NMR) spectroscopy was employed to characterize the molecular structures of the synthesized compounds. The freeze-dried product was dissolved in Deuterium oxide (D_2O) at a concentration of 10 mg/mL, ensuring complete dissolution by thorough mixing. Once fully dissolved, the sample was carefully transferred to an NMR tube, making sure no air bubbles were present. The tube was then sealed securely to prevent contamination or evaporation. D_2O, also known as heavy water, is used as a solvent in NMR spectroscopy because it contains deuterium instead of hydrogen, which does not interfere with the detection of hydrogen signals in the sample [19]. The prepared NMR tube was inserted into the spectrometer, ensuring proper alignment and secure placement.

Data acquisition was carried out at a frequency of 400 MHz for ^{1}H NMR. The acquisition parameters, including pulse sequence, relaxation delay, and acquisition time, were configured to optimize the signal-to-noise ratio and spectral resolution. After data acquisition, the obtained signals were processed using specialized software. Fourier transformation converted the time-domain signals into frequency-domain spectra, and subsequent phase correction, baseline adjustment, and peak integration were performed as necessary.

The resulting spectra were analyzed to identify chemical shifts, coupling constants, and integration values, allowing for the structural elucidation of the synthesized molecules. During analysis, the integral of the alpha proton peak was set to 1, and a linear fit integration was performed to ensure accurate measurements. The spectral data were documented, including key chemical shifts, coupling patterns, and other relevant information, to provide a comprehensive structural characterization of the synthesized molecules.

2.4.3 Quartz Crystal Microbalance with dissipation

The Quartz Crystal Microbalance with Dissipation Monitoring (QCM-D) technique is instrumental in validating the functionalization of synthesized products, including PLL-OEG and PLL-OEG-Biotin, on platinum-plated (Pt-plated) electrodes. This method provides real-time measurements of changes in mass at the surface due to molecular adsorption

or binding, offering insights into the dynamics of each layer's formation on the electrode surface, such as PLL modified with Biotin, Streptavidin, and biotinylated antibodies [5].

For the QCM-D experiments, extensive preparation and cleaning of the Pt-plated chips were crucial. Initially, a piranha solution, composed of Milli-Q water, ammonia (25%), and hydrogen peroxide (30%) in a 50:10:10 ratio, was prepared. Given its highly reactive and corrosive nature, the solution was handled with extreme care. This solution was heated on a hotplate set to 300°C, aiming for an operational temperature of 75°C, marked by the emergence of oxygen bubbles at around 65°C. The chips were submerged in this heated solution using a Teflon holder and maintained at 75°C for five minutes. After the treatment, the chips were allowed to cool next to the hotplate, and the solution was safely discarded. Subsequently, the chips were thoroughly rinsed with Milli-Q water and then with 99% ethanol, followed by a sonication for five minutes to ensure complete cleanliness. The final step involved drying the chips with nitrogen to eliminate any moisture or residual solvents.

The QCM-D set up was prepared according to the manufacturer's specifications [5], ensuring all connections were secure. The cleaned and dried chips were installed in the device. The system was initially rinsed with PBS at a flow rate of 300 µL/min until the frequency signals stabilized. Following stabilization, the flow rate was reduced, and PLL derivatives were introduced at a concentration of 0.5 mg/mL, derived from diluting a 10 mg/mL stock solution. This allowed for the derivatives to bind to the chip surface. After a 10-minute exposure, the system was rinsed with PBS to remove any unbound substances.

The binding specificity and efficiency of further interactions were tested by introducing streptavidin at a flow rate of 50 µL/min to interact with any biotinylated sites on the PLL derivatives. Following another PBS rinse, a biotinylated anti-EpCAM antibody solution at a concentration of 10 µg/mL was introduced. This step was followed by the introduction of an EpCAM protein solution to demonstrate the system's capacity to detect specific protein attachments.

After completing the assays, the QCM-D device was cleaned with Hellmanex solution to ensure it remained free of any residues that might affect subsequent analyses. The data collected from these experiments, particularly the frequency shifts, were meticulously analyzed to confirm the mass of the adsorbed layers, thus verifying the successful functionalization of the chips. This comprehensive setup not only demonstrated the attachment and specificity of the PLL derivatives but also validated the operational readiness of the QCM-D system for detailed biomolecular interactions.

2.4.4 Cyclic Voltammetry

Cyclic Voltammetry (CV) is a powerful electrochemical technique used to investigate the redox properties of molecules by analyzing their oxidation and reduction behaviors. In this project, CV was utilized to measure real-time concentrations of the EpCAM protein using Methylene Blue as a redox mediator.

The flow cell was set up with Pt-plated electrodes, see Figure 2.7, which were thoroughly cleaned using 0.5 M sulfuric acid H_2SO_4 to ensure that all surfaces were free of organic contaminants and ready for functionalization. Initially, bare electrodes were tested with varying concentrations of Methylene Blue to establish a baseline electrochemical response. This step verified that the redox mediator behaves predictably on a clean electrode surface. Methylene Blue acts as a redox mediator by facilitating electron transfer between the electrode and the proteins bound to the surface. The current measured is inversely proportional to the amount of surface coverage, allowing for quantification of the bound protein.

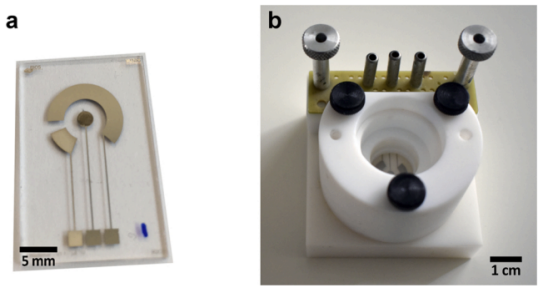

FIGURE 2.7: Experimental setup for electrochemical measurements. (a) Glass chip containing electrodes: Pt working electrode (WE), Ag/AgCl reference electrode (RE), Pt counter electrode (CE). (b) Teflon chip holder equipped with a pogo pins connection block. The setup is similar to the one used by Tanumihardja et al. [25].

After cleaning, the Pt-plated electrodes were functionalized with PLL-OEG-Biotin, streptavidin, and biotinylated anti-EpCAM antibodies to ensure selective binding of the target EpCAM protein. The electrodes were first treated with PLL-OEG-Biotin to provide a biotinylated surface. Streptavidin was then added, creating binding sites for biotinylated anti-EpCAM antibodies, which were subsequently flowed over the electrodes to selectively bind to the target EpCAM protein.

Various concentrations of the EpCAM protein were prepared in solutions alongside a 1 mM Methylene Blue solution in PBS. These protein concentrations were used to evaluate how the presence of proteins affects the electrochemical response. The CV was performed by flowing the solutions over the functionalized electrodes. Changes in current were recorded as the potential was cycled, detecting different levels of protein binding based on variations in current due to Methylene Blue.

The cyclic voltammograms were analyzed to observe peaks corresponding to the oxidation and reduction of Methylene Blue. The presence and intensity of these peaks were directly influenced by the interaction between Methylene Blue and the electrode surface. By comparing the cyclic voltammograms obtained from different protein concentrations, a relationship between the EpCAM concentration and the signal intensity was established, allowing for the quantification of protein levels based on electrochemical response.

The settings for CV measurements included a scan rate of 50 mV/s, 1 mM Methylene Blue in PBS as the redox mediator, and varied concentrations of EpCAM protein. This cyclic voltammetry approach provided a comprehensive method for detecting and quantifying EpCAM protein binding on functionalized electrodes using Methylene Blue as a redox mediator.

Chapter 3

Results and Discussion

3.1 Identification of potential PCa biomarkers using Proteome array

The identification of potential PCa biomarkers was conducted using a Proteome array as outlined in Section 2.2. The cells from the LnCAPs, PC-3, and 22Rv1 cell lines were initially seeded in 6-well plates at a density of 1×10^6 cells per well and cultured for two days. After this period, 2 mL of supernatant from each well was carefully collected. This duration was chosen to allow adequate protein secretion into the medium, ensuring a robust analysis. The collected supernatant was then processed using the Proteome array protocol. The results of this analysis are presented in Figure 3.1.

Concurrently, to assess the health and viability of the cells post-culture, they were harvested and subjected to viability testing using Trypan blue staining. The viability assessment revealed the following results:

- LnCAPs: 84% viability, which may be attributed to rapid growth potentially leading to overcrowding in the culture environment.
- PC-3: 93% viability, indicating a robust cell line under the given culture conditions.
- 22Rv1: 55% viability, suggesting that this cell line may require more time to adapt and stabilize within the culture, possibly due to its inherent instability or slower attachment and growth rates.

These observations suggest that variations in cell growth dynamics and environmental adaptability among the cell lines could significantly influence their viability and, consequently, the protein secretion profiles observed in the supernatant analysis. The differential viability rates may reflect the intrinsic biological variability of these cell lines, impacting their response to the cultured conditions and affecting the overall experimental outcomes.

To account (or normalize) for the fluorescence from the proteins present in cell culture medium, a control sample consisting only of the culture medium was analyzed concurrently. The intensities of the spots on the Proteome array were carefully analyzed and processed, with the detailed results documented in Appendix J. This analysis was crucial for differentiating between background protein levels and those significantly elevated due to cellular activity.

The experiment aimed to discern distinct protein secretion profiles among the different cell lines under study, providing insights into the heterogeneity of protein expression in PCa cells. These findings are integral to understanding the variable nature of PCa and refining biomarker-based diagnostics.

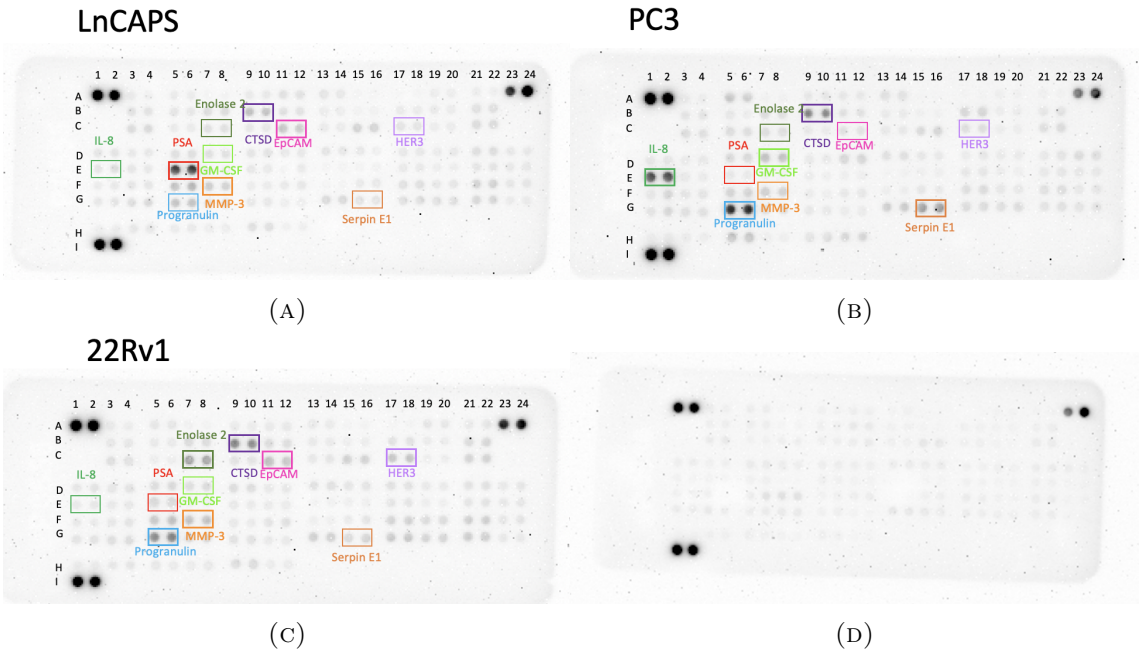

(A) (B)

(C) (D)

FIGURE 3.1: These figures display proteome array analyses for three different prostate cancer cell lines: LnCAPs, PC3, and 22Rv1. Each array highlights the expression of selected proteins crucial in cancer biology, including IL-8, PSA, GM-CSF, MMP-3, Enolase, CTSD, EpCAM, HER3, Serpin E1, and Progranulin. The spot intensities indicate the relative abundance of these proteins within each cell line, providing insights into the unique proteomic signatures that could potentially distinguish between different types of prostate cancer. The initial proteins of interest are encased in colored boxes for each cell line to facilitate direct comparison and visualization of differential expression across the arrays. Figure D) displays the control membrane tested with cell culture medium.

To analyze the proteome array data, pixel intensities were initially measured to obtain quantitative information on protein concentrations. The following steps were undertaken to process and analyze these data, as illustrated in the accompanying flowchart in Figure 3.2:

1. **Data Collection**: Pixel intensity values were extracted from the array images, representing the relative abundance of each protein.

2. **Normalization**: Values were normalized against a negative control to correct for background noise and variability in staining intensity.

3. **Threshold Setting**: A threshold was set to distinguish between meaningful signals and background noise, enhancing the reliability of the data interpretation.

4. **Data Compilation**: The processed data were compiled into a structured format for further statistical analysis and visualization.

This methodical approach enabled a robust analysis of the proteome array, facilitating a deeper understanding of the protein expression patterns associated with the sample.

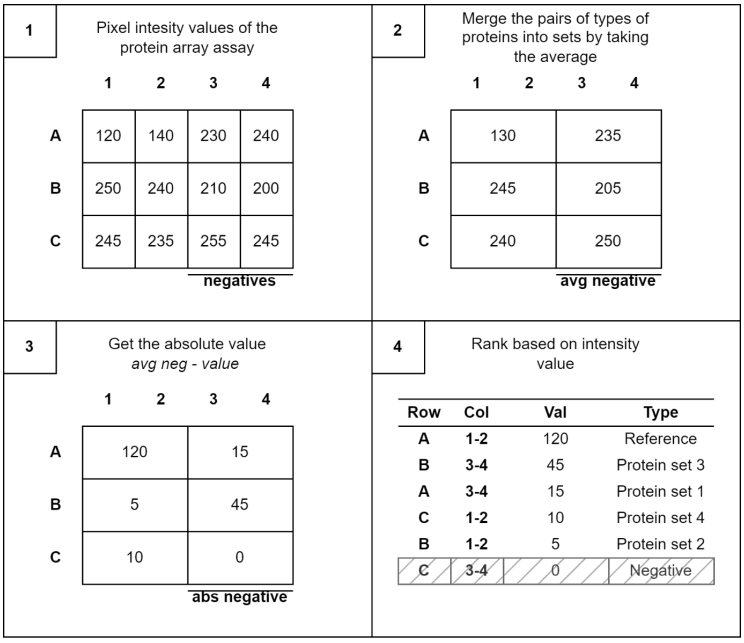

FIGURE 3.2: Flowchart illustrating the analysis of proteome array results. The data were first collected as pixel intensity values, with example values shown in each grid. C3,4 being an example for the negative reference, which is used to get the absolute values of the results and ensure accuracy when comparing various sets of results.

The results, plotted in Figure 3.3, illustrate distinct proteomic profiles among the different cell lines, indicating variable expression and secretion levels of specific proteins. Notably:

- **Progranulin** and **IL-8** show significantly higher concentrations in LnCAP cells compared to other cell lines and controls, suggesting a potential role of these proteins in the specific biology of LnCAP cells.
- **Prostate-Specific Antigen (PSA)**, a well-known marker for prostate cancer, is predominantly expressed in LnCAP and PC-3 cells, aligning with their prostate cancer origin.
- **Cathepsin D** and **Serpin E1** are expressed variably across all samples, indicating differential regulation across cell types which could be linked to distinct cellular processes or states of cancer progression.
- **Enolase**, **Thrombospondin-1**, and **MMP-2** display modest expression across the cell lines but are notably low in the control, suggesting these proteins may be specifically upregulated in prostate cancer cells.

The presence of these proteins in different concentrations across cell lines and the control suggests a complex interplay of factors driving protein secretion in cancer cells. This heterogeneity could be pivotal for understanding the mechanisms of prostate cancer progression and for developing targeted diagnostic and therapeutic strategies. Further investigation into these proteins may reveal their potential as biomarkers for prostate cancer progression and treatment response. Additionally, the lower concentrations in control medium underscore the specificity of these proteomic signatures to cancer cells, enhancing their diagnostic value

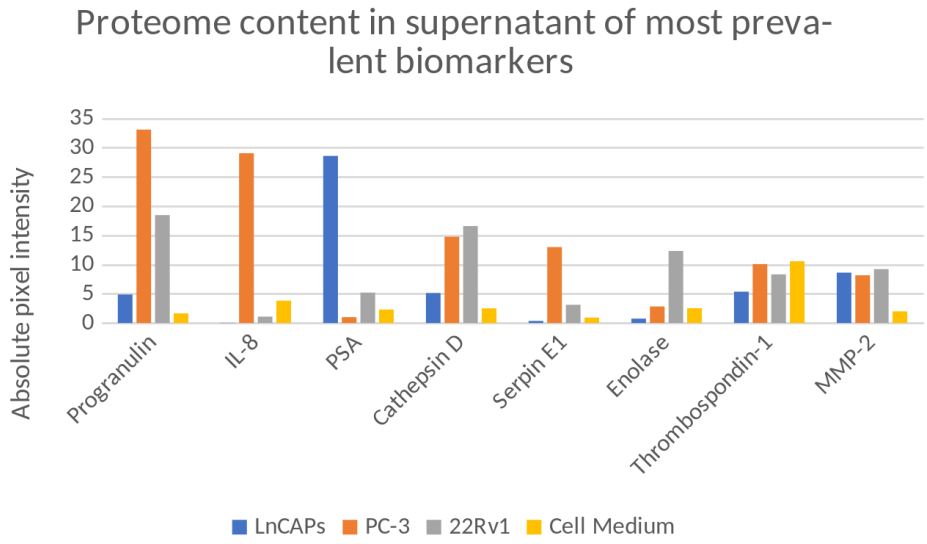

FIGURE 3.3: This graph displays the proteome content in the supernatant of three prostate cancer cell lines—LnCAP, PC-3, 22Rv1—and a control cell medium. The y-axis represents protein concentration (arbitrary units), and the x-axis lists different proteins: Progranulin, IL-8, PSA, Cathepsin D, Serpin E1, Enolase, Thrombospondin-1, and MMP-2. Each bar color corresponds to a different sample: blue for LnCAP, orange for PC-3, grey for 22Rv1, and yellow for the cell medium.

The data, plotted in Figure 3.4, showcase distinct secretion profiles which could be pivotal in the diagnosis and understanding of different prostate cancer subtypes:

- **PSA**, renowned for its application in prostate cancer diagnosis, is significantly more abundant in the LnCAPs cell line, suggesting its utility in identifying cancer activity in prostate tissues [3].
- **IL-8**, a key player in inflammatory and angiogenic pathways, is notably elevated in the PC-3 line, indicating its potential role in the aggressive behavior and metastatic potential of this particular subtype [26].
- **MMP-3**, involved in the breakdown of extracellular matrix, shows moderate expression across all lines, implicating its role in tumor invasion and metastasis [10].
- **EpCAM**, another important marker often associated with epithelial cancers, shows varied expression across the cell lines, with notable levels in 22Rv1, suggesting differences in epithelial cell properties or tumor characteristics [14].

This variability in protein expression underscores the heterogeneity of prostate cancer and highlights the importance of considering a range of biomarkers in both diagnostics and targeted therapy development. The significant differences in protein secretion levels among the cell lines emphasize the potential of these markers to serve as differential indicators for prostate cancer subtypes. Further detailed analysis of these proteins could lead to more effective, personalized therapeutic approaches, improving outcomes by aligning treatments more closely with the biological specifics of each cancer subtype.

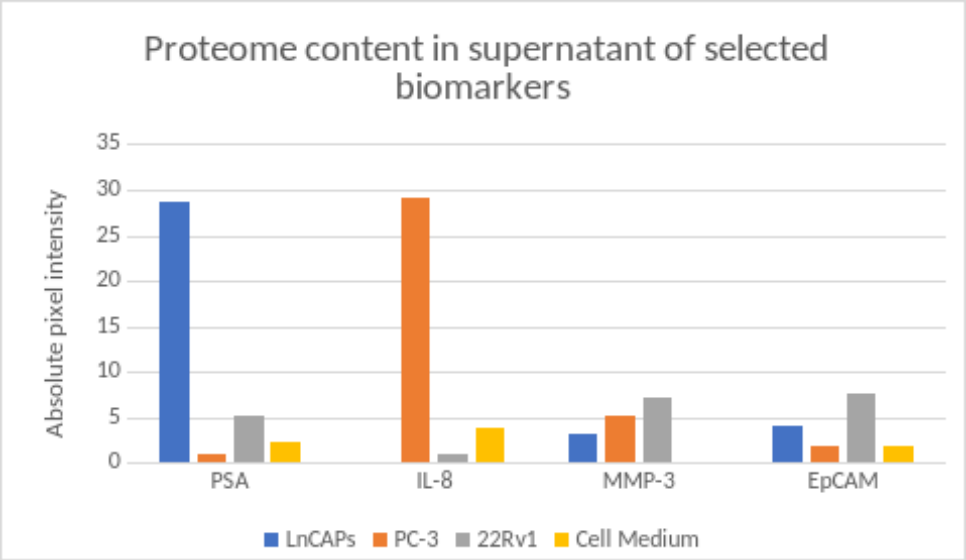

FIGURE 3.4: Graph x presents the comparative analysis of proteome content, specifically PSA, IL-8, MMP-3, and EpCAM, in the supernatants of three different prostate cancer cell lines—LnCAPs, PC-3, and 22Rv1—alongside a control of just cell medium.

3.2 Intracellular PSA of PCa's cell lines

In an effort to better understand the protein expression within PCa cells, we utilized specific antibodies to visualize the intracellular content of several proteins. The proteins targeted in this analysis included PSA, GAPDH, EpCAM, MMP-3, and IL-8. This intracellular staining was not only aimed at confirming the presence of these proteins but also at validating the efficacy of the antibodies used for detecting them, which is critical due to potential variations in epitope accessibility.

Experimental Approach and Observations:

- **Antibodies and Staining**: The antibodies were selected based on their ability to bind distinct epitopes within the target proteins. Staining was performed as detailed in the protocol from subsection 2.3.1. The primary aim was to assess whether these antibodies could effectively recognize and bind to their corresponding proteins within the cells.
- **Visualization**: The results of the staining are shown in Figure 3.5. PSA was clearly visible in the FITC channel, indicating successful staining and the presence of this protein within the cells. The nucleus was stained with DAPI, providing a clear demarcation of the cell nuclei and the images were put into overlay.
- **Additional Protein Analysis**:
  - GAPDH was also successfully visualized in the FITC channel, confirming the antibody's effectiveness and the protein's intracellular expression, as well as the staining of EpCAM.

– However, the analysis for MMP-3 in the PerCP channel and IL-8 in the APC channel did not yield reliable signals, suggesting that the antibodies might not have bound effectively, or the levels of these proteins were below the detection threshold under the experimental conditions used.

Significance of Findings: The visualization of these proteins is not only crucial for confirming the specificity and functionality of our antibodies but also provides insights into the protein profiles that could be linked to different stages of PCa. Although proteins like MMP-3 and IL-8 are not specific to PCa, their combination with PSA could potentially serve as an indicator of cancer stage. This intracellular staining serves as a preliminary step towards further analyses where these proteins will be assessed for their secretion patterns on PVDF membranes, aiming to correlate intracellular expression with extracellular secretion.

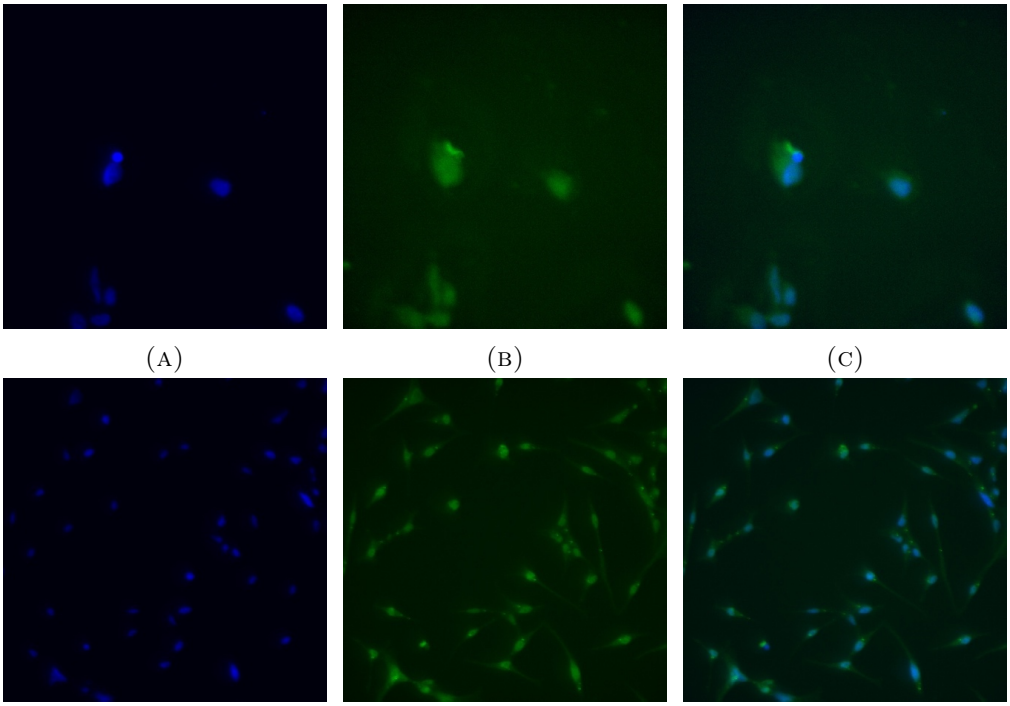

FIGURE 3.5: LnCAPs intracellular staining of the A) nucleus (DAPI in blue); B) PSA (FITC in green); C) overlay of nucleus and PSA; D) nucleus (DAPI); E) GAPDH (FITC); and F) overlay of nucleus and GAPDH

3.3 Visualisation of the cells using cytospin

To confirm the accuracy of cell sorting and validate the presence of each cell cycle phase, the Cytospin method was used to spin down the sorted PCa cells onto glass slides. Once deposited onto the slides, the cells were fixed using a mounting medium containing DAPI to stain the nuclei, thereby allowing us to visualize the DNA content and determine whether each sorted condition corresponded to the expected cell cycle phase.

Observations and Analysis:

- **G1 Phase Cells:** As shown in Figure 3-1, the cells sorted for the G1 phase appear predominantly as single cells with a single nucleus, consistent with cells that are in the initial growth phase of the cell cycle.
- **S Phase Cells:** The cells sorted for the S phase exhibit signs of DNA replication and are often seen growing or in the process of division. The DAPI staining highlights some nuclei that show indications of DNA synthesis and the early stages of cellular division.
- **G2/M Phase Cells:** The cells sorted for the G2/M phase display multiple nuclei or a single nucleus with doubled DNA content. Many of the cells appear to be on the verge of dividing into two cells, confirming that they are in the final stages of the cell cycle before mitosis.

Significance of Findings: These findings, shown in Figure 3.6, validate the accuracy of the cell sorting protocol and demonstrate that the Cytospin method effectively visualizes the sorted cells in their respective phases. The use of DAPI staining provides a clear view of the nuclear DNA content, enabling researchers to distinguish between different cell cycle phases based on nuclear morphology. This validation step is crucial for subsequent analyses that aim to correlate cell cycle phase with proteome secretion patterns in PCa cells.

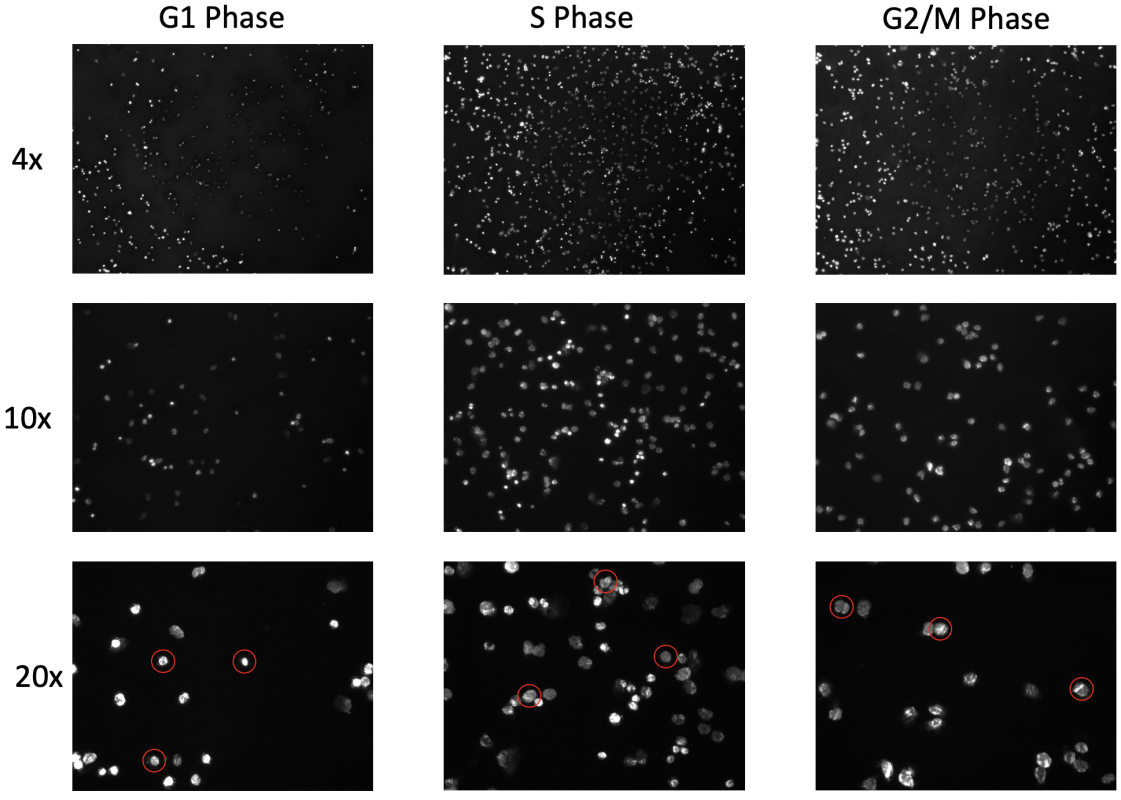

FIGURE 3.6: Microscopic images of sorted LnCAP cells spinned down using the cytospin and stained for DNA content with DAPI

3.4 Spotting device for multiplexing

To explore a multiplexing approach for analyzing protein secretion, a specialized spotting device was employed, as described in section 2.3.2. This device, illustrated in Figure 2.6, consists of 11 mini well chambers, each of which can be filled with a different antibody solution. The antibodies are then spotted onto a PVDF membrane, enabling the simultaneous analysis of various proteins on a single membrane.

For proof of concept, we utilized IgG-PE, an antibody that already contains a fluorophore, to assess the efficacy of the antibody coating process. The PVDF membrane was incubated with IgG-PE solutions placed in the spotting device chambers, and the antibody spotting was visualized using fluorescence imaging. As seen in Figure 3.7, the preliminary results indicate that the spotting device holds promise for multiplex protein analysis, as some spots were distinctly visible on the PVDF membrane, confirming successful antibody coating. However, the method did not yield consistent results across all chambers, with some spots appearing faint or inconsistent in intensity. This variability suggests that further optimization is required to ensure uniform antibody coating and reliable detection of protein secretion.

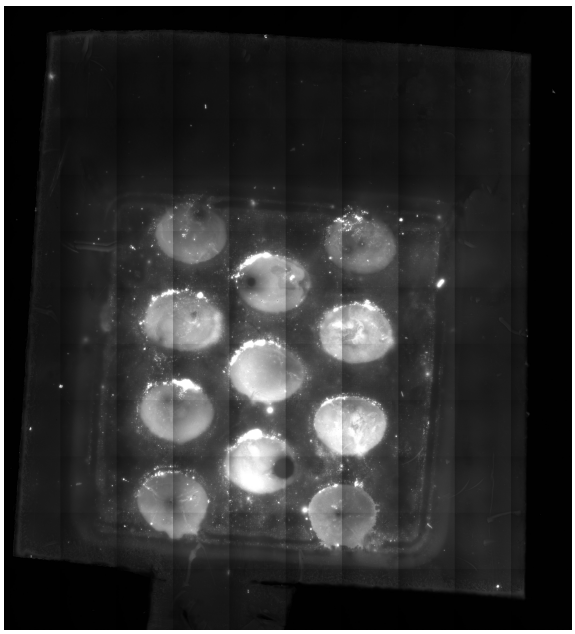

FIGURE 3.7: PVDF membrane stained with IgG-PE after 24 hour incubation, spotted with the spotting device described in section 2.3.2

In summary, while the spotting device offers a promising platform for multiplex protein analysis, especially for studying proteome secretion at a single-cell level, additional adjustments to the protocol are necessary to improve reproducibility and accuracy. These optimizations will be critical for achieving reliable and comprehensive analysis of multiple proteins on a single membrane.

3.5 Measuring PSA secretion from PCa's cell lines

To visualize and quantify proteome secretion, particularly PSA, cells from the PCa lines were seeded onto PVDF membranes. This process was designed to capture and analyze PSA secretion directly from the cells. The ELISpot assay was employed on the membranes

to detect and measure PSA secretion. After staining, the membranes were visualized using the VyCAP spot software, and the spots were further analyzed using ImageJ. In this experiment, the cells were seeded onto the PVDF membranes at a density of 5000 cells per membrane to provide a consistent starting point. Following the staining protocol, the VyCAP spot software enabled accurate visualization of PSA spots on the membranes, allowing us to identify and count individual spots indicative of PSA secretion.

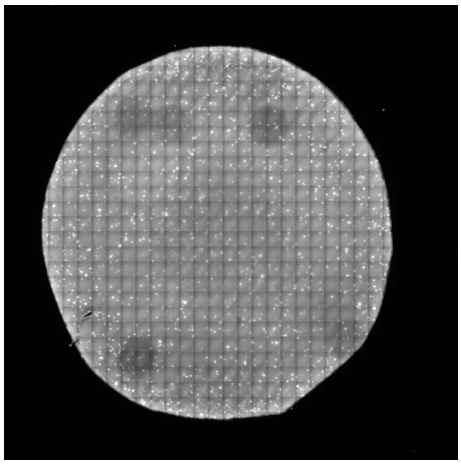

FIGURE 3.8: PVDF membrane with captured and stained PSA secretion from 5000 LnCAP cells

After sorting the cells into their respective phases, we evaluated the secretion patterns of PSA for each cell cycle phase (G1, S and G2/M). The images analyzed using ImageJ provided distinct secretion profiles across the different phases, as illustrated in Figure 3.9.

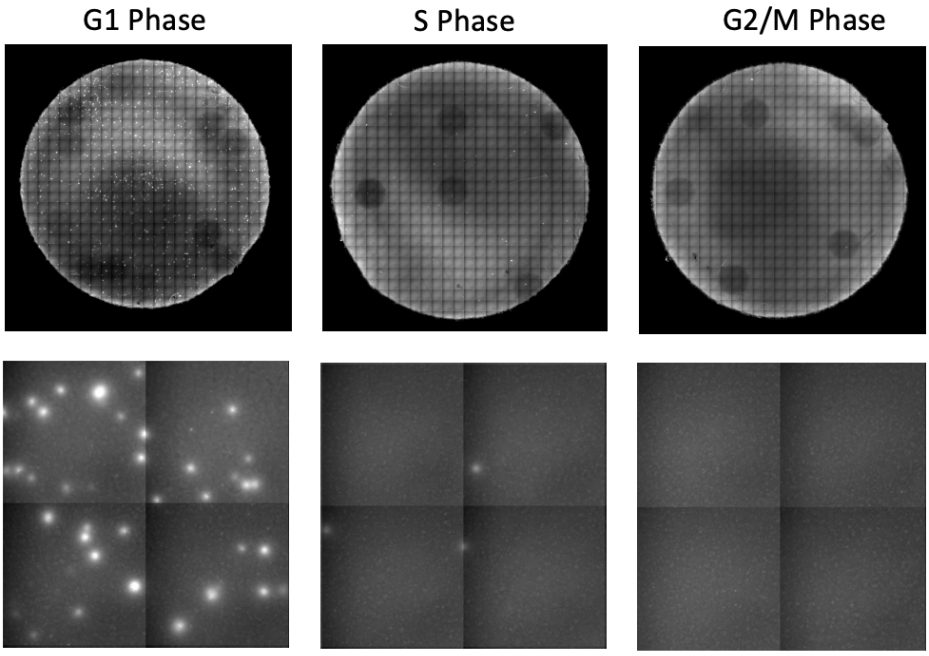

FIGURE 3.9: PVDF membranes with captured and stained PSA secretion from 5000 LnCAP sorted cells according to cell phase

From the analyzed images, it was evident that cells in the G1 phase were actively secreting PSA, as indicated by the distinct spots visible on the PVDF membranes. In contrast, cells sorted into the S and G2/M phases did not exhibit significant PSA secretion, with minimal or no spots detected on the membranes. These results underscore the importance of considering cell cycle phases when analyzing proteome secretion at a single-cell level. The findings suggest that PSA secretion is predominantly active during the G1 phase, while cells in theSand G2/M phases contribute negligibly. Understanding these variations can provide insights into the heterogeneity of PCa and aid in developing more precise diagnostic and therapeutic strategies.

3.6 Identification and sorting of cells in different cell cycle phases

To investigate the proteome secretion patterns across different cell cycle phases, PCa cells were harvested and sorted based on their DNA content using Fluorescence-Activated Cell Sorting (FACS). The cells were collected when they reached approximately 80% confluency, stained with Hoechst 33342 for 30 minutes on ice, and then analyzed using the FACS technique, see Figure 3.10.

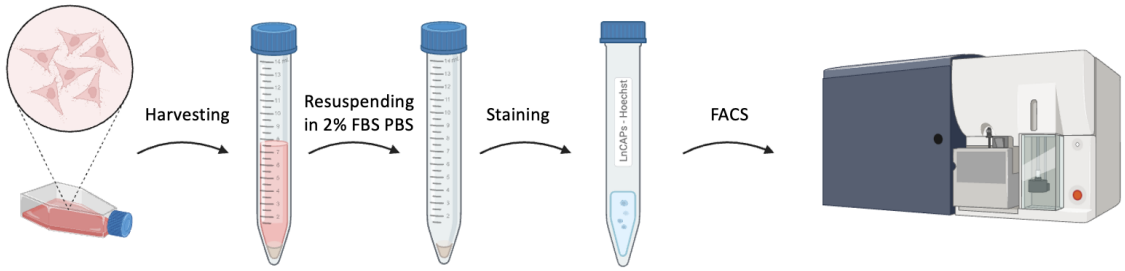

FIGURE 3.10: Workflow of cell preparation for FACS analysis

In the initial phase of the analysis, a negative control sample of unstained cells was measured to establish a baseline signal and to adjust the parameters of the FACS machine. This baseline measurement ensured that any background signals were accounted for, providing a reliable reference point for the subsequent analysis. Following this, the stained samples were analyzed by measuring the fluorescence of Hoechst 33342 at its specific wavelength. This enabled the identification of distinct peaks corresponding to the G1, and G2/M phases based on the DNA content of the cells. Using these peaks, the appropriate gates were set on the FACS machine to differentiate between the different cell cycle phases. After the gates were set, the cells were sorted into tubes according to their respective cell cycle phases. The sorted cells were then used for two main purposes. First, they were spun down onto glass slides using the Cytospin method to confirm their cell cycle phase and validate the sorting process, as described in section 3.3. Second, the cells were directly sorted into a 24-well plate containing pre-coated PVDF membranes for PSA secretion analysis. See Figure 3.11 for the schematic. The PVDF membranes were prepared following the protocol outlined in subsection 2.3.2.

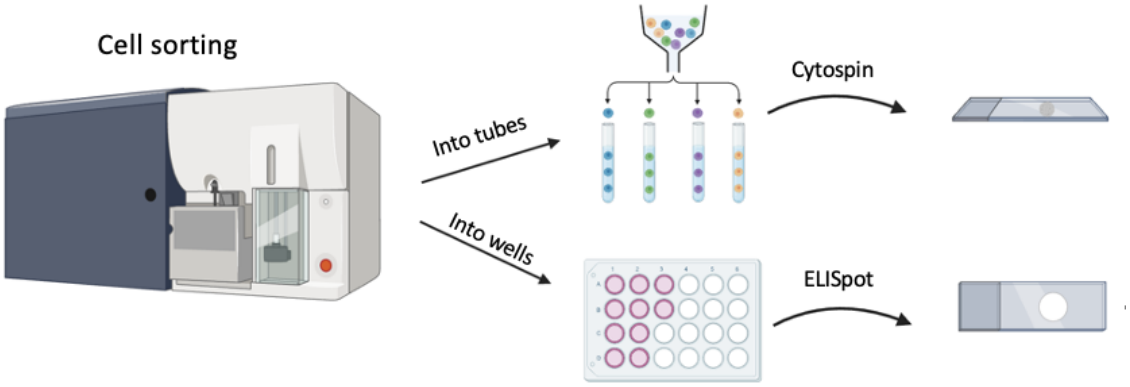

FIGURE 3.11: Workflow of cell sorting and analysis, depicting steps from sorting to application in cytospin and ELISpot assays

Once the cells were sorted and placed onto the membranes, they were incubated overnight to allow sufficient time for protein secretion. The next day, the membranes were analyzed using the ELISpot assay and visualized with the VyCAP spot software, as detailed in subsection 2.3.4. This setup enabled a comprehensive assessment of PSA secretion patterns across the different cell cycle phases (G1, S and G2/M).

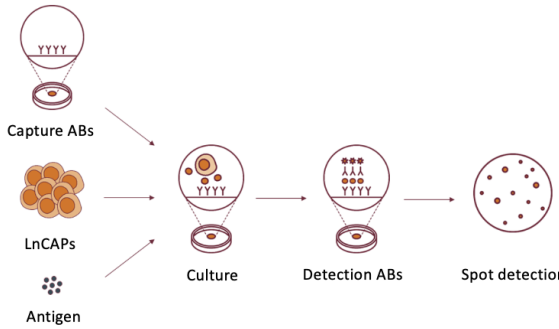

FIGURE 3.12: This figure illustrates the sequential steps involved in an ELISpot assay to detect specific protein secretion. The process begins with the capture antibodies (Abs) that are pre-coated on a PVDF membrane to bind specific antigens. Next, LnCAPs cells are cultured on the membrane, allowing them to secrete proteins such as antigens, which are captured by the antibodies. Following the culture phase, detection antibodies are added, which bind to the antigens. The final step, spot detection, involves visualizing these bound complexes, revealing the protein secretion profile of the LnCAPs cells in the form of discrete spots on the membrane. Each spot corresponds to the secretion activity of individual cells. [2])

The FACS analysis successfully identified distinct peaks corresponding to each cell cycle phase, enabling accurate sorting of cells into the G1, S and G2/M phases. Following the sorting process, the Cytospin measurement confirmed that the majority of cells in the G1 phase were predominantly single cells, while the S phase cells exhibited evidence of DNA replication, and the G2/M phase cells displayed characteristics indicative of division. The analysis of PSA secretion revealed that only cells in the G1 phase secreted significant levels of PSA, while cells in the S and G2/M phases did not secrete detectable amounts of the protein. Figure 3.12 depicts the steps of the protein detection on the membranes.

This finding aligns with the known biology of PCa cells, where PSA secretion is linked to specific cellular states. Understanding these patterns improves the interpretation of PSA levels in clinical diagnostics and underscores the need to consider cell cycle phases in single-cell proteome studies. In summary, the FACS sorting and subsequent analyses provided valuable insights into the heterogeneity of PSA secretion among PCa cells. These results underscore the importance of distinguishing cell cycle phases to obtain accurate and meaningful data on proteome secretion patterns.

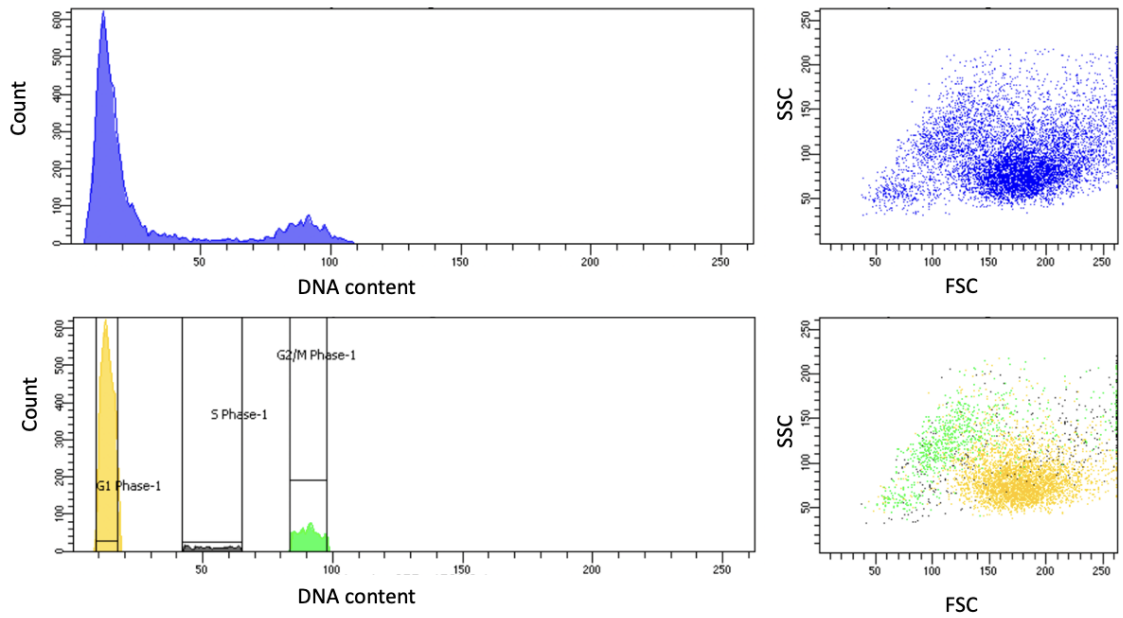

FIGURE 3.13: This figure presents flow cytometry results used to analyze cell cycle phases and cellular granularity in LnCAP cells. The left panels display histograms of DNA content with the initial plot showing a unimodal distribution indicative of a homogeneous population, and the subsequent plot segmented into G1, and G2/M phases, highlighted in yellow, green, and gray respectively. The right panels are scatter plots correlating Forward Scatter (FSC), which indicates cell size, with Side Scatter (SSC), which reflects internal complexity or granularity. The top scatter plot shows the entire cell population, while the bottom plot highlights cells gated from specific cell cycle phases, color-coded to match the histogram.

The flow cytometry analysis depicted in the Figure 3.13 was critical for identifying and quantifying the distribution of LnCAP cells across different cell cycle phases. By establishing gates on the DNA content histograms, we were able to effectively segregate cells in G1, S and G2/M phases, as indicated by the distinct peaks. This separation is essential for subsequent experiments, particularly for sorting cells based on their specific phase of the cell cycle. Following the identification of cell cycle phases, the sorted cells were used in downstream analyses to investigate phase-specific secretion patterns. This sorting is crucial for understanding how cellular behavior and secretion profiles vary with cell cycle progression, which can impact the understanding of secretion profiles at the single-cell level is crucial for unraveling complex cell cycle dynamics in cancer biology. The scatter plots further assisted in refining our selection process by allowing us to visually confirm the granularity and size of the cells, attributes that are often altered by cell cycle changes and can influence cellular functions including secretion. By utilizing both DNA content and

physical properties for gating, we ensured a more accurate and representative sorting of cells, thereby enhancing the reliability of subsequent analyses regarding cellular secretion.

3.7 Evaluation of Pharmacological Agents for Synchronization of Cells into the G1 Phase

In the experiments conducted to assess the efficacy of pharmacological agents in synchronizing cells into the G1 phase, no significant effects were observed. The experimental setup, as detailed in section 2.1 and subsection 2.3.3, involved varying cell seeding densities and performing multiple timepoint measurements (1, 3, 6, 18, 21, 24, and 48 hours). Despite the use of different concentrations of Ciclopirox olamine, Aphidicolin, and Palbociclib, the FACS analysis revealed that the majority of cells, including those in control groups, predominantly remained in the G1 phase, seen in the plots of Figure 3.14 and Figure 3.15. This uniformity in cell cycle phase across treated and control samples suggests that the pharmacological agents did not effectively induce synchronization. Several factors could be responsible for this outcome. First, the cells may not have adapted well to the well plate environment, potentially impacting their responsiveness to the treatments. Additionally, there might have been insufficient time for cells to adhere properly within the wells before the initiation of treatment, affecting the drug's efficacy. It is also possible that the natural cell cycle dynamics of the cell lines used did not align well with the expected intervention points of the pharmacological agents. Further investigation into these aspects could help in optimizing the experimental conditions and achieving more discernible effects on cell cycle synchronization.

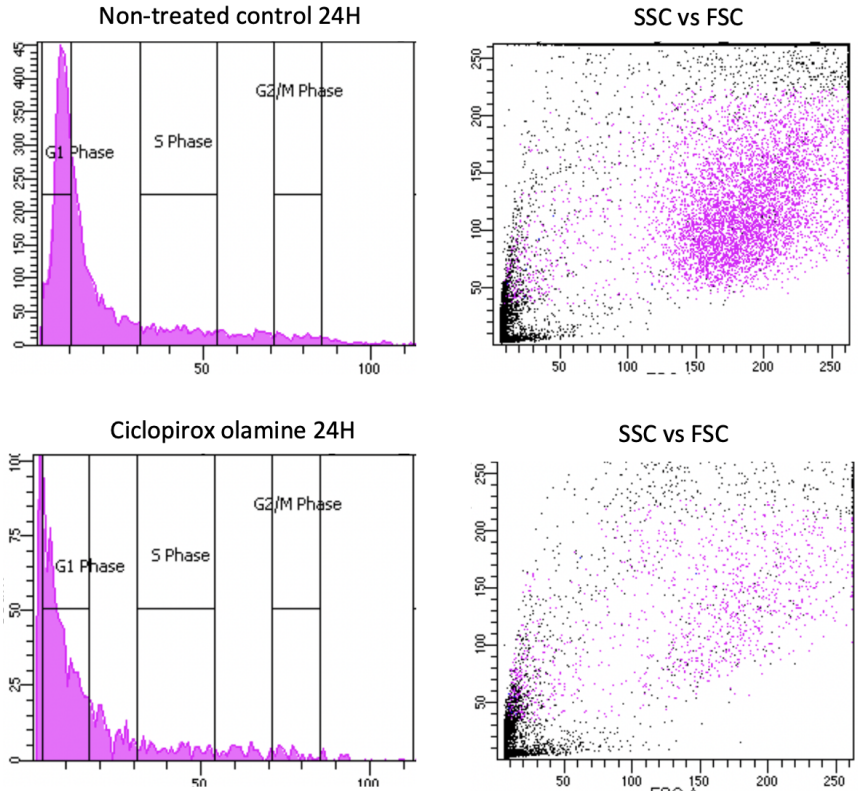

FIGURE 3.14: FACS analysis of Ciclopirox olamine effect on LnCAP cells after 24 hour incubation

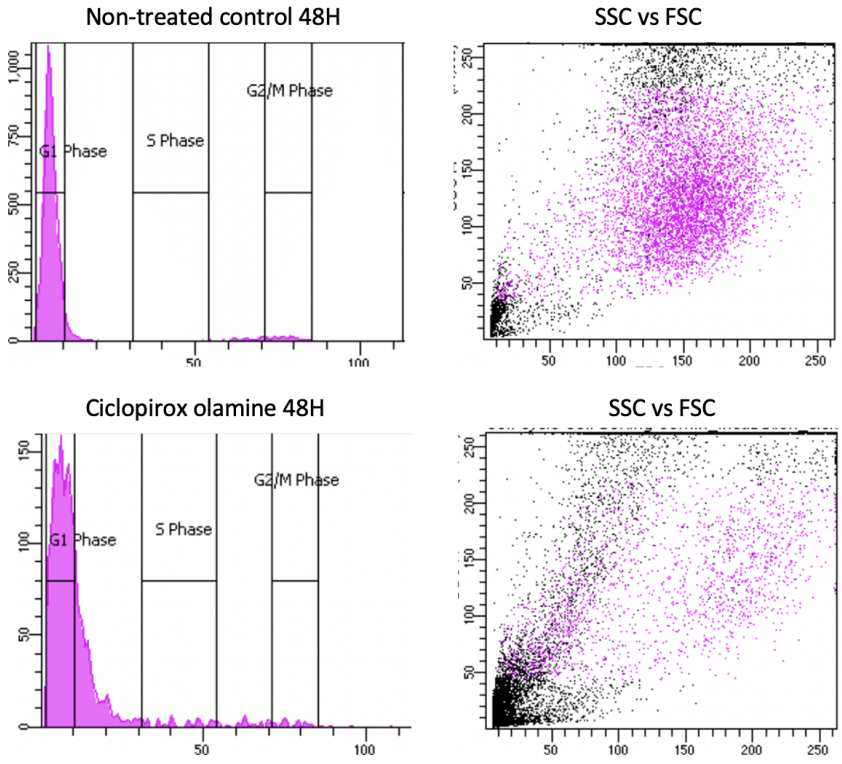

FIGURE 3.15: FACS analysis of Ciclopirox olamine effect on LnCAP cells after 48 hour incubation

3.8 PLL synthesis and NMR

PLL is utilized in research primarily because it exhibits strong adsorption properties on a variety of metal oxide surfaces, which is vital for the immobilization of biomolecules on biosensor surfaces. The use of PLL enhances the functionalization of these surfaces, allowing for a controlled and efficient binding of biomolecules. This ensures that the biosensors maintain high sensitivity and specificity in detecting biological targets. Furthermore, PLL's ability to form multivalent electrostatic interactions facilitates the stable attachment of functional groups, which is crucial for achieving consistent biosensor performance. This makes PLL an invaluable component in the development of advanced biosensing platforms aimed at diagnosing and monitoring diseases [21].

To explore the attachment efficiency and specificity of different PLL derivatives on Pt-plated electrodes, we synthesized PLL-OEG-Biotin 4%, PLL-OEG-Biotin 1%, and PLL-OEG. These derivatives were crucial for understanding their impact on biomarker detection and minimizing non-specific binding. Figure 3.16 depicts the customised options of PLL modified molecule possibilities. The incorporation of oligoethylene glycol (OEG) in these derivatives is specifically due to its antifouling properties, which help to reduce undesirable protein adsorption and surface fouling, thus enhancing the sensitivity and selectivity of the sensors. Figure 3.17 depicts the schematic of PLL modified surface including the antifouling groups of OEG.

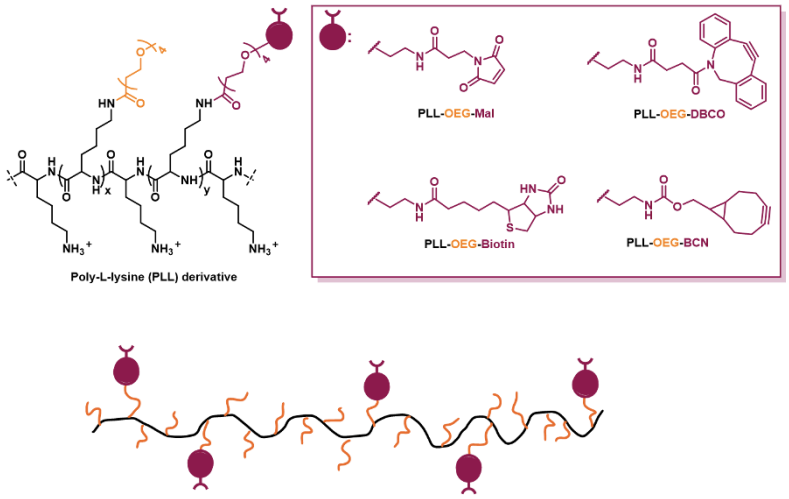

FIGURE 3.16: The diagram illustrates the structural modifications of Poly-L-Lysine (PLL) to create different derivatives for targeted bioconjugation applications. It includes the base structure of a PLL derivative, followed by several functionalized forms: PLL-OEG-Mal (maleimide), PLL-OEG-DBCO (dibenzocyclooctyne), PLL-OEG-Biotin, and PLL-OEG-BCN (bicyclo[6.1.0]nonyne). Each derivative is designed for specific reactive functionalities, facilitating the conjugation to various biomolecules or surfaces, enhancing the versatility of PLL in biomedical research and development (figure provided by Dr. Sevil Sahin).

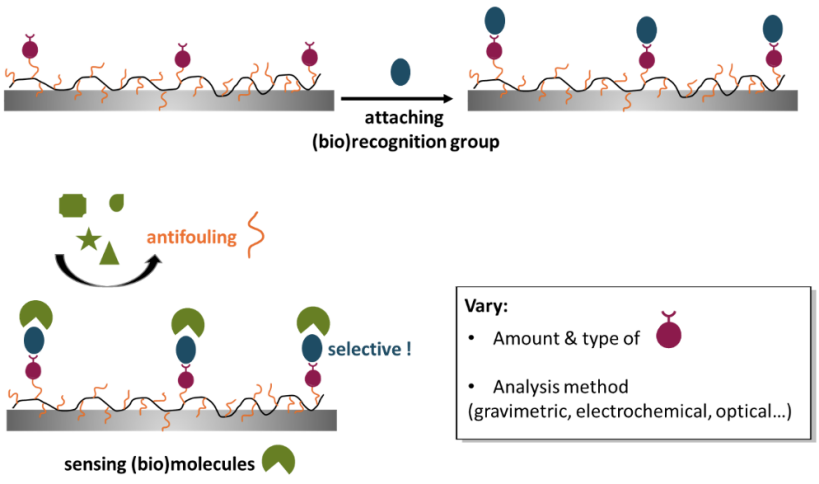

FIGURE 3.17: This diagram outlines the process of modifying surfaces for targeted biomolecule detection. It starts with attaching functional groups to the surface, followed by linking specific (bio)recognition molecules. These modifications aim to achieve selective sensing while incorporating antifouling properties to reduce unspecific binding. The figure also highlights variables like the type and amount of recognition molecules and detection methods (e.g., electrochemical, optical). (figure provided by Dr. Sevil Sahin).

Synthesis Process: The synthesis of the PLL derivatives followed the protocol outlined in subsection 2.4.1. Initially, a stock solution of 10 mg/mL poly-L-lysine (PLL) was prepared to serve as the base for all derivatives. For the PLL-OEG-Biotin derivatives, we synthesized two variants by varying the proportion of biotinylated OEG-NHS ester (0.25 M in DMSO) relative to the PLL base. A consistent amount of OEG-NHS ester was mixed with PLL to obtain a stable PLL-OEG backbone, maintaining a 30% OEG concentration for its optimal antifouling properties. Subsequently, biotinylated OEG-NHS ester was added to achieve different biotin concentrations, see Figure 3.18 for the chemical schematic:

- **PLL-OEG-Biotin 4%:** 4% of the total OEG content was biotinylated.
- **PLL-OEG-Biotin 1%:** 1% of the total OEG content was biotinylated.

The mixtures were stirred vigorously for 4 hours to ensure complete reaction, followed by dialysis to remove unreacted reagents and freeze-drying for storage. Similarly, the PLL-OEG derivative was synthesized without biotin to study non-specific binding. After stirring for 4 hours, this derivative also underwent dialysis and freeze-drying.

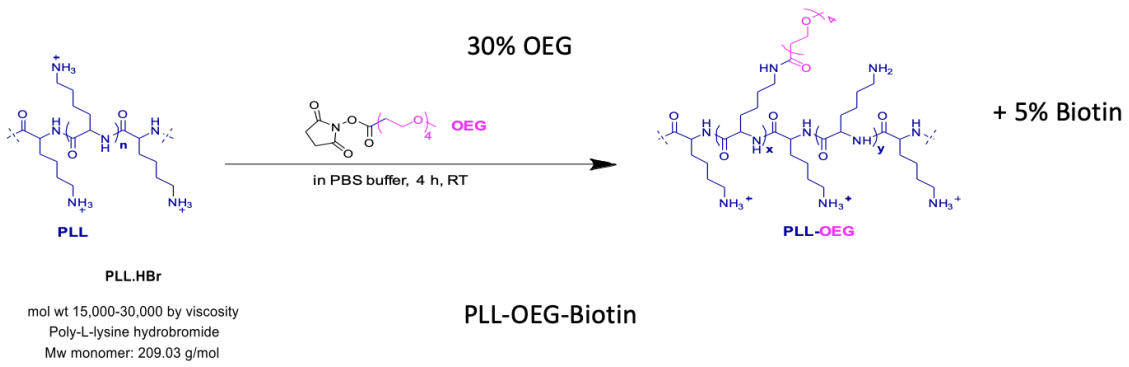

FIGURE 3.18: This figure depicts the synthesis process of PLL-OEG-Biotin from PLL. Initially, PLL is reacted with OEG (Oligoethylene glycol) to form PLL-OEG, representing 30% of the final compound. Subsequently, 5% biotin is added to the PLL-OEG to create PLL-OEG-Biotin. The reaction occurs in PBS buffer at room temperature over four hours. The structural changes at each step are illustrated, showing the incorporation of OEG and biotin into the PLL backbone, transforming it into a functionalized polymer suitable for biosensing applications (figure provided by Dr. Sevil Sahin, July 2023).

Purpose of Different PLL Derivatives : The variation in the proportion of biotinylated OEG aimed to assess the effect of different biotin concentrations on attachment efficiency and specificity. The higher proportion of biotin in the PLL-OEG-Biotin 4% derivative was expected to enhance attachment due to increased biotin-streptavidin binding. In contrast, the lower biotin concentration in the PLL-OEG-Biotin 1% derivative aimed to reduce non-specific interactions while maintaining adequate attachment. Meanwhile, the PLL-OEG derivative served as a control to evaluate non-specific binding. Since it lacks biotin, it was expected that the PLL-OEG derivative would not specifically interact with streptavidin, providing a baseline for non-specific adsorption.

NMR spectroscopy and Findings : After synthesis, the PLL derivatives were characterized using NMR spectroscopy to confirm the successful conjugation of the biotinylated

OEG-NHS ester to the PLL backbone. For each derivative, distinct peaks were observed in the 1H NMR spectra, allowing for the identification of the molecular structures and verification of the conjugation. The characteristic peaks of the biotinylated OEG confirmed its presence in the PLL-OEG-Biotin derivatives, whereas the PLL-OEG spectrum showed no such peaks, as expected. Further validation using QCM-D demonstrated that both PLL-OEG-Biotin derivatives exhibited specific binding to streptavidin-coated surfaces, with the PLL-OEG-Biotin 4% derivative showing stronger attachment compared to the PLL-OEG-Biotin 1% derivative. In contrast, the PLL-OEG derivative showed negligible binding to streptavidin-coated surfaces, confirming the specificity of the biotin-streptavidin interaction and the effectiveness of the PLL-OEG-Biotin derivatives. In summary, the synthesis and characterization of these derivatives provided valuable insights into the importance of biotin concentration in attachment efficiency and the necessity of controlling non-specific binding in electrochemical detection assays.

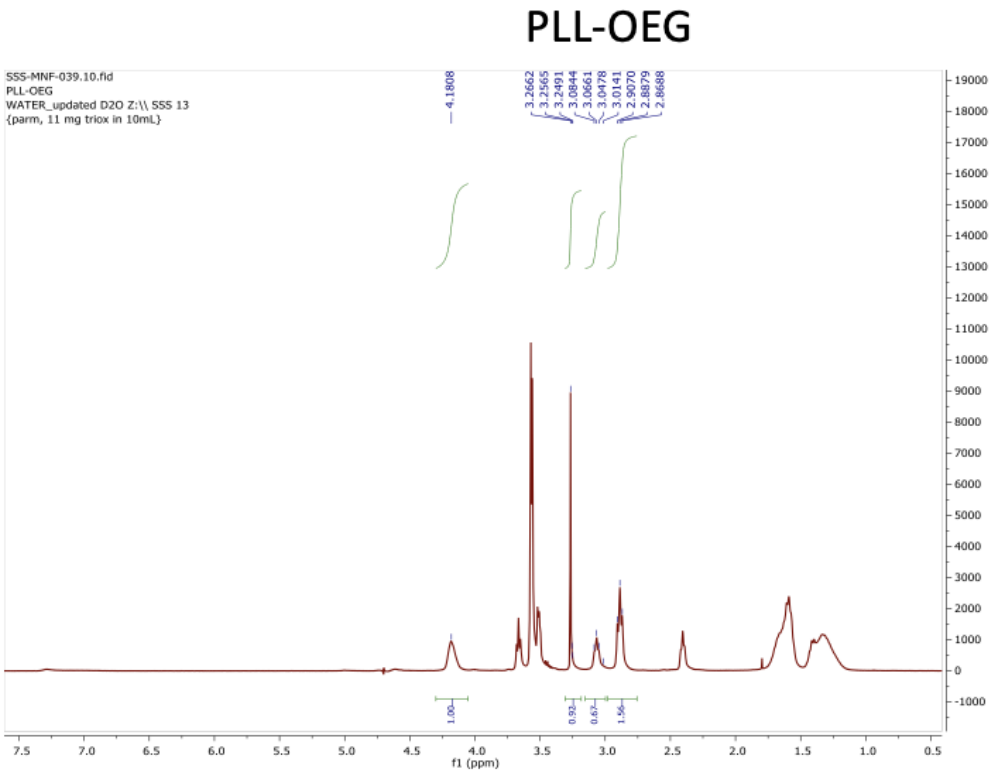

FIGURE 3.19: This figure presents the NMR spectrum of PLL-OEG, demonstrating the characteristic peaks corresponding to different protons in the polymer structure. The spectrum was obtained using water-suppressed D_2O as a solvent, with a concentration of the sample at 1 mg/mL. Key peaks are labeled with their respective chemical shift values (in ppm), providing insights into the molecular structure of PLL-OEG. This NMR analysis aids in confirming the chemical modification of poly-L-lysine with oligoethylene glycol (OEG), indicated by specific shifts and peak patterns associated with the OEG component within the polymer backbone.

This NMR spectrum of PLL-OEG found in Figure 3.19 illustrates several distinct peaks, indicating the chemical environment of protons within the molecule, refer to Figure 3.21 see which chemical group each peak represents:

- **Peak around 3.7 ppm:** Represents the methylene protons (-CH2-) in the oligoethy-

lene glycol (OEG) chains. This region typically shows peaks due to the flexible, repeating ether units in the OEG.

- **Peaks between 2.0 and 3.0 ppm:** Likely correspond to the backbone methylene protons adjacent to the amine groups in the poly-L-lysine structure.
- **Sharp peaks around 1.0 to 2.0 ppm:** These could be associated with the methylene groups further along the PLL chain, away from the more reactive sites of substitution.

Each peak's intensity and position provide critical information about the environment of these protons and the successful grafting of OEG and biotin groups onto the PLL backbone. This detailed peak analysis is essential for verifying the structure of the synthesized PLL-OEG and its expected modifications.

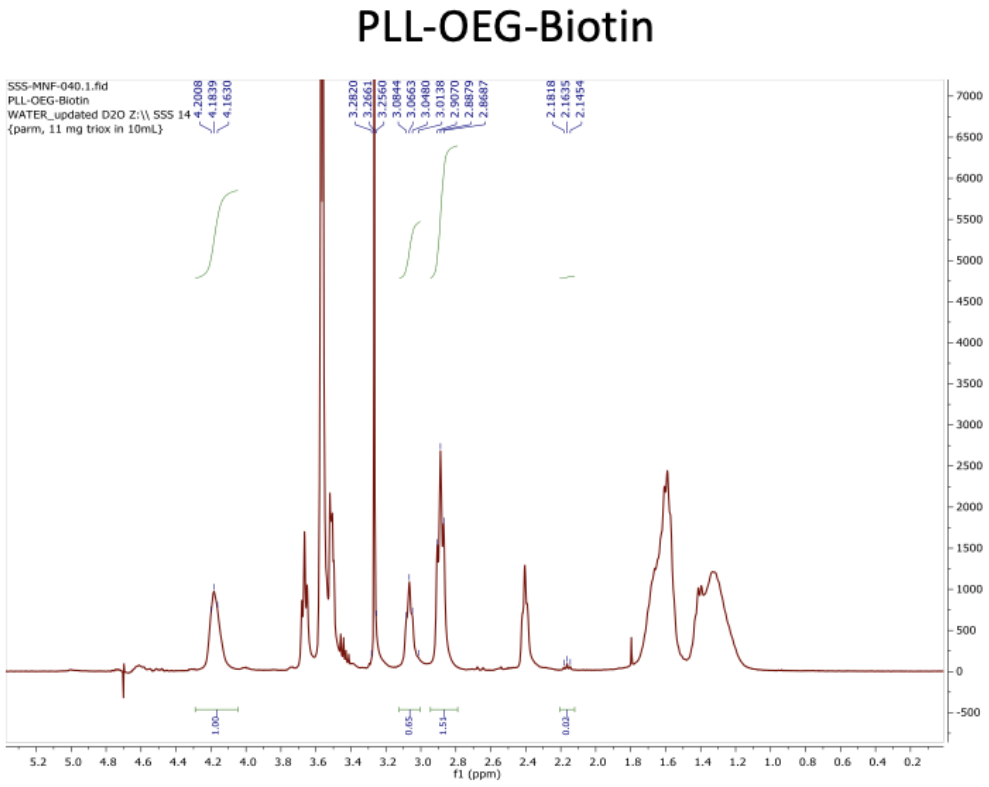

FIGURE 3.20: This figure displays the NMR spectrum of PLL-OEG-Biotin, highlighting the chemical shifts associated with various atomic environments within the molecule. The spectrum is rich with information that reflects the chemical structure and the successful incorporation of biotin and oligoethylene glycol (OEG) into the PLL backbone.

Figure 3.20 shows the NMR spectrum of PLL-OEG-Biotin illustrating the distinct peaks indicating the chemical environment of protons within this molecule:

- **Peaks around 4.2 to 4.5 ppm:** These peaks typically correspond to the methylene protons adjacent to the oxygen in the ether linkages of the OEG. Their relatively downfield shift compared to simple alkyl chains indicates the influence of the electronegative oxygen atoms.

- **Peaks at 3.0 to 3.8 ppm:** These peaks are likely related to the protons of the OEG backbone. The multiplicity and pattern suggest flexibility in the polymer chain, indicating good solubility and potential for effective biotin conjugation.
- **Sharp peaks at 1.2 to 2.2 ppm:** These represent the backbone methylene groups of PLL. These protons are typically more shielded and appear upfield due to their distance from the more electronegative groups.
- **Lower intensity peaks near 2.8 ppm:** These could be associated with the protons near the biotin moiety, indicating successful conjugation. The integration and splitting patterns of these peaks would be crucial for confirming the presence and environment of biotin within the PLL structure.

This spectrum is an essential tool for confirming the molecular structure of PLL-OEG-Biotin and for ensuring the functionality of the biotin conjugation, which is critical for subsequent biomedical applications.

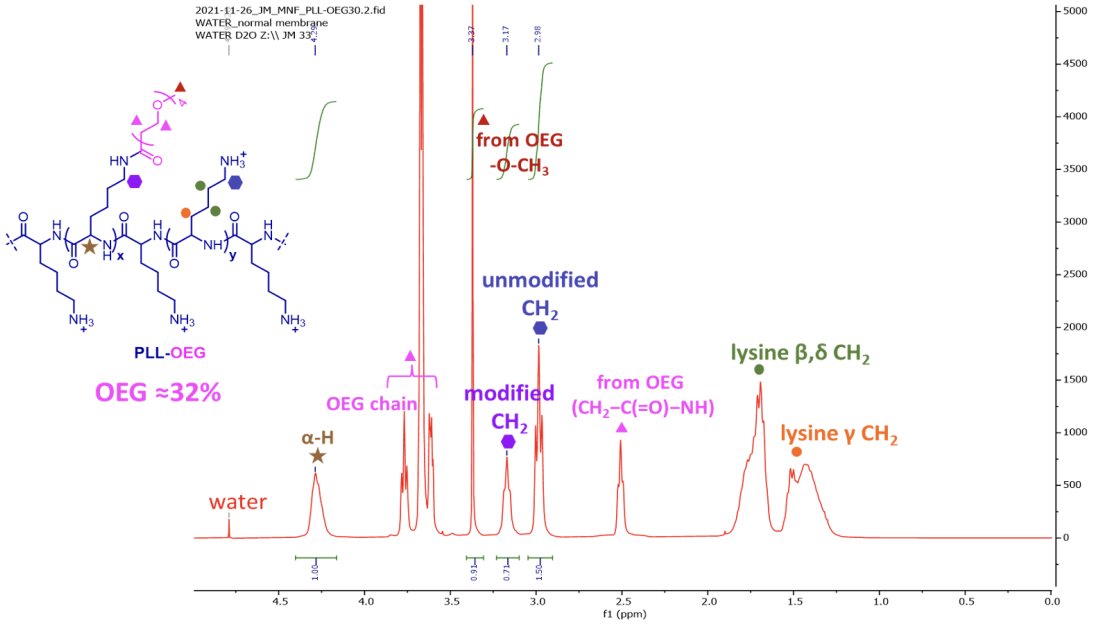

FIGURE 3.21: Reference figure that displays the NMR spectrum of PLL-OEG-Biotin, highlighting the chemical shifts associated with various atomic environments within the molecule. The spectrum is rich with information that reflects the chemical structure and the successful incorporation of biotin and oligoethylene glycol (OEG) into the PLL backbone. This figure describes each peak and the relevant molecules that each peak represents (figure provided by Dr. Sevil Sahin).

3.9 QCM-D experiments

The attachment efficiency and specificity of the synthesized PLL derivatives were validated using Quartz Crystal Microbalance with Dissipation Monitoring (QCM-D). The primary goal was to evaluate the selective binding capabilities of each derivative to the Pt-plated surface and subsequently interact with streptavidin, antibodies, and target proteins.

Attachment of PLL Derivatives: In the initial phase of the validation, the PLL derivatives (PLL, PLL-OEG, PLL-OEG-Biotin 4%, and PLL-OEG-Biotin 1%) were tested for their ability to attach to Pt-plated surfaces. The QCM-D data confirmed that all derivatives successfully adhered to the platinum surface, as indicated by a decrease in frequency and an increase in dissipation. In a QCM-D plot, a decrease in frequency (Δf) signifies mass gain on the surface due to the attachment of the derivatives. The increase in dissipation (ΔD) reflects changes in the viscoelastic properties of the layer, indicating the formation of a stable layer on the surface that provides a suitable foundation for further interactions.

The QCM-D graph in Figure 3.22a displays the dynamic monitoring of frequency (Hz) and dissipation (ppm) changes over time (minutes) for a PLL coated surface. Initially, the system stabilization with Phosphate-Buffered Saline (PBS) leads to a sharp decrease in frequency, marked by a shift of approximately 16 Hz, indicating the specific attachment of PLL to the surface. This primary frequency drop is attributed to the adsorption of PLL molecules forming a stable layer on the sensor's surface. After the PLL adsorption, the system undergoes a rinsing phase with PBS to remove any non-specifically bound molecules, ensuring that only firmly attached PLL remains on the surface. Following the rinse, streptavidin is introduced into the system, resulting in a minor frequency shift of about 3 Hz. This change is likely due to unspecific binding or inherent system frequency fluctuations since there is no biotin present on the PLL layer to facilitate specific binding. The minimal change in dissipation throughout this process supports the conclusion of a rigid and stable PLL layer. The overall stability observed post-streptavidin addition and the minimal dissipation changes underscore the integrity of the PLL coating, confirming its functionality for potential biomolecular interactions on the surface. This setup effectively demonstrates the use of QCM-D in verifying the selective binding capabilities of surface coatings in the absence of target-specific interactions.

This QCM-D graph in Figure 3.22b illustrates the real-time monitoring of frequency (Hz) and dissipation (ppm) changes for a PLL-OEG-Biotin coated surface. The experiment begins with system stabilization using PBS, which results in an initial frequency drop of approximately 18 Hz. This decrease, slightly greater than observed with PLL alone, signifies the effective functionalization of the surface with the biotinylated PLL-OEG compound. Following the PLL-OEG-Biotin adsorption and PBS rinse to remove unbound elements, streptavidin is introduced into the system, resulting in a significant frequency shift of approximately 32 Hz. This pronounced change, alongside an increase in dissipation, indicates substantial binding interactions between the biotin on the PLL-OEG and the streptavidin. The rise in dissipation points to a less rigid molecular layer compared to PLL alone, suggesting that the dynamic nature of the biotin-streptavidin binding affects the structural integrity of the surface layer. The notable changes in both frequency and dissipation upon streptavidin introduction validate the specific attachment of PLL-OEG-Biotin and streptavidin, confirming the functionality and enhanced molecular binding capabilities of the biotin-modified surface. This successful demonstration of specific biotin-streptavidin interaction highlights the potential of PLL-OEG-Biotin as an effective surface coating for biosensing applications.

These figures illustrate the utility of QCM-D in monitoring real-time interactions and modifications on sensor surfaces, providing quantitative data on the binding efficiency and stability of functional layers.

Specific Binding of Streptavidin: After establishing the base PLL layers, streptavidin was introduced to the surfaces to verify its selective binding to the biotinylated

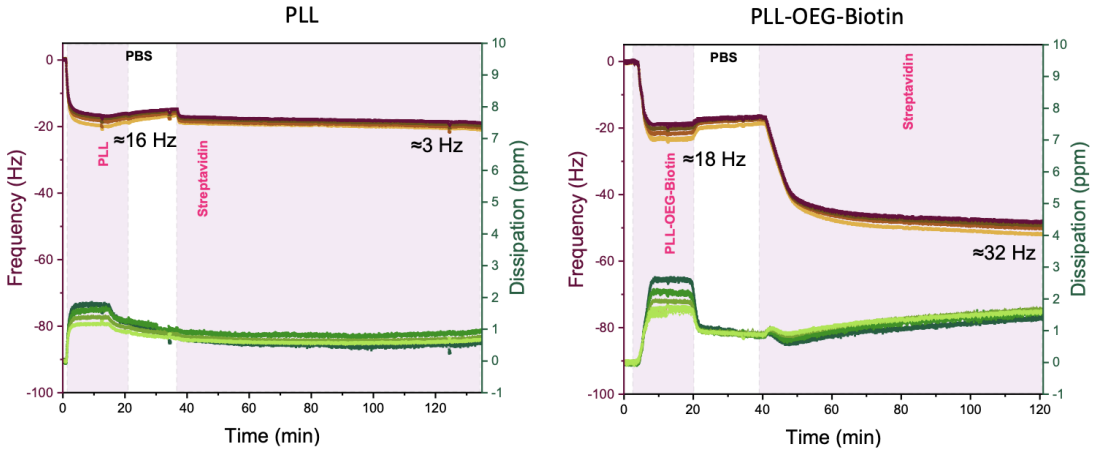

(A) (B)

FIGURE 3.22: QCM-D analysis of Streptavidin binding on (A) PLL and (B) PLL-OEG-Biotin functionalized Pt surface electrode

PLL derivatives. The QCM-D data revealed that streptavidin specifically attached to the PLL-OEG-Biotin 4% and PLL-OEG-Biotin 1% derivatives, indicating the specificity of the biotin-streptavidin interaction. This specific binding was demonstrated by a further decrease in frequency (mass gain) and an increase in dissipation, suggesting a flexible but stable attachment. Conversely, no significant attachment was observed on the PLL and PLL-OEG surfaces, validating the absence of non-specific binding.

According to Hamming and Huskens [15], the density of streptavidin on biotinylated surfaces can be quantitatively predicted, allowing for precise control over the functionalization of biosensor surfaces. Their findings underscore the importance of controlling streptavidin coverage, which directly impacts the performance and specificity of biotin-streptavidin interactions in various biosensing applications. This aligns with our observations of specific streptavidin attachment and supports the robustness of our surface functionalization approach.

Attachment of Anti-EpCAM Antibody: Following streptavidin attachment, the anti-EpCAM antibody was introduced to the biotinylated PLL layers. The QCM-D data indicated successful binding of anti-EpCAM to the PLL-OEG-Biotin surfaces, as evidenced by a further decrease in frequency and increase in dissipation. This confirmed that the antibody specifically attached to the streptavidin-coated surface, enabling the subsequent detection of the EpCAM protein.

Figure 3.23 depicts the QCM-D monitoring of anti-EpCAM antibody binding on different surface modifications. Panel (A) shows the frequency and dissipation responses when anti-EpCAM is introduced to a PLL-coated surface without biotin modification, illustrating negligible frequency changes indicative of minimal nonspecific binding. Panel (B) explores the interaction of anti-EpCAM with a PLL-OEG-Biotin modified surface, demonstrating a distinct frequency shift (of approximately 12Hz) as the antibody specifically binds to the biotinylated surface.

Figure 3.23 illustrates the step-by-step functionalization of PLL-OEG-Biotin surfaces and subsequent specific antibody binding, monitored using QCM-D. The graph depicts the initial PBS stabilization, followed by the binding of PLL-OEG-Biotin which results in a frequency shift of approximately 17 Hz. The introduction of streptavidin to the function-

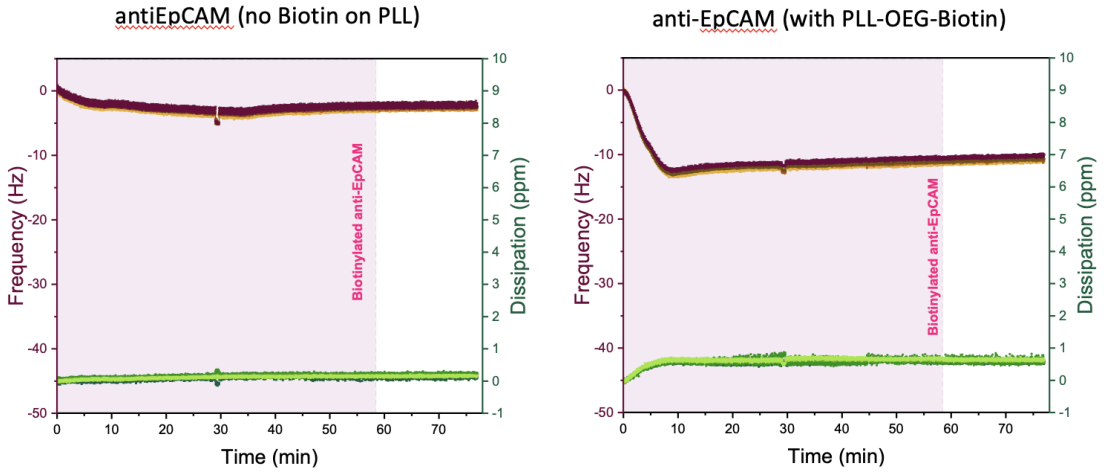

FIGURE 3.23: QCM-D Analysis of anti-EpCAM Antibody Binding to (A) PLL and (B) PLL-OEG-Biotin modified surface after the modification with streptavidin

alized surface leads to a further frequency shift of about 30 Hz, indicating strong biotin-streptavidin interaction. After a subsequent PBS wash to remove unbound molecules, anti-EpCAM antibody is introduced, causing an additional frequency shift of around 10 Hz, which signifies the specific binding of the antibody to the biotinylated surface. The dissipation data across these steps show minimal fluctuations, underscoring the stability and rigidity of the molecular layers formed during each binding event.

Dissociation Constant Analysis: The dissociation constant (Kd) of anti-EpCAM binding to EpCAM provides a measure of the antibody's affinity for the antigen. A lower Kd value indicates stronger binding. Previous studies have reported the dissociation constant of anti-EpCAM to EpCAM to be around 2.3 nM , which indicates a high-affinity interaction.

Validation of EpCAM Protein Binding: To complete the validation process, the EpCAM protein was introduced to the surface to assess its binding to the anti-EpCAM antibody. The QCM-D data showed a significant decrease in frequency and a concurrent increase in dissipation, confirming the successful attachment of the EpCAM protein to the surface. The increase in dissipation indicated that the EpCAM protein was not rigidly bound but formed a flexible layer on the surface.

The QCM-D validation provided comprehensive insights into the attachment specificity of the synthesized PLL derivatives. The results showed that the PLL derivatives could effectively bind to the Pt-plated surface, providing a stable platform for further interactions. Streptavidin was observed to selectively bind only to the biotinylated PLL derivatives (PLL-OEG-Biotin 4% and PLL-OEG-Biotin 1%), proving the specificity of the biotin-streptavidin interaction and the absence of non-specific binding. Moreover, the anti-EpCAM antibody and the EpCAM protein were both able to attach specifically to the biotinylated PLL derivatives, demonstrating the suitability of these derivatives for specific protein detection. The differences between PLL-OEG-Biotin 4% and PLL-OEG-Biotin 1% in streptavidin attachment were minimal but noticeable, with the higher biotin concentration (4%) providing a slightly stronger attachment. The PLL-OEG derivative served as an excellent control to confirm the absence of non-specific binding, as it lacked biotin

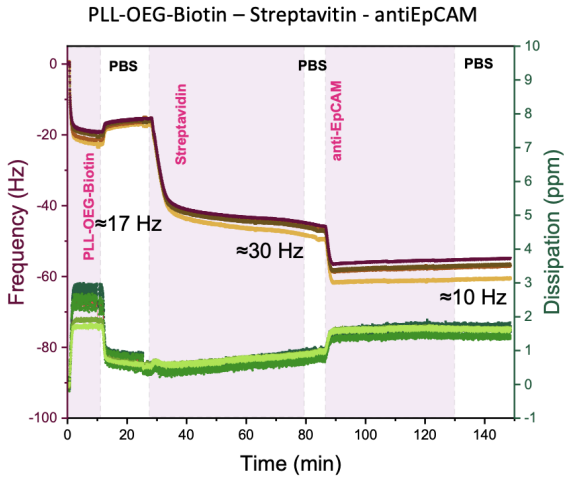

FIGURE 3.24: Comprehensive QCM-D analysis of PLL-OEG-Biotin surface functionalization and specific anti-EpCAM antibody binding

and showed negligible interaction with streptavidin. In summary, the QCM-D validation successfully demonstrated the specificity and attachment efficiency of the PLL derivatives, making them ideal candidates for selective protein detection with minimal non-specific binding.

The data from the QCM-D measurements are critical in demonstrating the specificity and effectiveness of surface functionalization using biotinylated PLL derivatives for specific biomolecular interactions.

Discussion of QCM-D Results

Specificity and Negligible Nonspecific Binding

- **PLL and PLL-OEG Baseline:** The minimal frequency shifts observed with PLL (average ≈ 3.0 Hz) and PLL-OEG (average ≈ 1.7 Hz) when exposed to Streptavidin suggest negligible nonspecific binding. These controls are crucial as they establish that without biotin, Streptavidin does not adhere significantly to the surfaces, underlining the specificity of the biotin-streptavidin interaction on modified surfaces.

Biotin-Streptavidin Specific Binding

- **Biotinylated Derivatives (PLL-OEG-Biotin 4% and 1%):** Both derivatives show significant frequency shifts upon Streptavidin introduction (average ≈ 30.0 Hz for 4% and ≈ 20.7 Hz for 1%), which are substantially higher compared to the controls. This directly correlates to the presence of biotin and confirms the high specificity and effective binding capacity of Streptavidin to biotin-modified surfaces. The low standard deviations indicate consistent functionalization and reliable Streptavidin binding.

Specific Antibody-Antigen Interactions

- **Anti-EpCAM Binding:** The considerable shifts observed for PLL-OEG-Biotin 4% (average ≈ 13.8 Hz) and PLL-OEG-Biotin 1% (average ≈ 21.2 Hz) upon anti-EpCAM application illustrate the effective capture and specific detection of this

cancer marker. These results not only validate the biotin-streptavidin layer as a foundational binding platform but also highlight its utility in specifically detecting targeted antigens through antibody interactions.

Conclusion The data discussed, support the hypothesized efficacy of the surface functionalization strategy, demonstrating that:

1. **There is minimal to no nonspecific binding on PLL and PLL-OEG surfaces.**
2. **Streptavidin binding is highly specific to the biotinylated PLL derivatives, and the density of biotin influences the degree of interaction.**
3. **Biotinylated surfaces effectively capture and specifically detect targeted antibodies, exemplified by anti-EpCAM.**

These findings conclusively demonstrate the potential of these surface functionalizations in biosensing applications, where the specificity of interaction is paramount. By ensuring that only the targeted interactions occur, these functionalized surfaces can be further utilized for the detection of specific analytes and biomarkers The results discussed can be found in the supplementary data in Table K.1 in the Appendix K.

3.10 Cyclic Voltammetry validation

Initial Testing with Methylene Blue as a Redox Mediator: Cyclic Voltammetry (CV) measurements were conducted to analyze the binding of the EpCAM protein on functionalized Pt-plated electrodes. Initially, various concentrations of methylene blue, a redox mediator, were tested on bare electrodes to establish a baseline. Methylene blue acts as an electron shuttle between the electrode surface and the electrolyte solution, enhancing the detection of electrochemical signals. This redox mediator is essential because it facilitates electron transfer, providing a measurable signal that corresponds to the accessibility of the electrode surface. The CV data from these tests demonstrated distinct signals based on the concentration of methylene blue, with higher concentrations producing stronger signals. This result confirmed that the signal intensity changes with different levels of the redox mediator reaching the electrode surface.

Figure 3.25 displays cyclic voltammetry measurements of methylene blue at different concentrations on Pt-plated electrodes. The CV curves illustrate the redox behavior of methylene blue across a range of applied potentials. The curves labeled Pt_bare_MB_0.37, Pt_bare_MB_0.75, and Pt_bare_MB_1.5 correspond to increasing concentrations of methylene blue, depicted by progressively higher peaks in current response. This graph highlights the electrochemical activity of methylene blue as a function of its concentration, showing marked peaks at specific potentials, which represent the oxidation and reduction events of the redox mediator on the electrode surface.

Measuring EpCAM Protein Binding: After baseline testing with methylene blue, the functionalized electrodes were prepared for measuring the attachment of EpCAM protein. The electrodes were coated with the PLL-OEG-Biotin derivatives and then incubated with streptavidin and anti-EpCAM antibody, following the protocol described in subsection 2.4.4.

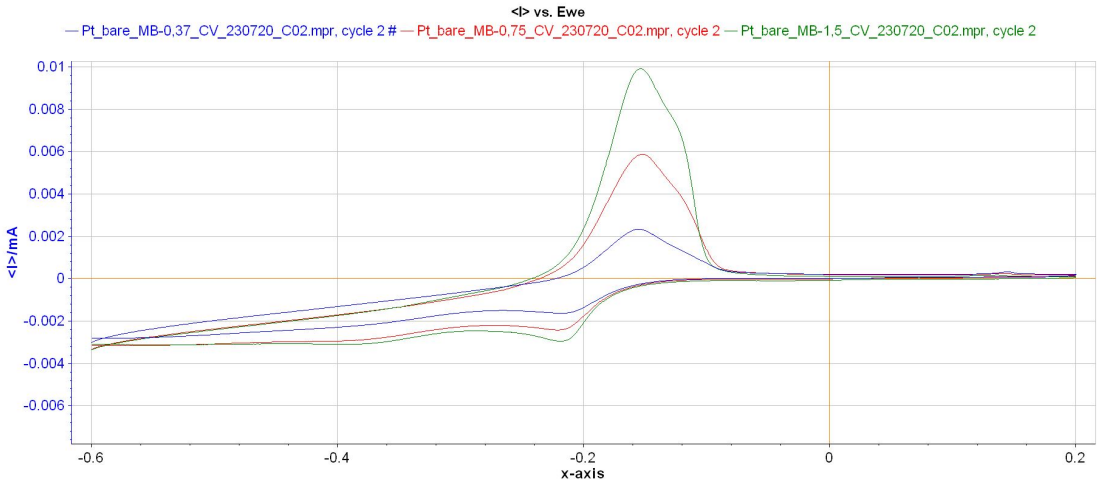

FIGURE 3.25: Cyclic Voltammetry analysis of Methylene Blue redox activity on Pt electrodes

Cyclic Voltammetry Analysis: The CV measurements, plotted in Figure 3.26 were then conducted using methylene blue mixed with different concentrations of EpCAM protein. The specific settings used for the CV measurements included a scan Rate of 50 mV/s, redox mediator: 1 mM methylene blue in PBS and varied concentrations of EpCAM protein.

The results revealed a significant relationship between protein concentration and signal intensity:

- As the concentration of EpCAM increased, the measured signal intensity decreased.
- This inverse relationship occurred because higher concentrations of the protein blocked more of the electrode surface, reducing the ability of the redox mediator to reach the surface and participate in electron transfer.

In Figure 3.25, the CV plots show this trend clearly. The bare electrode produced a strong signal with methylene blue alone, indicating full accessibility of the redox mediator to the electrode surface. However, as the concentration of EpCAM protein increased, the signal gradually diminished, confirming that the protein effectively blocked the surface.

Figure 3.26 demonstrates cyclic voltammetry responses for varying concentrations of an EpCAM-specific probe molecule, ranging from 0 nM to 50 nM, used to measure EpCAM protein binding. Each trace corresponds to a different probe concentration, highlighting the electrochemical activity on surface functionalized platinum electrodes. The results depict distinct redox behavior and current changes, which increase with the probe concentration, crucial for quantifying EpCAM protein levels.

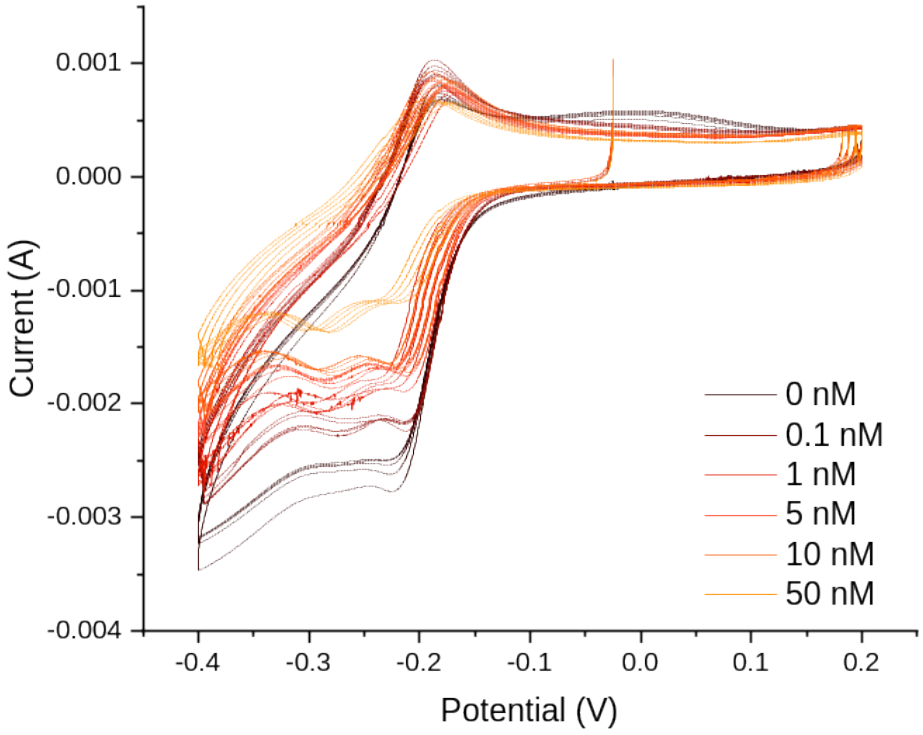

FIGURE 3.26: Electrochemical detection of EpCAM protein binding at varying concentrations on surface functionalised on Pt-plated electrodes

Discussion: These results illustrate the effectiveness of cyclic voltammetry and methylene blue as a redox mediator in detecting protein binding on functionalized electrodes. The inverse relationship between EpCAM concentration and signal intensity demonstrates that the functionalized electrodes can successfully measure protein attachment by monitoring changes in surface accessibility. The redox mediator plays a crucial role in this process by providing a measurable signal based on electron transfer. When the electrode surface is partially or fully blocked by proteins, the mediator cannot reach the surface as effectively, leading to a decrease in signal. This principle underlies the utility of cyclic voltammetry in protein detection. In summary, the cyclic voltammetry measurements confirmed that the more EpCAM protein was present, the lower the signal measured. This relationship provides a reliable means of quantifying protein attachment and reinforces the value of cyclic voltammetry for proteome analysis in PCa research.

3.11 Conclusion

This study aimed to evaluate the proteome secretion of Prostate Cancer (PCa) cells based on their cell cycle phases and develop a multiplexing platform to identify potential biomarkers. Furthermore, the project sought to compare the efficacy of optical measurement versus electrochemical measurement setups in analyzing proteome secretion.

Key Findings: The results demonstrated significant heterogeneity in the secretion of PSA depending on the cell cycle phase. The G1 phase secretes PSA, while theSphase and G2/M phase exhibit no detectable secretion of the protein. This finding underscores the importance of considering cell cycle phase heterogeneity in biomarker analysis and its potential impact on PCa diagnostics and therapeutics. Using the proteome array, we identified the secretion of multiple proteins from PCa cell lines. Apart from PSA, several proteins showed potential as biomarkers for PCa, providing a foundation for further research into their diagnostic and prognostic utility. In addition, the spotting device was successfully used to multiplex multiple antibodies onto a PVDF membrane. Although the concept was proven feasible, the results indicated the need for further optimization to achieve consistent and reliable data. The synchronization protocol for aligning PCa cells to the G1 phase needs further refinement. Achieving effective synchronization is crucial for accurate comparison of proteome secretion across different cell cycle phases. Detection using the electrochemical measurement setup was validated and found to be possible. The QCM-D validation confirmed the specific binding of the synthesized PLL derivatives and demonstrated the specificity of biotin-streptavidin interactions on the Pt-plated electrodes. Cyclic voltammetry results showed that the attachment of EpCAM protein to the functionalized electrodes led to a decrease in signal intensity, proving the ability of the electrochemical setup to detect protein attachment.

Comparison Between Optical and Electrochemical Methods: The comparison between optical and electrochemical measurement methods revealed distinct advantages and disadvantages for each approach. Optical methods, such as the Proteome array and spotting device, enable simultaneous detection of multiple biomarkers, providing a comprehensive profile of proteome secretion. They are also highly sensitive to changes in protein concentration, enabling the detection of low-abundance biomarkers, and direct visualization of stained proteins offers clear confirmation of the presence and localization of specific proteins. However, optical methods often require complex protocols, such as immunofluorescence staining and ELISpot assays, which involve multiple preparation steps and careful optimization. Additionally, these protocols can be time-consuming, from sample preparation to data analysis, and the spotting device requires further refinement for consistent and reliable antibody coating. On the other hand, electrochemical methods, including cyclic voltammetry, offer real-time monitoring of protein attachment, providing immediate insights into binding kinetics. The QCM-D validation showed specific binding of streptavidin to the biotinylated PLL derivatives and subsequent protein attachment, demonstrating high specificity. Furthermore, electrochemical methods often require less sample preparation compared to optical methods. Nonetheless, electrochemical methods are typically focused on a single biomarker at a time, limiting the comprehensiveness of the analysis. Signal interpretation requires careful calibration due to potential interference or non-specific binding, and high-quality instrumentation is required to detect low-abundance proteins.

Societal Impact: The societal impact of this research lies in its potential to improve the early detection and personalized treatment of prostate cancer. By identifying the heterogeneity in PSA secretion across different cell cycle phases, the findings emphasize the need for more accurate diagnostic tools that consider this variability. Furthermore, the development of a multiplexing platform to identify multiple potential biomarkers could pave the way for better understanding tumor heterogeneity, leading to more effective and personalized therapeutic strategies.

A significant benefit of this research is the emphasis on liquid biopsy as a diagnostic approach. Liquid biopsy, involving the analysis of Circulating Tumor Cells (CTCs) and Cell-free DNA (cfDNA), is less invasive than traditional tissue biopsies, offering an easier and safer way to monitor patients. By enabling the understanding of tumor type through liquid biopsy, patients can avoid the discomfort and risks associated with conventional biopsies. Additionally, this method allows for real-time monitoring of disease progression and treatment response, enabling clinicians to tailor treatments to individual patients more effectively.

The multiplexing platform developed in this research, which can identify multiple potential biomarkers in a single test, offers a comprehensive view of the proteome secretion profile. This level of detail is crucial for understanding tumor heterogeneity and selecting the most appropriate therapeutic strategies for each patient. Personalized treatment strategies that consider the heterogeneity of PCa can lead to improved outcomes, reducing over-treatment and unnecessary side effects for patients.

Furthermore, by highlighting the differences in protein secretion based on cell cycle phases, this study contributes to the broader understanding of PCa biology. This understanding can inform the development of targeted therapies that are more effective for specific tumor types. Ultimately, this research provides a foundation for the future development of more accurate diagnostic tools and treatment approaches, directly benefiting patients through improved prognosis, quality of life, and survival rates.

The comparison between optical and electrochemical measurement methods offers valuable insights into how different analytical approaches can complement each other, ultimately contributing to the development of more comprehensive diagnostic technologies. By refining the synchronization protocol and optimizing the multiplexing device, this research provides a strong foundation for future investigations aimed at identifying novel biomarkers and improving PCa diagnosis and treatment.

3.12 Future recommendations

The findings from this study have provided valuable insights into proteome secretion from PCa cells and have paved the way for further research into optimizing multiplexing and synchronization protocols. However, several aspects require further investigation and improvement to enhance the understanding of tumor heterogeneity and improve diagnostic and therapeutic strategies.

One of the primary recommendations is to optimize the GAPDH antibody protocol for normalization. GAPDH serves as a housekeeping protein, enabling accurate normalization of PSA secretion across various cell lines. Developing a dualplex assay that simultaneously coats PSA and GAPDH antibodies on a PVDF membrane will help determine if there is genuine heterogeneity in PSA secretion from PCa cells.

To further advance multiplexing, the spotting device used in this study should be refined to ensure consistent and accurate antibody coating. Moreover, other multiplexing methods, such as barcode-based techniques, should be explored to increase the detection efficiency of multiple biomarkers. The ultimate goal is to develop a multiplexing platform capable of simultaneously detecting up to four antibodies on a single membrane, providing a comprehensive proteome profile.

The synchronization protocol also requires further refinement. Improving the protocol to arrest cells in the G1 phase will ensure homogeneous PSA secretion, enabling more reliable comparisons between different cell cycle phases. In addition, measuring the secretion differences in cell cycle phases of other PCa cell lines will provide deeper insights

into tumor heterogeneity and potentially identify more relevant biomarkers. In the field of electrochemical measurement setups, exploring alternative approaches is crucial for improving detection sensitivity and throughput. Multielectrode sensors can significantly enhance time efficiency by allowing parallel measurements across multiple electrodes. This approach would also facilitate the simultaneous analysis of multiple biomarkers, complementing the multiplexing achieved through optical methods.

Bibliography

[1] Eurocare-5 data. *European Journal of Cancer*, 50(15):2545–2568, 2021.

[2] Elispot, n.d. Retrieved May 12, 2024. URL: https://www.sanquin.org/products-and-services/immunomonitoring-services/clinical-immunomonitoring/assays/elispot.

[3] Fikri Abali, Narghes Baghi, Arjan Tibbe, and Leon Terstappen. Detection of psa secretion from single prostate cancer cells with and without drug stimulation [abstract]. In *Proceedings of the Annual Meeting of the American Association for Cancer Research 2020*, volume 80, page Abstract nr 2693, Philadelphia (PA), Apr 27-28 and Jun 22-24 2020. AACR.

[4] S. P. Balk, Y. J. Ko, and G. J. Bubley. Biology of prostate-specific antigen. *Journal of Clinical Oncology*, 21(2):383–391, 2003.

[5] Biolin Scientific. Qcm-d measurements, n.d. Retrieved 2024. URL: https://www.biolinscientific.com/measurements/qcm-d.

[6] William J. Catalona, Alan W. Partin, Martin G. Sanda, John T. Wei, George G. Klee, Chris H. Bangma, Kevin M. Slawin, Leonard S. Marks, Stacy Loeb, Dennis L. Broyles, Sanghyuk S. Shin, Amabelle B. Cruz, Daniel W. Chan, Lori J. Sokoll, William L. Roberts, Ron H.N. Van Schaik, and Isaac A. Mizrahi. A multicenter study of [-2]pro-prostate specific antigen combined with prostate specific antigen and free prostate specific antigen for prostate cancer detection in the 2.0 to 10.0 ng/ml prostate specific antigen range. *Journal of Urology*, 185(5):1650–1655, May 2011. doi:10.1016/j.juro.2010.12.032.

[7] P. Chen, Y.-L. Zhang, B. Xue, and G.-Y. Xu. Association of caveolin-1 expression with prostate cancer: A systematic review and meta-analysis. *Frontiers in Oncology*, 10:562774, 2021. doi:10.3389/fonc.2020.562774.

[8] A. Ciccia and S. J. Elledge. The dna damage response: making it safe to play with knives. *Molecular Cell*, 40(2):179–204, 2010.

[9] M. K. David and S. W. Leslie. Prostate specific antigen. In *StatPearls [Internet]*. StatPearls Publishing, Treasure Island, FL, 2022. Available from: https://www.statpearls.com.

[10] H. Eba, Y. Murasawa, K. Iohara, Z. Isogai, H. Nakamura, H. Nakamura, and M. Nakashima. The anti-inflammatory effects of matrix metalloproteinase-3 on irreversible pulpitis of mature erupted teeth. *PLOS ONE*, 7(12):e52523, 2012. doi:10.1371/journal.pone.0052523.

[11] T. del N. J. Flores-Téllez and E. Baena. Experimental challenges to modeling prostate cancer heterogeneity. *Cancer Letters*, 2021. doi:10.1016/j.canlet.2021.10.012.

[12] G. Garudadri, B. V. Rao, C. Sundaram, D. Fonseca, S. S. Murthy, R. Sharma, and T. S. Rao. Diagnostic utility of immunohistochemical marker prostein for evaluation of primary and metastatic prostatic carcinomas. *Indian Journal of Pathology and Microbiology*, 63(Supplement):S18–S24, 2020. doi:10.4103/IJPM.IJPM_852_18.

[13] S. Ghosh, R. Bhowmick, S. Nandi, and S. Bhattacharjee. Facs: application in cancer research. *Advances in clinical chemistry*, 51:151–182, 2010.

[14] O. Gires, M. Pan, H. Schinke, M. Canis, and P. A. Baeuerle. Expression and function of epithelial cell adhesion molecule epcam: where are we after 40 years? *Cancer Metastasis Review*, 39(3):969–987, 2020. doi:10.1007/s10555-020-09898-3.

[15] P. H. Hamming and J. Huskens. Streptavidin coverage on biotinylated surfaces. *ACS Applied Materials & Interfaces*, 13(48):58114–58123, 2021. doi:10.1021/acsami.1c16446.

[16] X. Huang, T. Yuan, M. Liang, M. Du, S. Xia, R. Dittmar, et al. Exosomal mir-1290 and mir-375 as prognostic markers in castration-resistant prostate cancer. *European Urology*, 67(1):33–41, 2017.

[17] S. Janetzki, J. H. Cox, N. Oden, and G. Ferrari. Standardization and validation issues of the elispot assay. *Methods in molecular biology*, 302:51–86, 2005.

[18] P. Kanyong, S. Rawlinson, and J. Davis. Immunochemical assays and nucleic-acid detection techniques for clinical diagnosis of prostate cancer. *Journal of Cancer*, 7(5):523–531, 2016. doi:10.7150/jca.13821.

[19] L. Kneppers, A. Palapanis, T. Bonfill, J. Bierau, J. Schalkwijk, and S. Pouwels. Advances in plasma protein glycation: from diabetes to cardiovascular disease and beyond. *Glycobiology*, 33(4):339–354, 2023. doi:10.1093/glycob/cwad039.

[20] J. L. Mohler, E. S. Antonarakis, A. J. Armstrong, A. V. D'Amico, B. J. Davis, T. Dorff, et al. Prostate cancer, version 2.2019, nccn clinical practice guidelines in oncology. *Journal of the National Comprehensive Cancer Network*, 17(5):479–505, 2019.

[21] J. Movilli, A. Rozzi, R. Ricciardi, R. Corradini, and J. Huskens. Control of probe density at dna biosensor surfaces using poly(l-lysine) with appended reactive groups. *Bioconjugate Chemistry*, 29(12):3923–3934, 2018. doi:10.1021/acs.bioconjchem.8b00733.

[22] S. M. Rocha, J. Barroca-Ferreira, L. A. Passarinha, S. Socorro, and C. J. Maia. The usefulness of steap proteins in prostate cancer clinical practice. In S. R. J. Bott and K. L. Ng, editors, *Prostate Cancer*. Exon Publications, Brisbane, AU, 2021.

[23] ScienceFacts.net. Cell cycle: Definition, phases, and diagram, n.d. URL: https://www.sciencefacts.net/cell-cycle.html.

[24] D. G. Tang. Understanding and targeting prostate cancer cell heterogeneity and plasticity. *Seminars in Cancer Biology*, 82:68–93, 2022. doi:10.1016/j.semcancer.2021.11.001.

[25] E. Tanumihardja, A. Paradelo Rodríguez, J. T. Loessberg-Zahl, B. Mei, W. Olthuis, and A. van den Berg. On-chip electrocatalytic no sensing using ruthenium oxide nanorods. *Sensors and Actuators B: Chemical*, 334:129631, 2021. doi:10.1016/j.snb.2021.129631.

[26] G. Theil, C. Lindner, J. Bialek, and P. Fornara. Association of circulating tumor cells with inflammatory and biomarkers in the blood of patients with metastatic castration-resistant prostate cancer. *Life (Basel)*, 11(7):664, 2021. doi:10.3390/life11070664.

[27] Claire Tonry, Stephen Finn, John Armstrong, and Stephen R. Pennington. Clinical proteomics for prostate cancer: understanding prostate cancer pathology and protein biomarkers for improved disease management. *Clinical Proteomics*, 17(41), 2020. doi:10.1186/s12014-020-09305-7.

[28] J. J. Tosoian, S. Loeb, Z. Feng, S. Isharwal, P. Landis, D. J. Elliot, et al. Association of [-2] propsa with biopsy reclassification during active surveillance for prostate cancer. *JAMA Oncology*, 3(5):687–694, 2017.

[29] G. Wang, D. Zhao, D. J. Spring, and R. A. DePinho. Genetics and biology of prostate cancer. *Genes & Development*, 33(17-18):1090–1105, 2019.

[30] J. Wang. Electrochemical biosensors: Towards point-of-care cancer diagnostics. *Biosensors and Bioelectronics*, 21(10):1887–1892, 2008.

[31] J. Zapatero Rodríguez and R. O'Kennedy. New approaches for the development of diagnostic systems for prostate cancer. *Medical Science, Asian Hospital & Healthcare Management*, (36):20, 2017. URL: https://www.researchgate.net/publication/316550970_New_Approaches_For_The_Development_Of_Diagnostic_Systems_For_Prostate_Cancer.

Appendix A

Identification of potential PCa biomarkers using Proteome array

To identify potential biomarkers associated with Prostate Cancer (PCa), a proteome profiling array was utilized, specifically the Proteome Profiler™ Array Human XL Oncology Array Kit (Catalog Number ARY026). This array kit enabled us to detect and quantify multiple biomarkers simultaneously, providing insights into the proteomic variations across different PCa cell lines.

Kit Components and Storage Conditions The kit was stored unopened at 2-8°C. Following its instructions, the nitrocellulose membranes and reagents were stored as per the recommendations:

- **Human XL Oncology Array:** Contains 4 nitrocellulose membranes printed with 84 different capture antibodies, each printed in duplicate. Unused membranes were returned to their foil pouch, sealed along the entire edge, and stored for up to 3 months at 2-8°C.
- **Array Buffers 4 and 6:** Array Buffer 4 (21 mL) and two vials of Array Buffer 6 (21 mL each) served as blocking and dilution buffers, mixed fresh before use.
- **Wash Buffer Concentrate:** Two vials of a 25-fold concentrated wash solution, diluted to 1 L before use.
- **Detection Antibody Cocktail:** A biotinylated antibody cocktail, reconstituted in 200 µL of deionized water immediately before use.
- **Streptavidin-HRP:** 200 µL of streptavidin conjugated to horseradish peroxidase, diluted before use.
- **Chemi Reagents:** 2.5 mL each of Chemi Reagents 1 and 2, mixed equally to prepare a luminescent solution for membrane development.
- **4-Well Multi-Dish:** A clear rectangular dish for incubation steps.
- **Transparency Overlay Template:**For coordinate reference during analysis.

The reagents were prepared and used following the instructions, ensuring minimal contamination and optimal assay conditions.

Sample Collection and Processing Cell culture supernatants were collected from LnCAP, PC-3, and 22Rv1 cell lines. A control sample consisting only of the cell culture medium was also included to account for proteins already present in the medium.

- **Supernatant Collection:** The supernatants were centrifuged to remove particulates, aliquoted, and stored at $\leq$ -20°C to avoid repeated freeze-thaw cycles.

Assay Procedure All reagents were brought to room temperature, and the assays were conducted as follows:

1. **Blocking: Membranes were placed in a 4-Well Multi-Dish, each with 2 mL of Array Buffer 6, and rocked for 1 hour.**
2. **Sample Preparation: Samples were diluted with Array Buffer 4, then adjusted to 1.5 mL with Array Buffer 6.**
3. **Incubation: Samples were added to the membranes and incubated overnight at 2-8°C.**
4. **Washing: Membranes were washed three times with 1X Wash Buffer.**
5. **Detection Antibody Cocktail: Each membrane was incubated with a diluted cocktail (30 µL per 1.5 mL) of Detection Antibody for 1 hour, followed by a wash.**
6. **Streptavidin-HRP: Membranes were incubated with Streptavidin-HRP for 30 minutes, then washed.**
7. **Chemi Reagent Mix: Chemi Reagents 1 and 2 were mixed in equal parts, and 1 mL was spread over each membrane, followed by incubation in a plastic protector.**
8. **Development: Membranes were exposed to X-ray film for 1-10 minutes for visualization.**

Data Analysis and Interpretation The resulting membranes were analyzed for relative biomarker expression, identifying key proteins indicative of PCa biology. The inclusion of a control sample without cells allowed for adjustment against proteins present in the culture medium alone. This comprehensive analysis provides a foundation for understanding biomarker profiles across different PCa cell lines and further characterizing their proteomic signatures.

Appendix B

Intracellular PSA of PCa's cell lines

Immunofluorescence Staining of Cells Immunofluorescence staining was conducted to visualize and quantify specific antigens within the PCa cell lines. The procedure was as follows:

1. **Fixation:** Cultured cells were fixed in 1% formalin in 1X PBS for 15 minutes at room temperature, stabilizing their structures and preserving cellular proteins for analysis.

2. **Washing:** The cells were washed twice with 1X wash buffer (PBS) to remove residual formalin and prepare for further processing.

3. **Permeabilization:** The cells were treated with 0.1% Triton X-100 in 1X PBS for 15 minutes at room temperature to permeabilize the cell membranes, allowing antibodies to access intracellular targets.

4. **Washing:** The permeabilization buffer was gently removed, and the cells were washed three times with PBS, ensuring complete removal of Triton X-100.

5. **Blocking:** To reduce nonspecific binding, the cells were blocked with 1% BSA (in PBS) for 60 minutes at room temperature.

6. **Primary Antibody Incubation:** A rabbit anti-PSA antibody was diluted to a working concentration of 10 µg/mL in 0.1% BSA/PBS and incubated with the cells for 1 hour at room temperature. This antibody targets the Prostate-Specific Antigen (PSA), a key biomarker in prostate cancer research. After incubation, the cells were washed three times (5-10 minutes each) with 1X wash buffer.

7. **Secondary Antibody Incubation:** An anti-rabbit PE-conjugated antibody (1:1000 v/v in PBS) was prepared and incubated with the cells for 60 minutes at room temperature. This secondary antibody binds to the primary antibody, creating a fluorescent signal. The cells were then washed three times (5-10 minutes each) with 1X wash buffer.

8. **Optional Counterstaining:** If desired, nuclei counterstaining was performed by incubating cells with DAPI or Hoechst for 15 minutes at room temperature, followed by washing three times (5-10 minutes each) with 1X wash buffer.

9. **Final Preparation:** Cells stained in a 24-well plate were covered with 1X PBS to prevent drying. For cells on coverslips, antifade mounting solution was used to mount them onto slides.

10. **Visualization:** Fluorescent images of the stained cells were visualized using a fluorescence microscope, ensuring the correct filters were used for specific fluorescent signals.

This staining technique enabled us to detect and quantify PSA expression within the PCa cell lines, providing valuable insights into their proteomic profiles. Further staining methods, including cytospin, membrane staining, and spotting device-based approaches, were also employed, as detailed in subsequent sections.

Visualisation of the stained cell on a cover slip using the cytospin To further examine the cellular structures and cycle phases, LnCAP cells were stained and analyzed as follows:

1. **Sample Preparation:** LnCAP cells were harvested and stained with Hoechst, a fluorescent dye that binds to DNA, highlighting the nuclei.

2. **FACS Analysis and Sorting:** The stained cells were then analyzed with FACS, where they were sorted according to their cell cycle phase, categorizing them into different groups.

3. **Cell Counting:** After sorting, the cells were counted, and 10,000 cells from each cycle phase group were selected.

4. **Cytospin:** These selected cells were then spun down onto coverslips using a cytospin technique. This involved placing the cells into a specialized chamber, where they were centrifuged, spreading them evenly across the surface of the coverslip.

5. **Mounting:** The coverslips with spun-down cells were mounted onto microscope slides using antifade mounting solution, preserving the fluorescent signal and allowing for extended analysis.

6. **Visualization:** The slides were then examined under a fluorescence microscope, using appropriate filters to visualize the Hoechst-stained nuclei. This allowed for a detailed examination of each cell cycle phase and comparison of cellular characteristics between the different phases.

By incorporating FACS sorting and cytospin staining, this approach provided a comprehensive analysis of LnCAP cells, offering insights into their cell cycle dynamics and biological profiles.

Appendix C

Measuring PSA secretion from PCa's cell lines

Staining PVDF Membranes to Visualize PSA Secretion To investigate the secretion of Prostate-Specific Antigen (PSA), LnCAP, PC-3, and 22Rv1 cells were seeded onto PVDF membranes and stained using a specific protocol, allowing for visualization of PSA secretion.

Membrane Preparation and Activation:

1. **Membrane Cutting:** PVDF membranes were cut into circles to fit into a 24-well plate.
2. **Activation:** The membranes were placed in the wells under sterile conditions and incubated with 500 µL of 100% methanol, ensuring complete coverage for 5-10 seconds.
3. **Washing:** The membranes were washed twice with 500 µL of 1X PBS.
4. **Antibody Coating:** Anti-PSA (capture) antibody solutions were prepared at a concentration of 25 µg/mL. The membranes were coated with 200 µL of the antibody solution, ensuring complete surface coverage.
5. **Incubation:** The membranes were incubated at 4°C overnight to allow the antibodies to bind effectively.

Membrane Blocking:

1. **Blocking:** The antibody solution was aspirated out, and the membranes were blocked with 200-300 µL of a 3% BSA in 1X PBS solution for 1 hour at 4°C or at room temperature.
2. **Washing:** The membranes were washed with 1X PBS and left in the solution if not immediately used.

Cell Seeding on Membranes:

1. **Cell Seeding:** The PBS was aspirated from the wells, and 500 µL of cell culture medium was added to each well.

2. **Cell Suspension:** 5,000 cells from each cell line were suspended and added to each membrane.

3. **Incubation:** The 24-well plate was incubated at 37°C overnight, allowing the cells to adhere and grow. Antibody Staining:

4. **Initial Washing:** The plate was removed from the incubator, and the membranes were washed with 0.1% Tween 20 (in 1% BSA PBS) for 15 minutes on a rocker shaker at 300 rpm.

5. **Second Washing:** The membranes were washed with 1% BSA in PBS for 15 minutes on a rocker shaker at 300 rpm.

6. **Primary Antibody:** A Rabbit anti-PSA antibody was prepared at 2 µg/mL in 1X PBS. 200 µL of this solution was added to each membrane and incubated for 1 hour on a shaker at 300 rpm, with the lid closed.

7. **Washing:** The membranes were washed three times with 1% BSA in PBS for 5 minutes each.

8. **Secondary Antibody:** A Goat anti-Rabbit antibody was prepared at 2 µg/mL in 1X PBS. 200 µL of this solution was added to each membrane and incubated for 1 hour on a shaker at 300 rpm, covered with aluminum foil.

9. **Final Washing:** The membranes were washed three times with 1% BSA in PBS for 5 minutes each.

10. **Storage:** The membranes were stored in PBS, covered in aluminum foil, and placed at 4°C for further use. For long-term storage, they were kept in Milli-Q water, sealed with parafilm, and covered in foil at 4°C.

Visualization: For imaging, the membranes were dried completely and placed on glass slides. The VyCAP spot software was used to visualize the PSA secretion, providing valuable insights into the secretion profiles of each cell line.

Spotting device for multiplexing As part of our ongoing efforts to analyze cellular characteristics and detect specific proteins, a novel approach was implemented using a spotting device to perform multiplex staining on PVDF membranes. This method allows for the simultaneous analysis of multiple antibodies on a single membrane.

Staining Membranes Using the Spotting Device:

1. **Membrane Preparation and Activation:**

   (a) **Prepare and activate the PVDF membrane:** Follow the previously established protocol outlined in the section on staining membranes. This involves cutting, activating with methanol, and blocking the membrane to prepare it for antibody application.

2. **Insertion into the Spotting Device:**

   (a) **Setup:** Place the prepared and activated membrane into the spotting device, ensuring it is positioned correctly to align with the wells of the device.

3. **Antibody Application:**

   (a) **Preparation of Antibody Solutions:** Antibody solutions were prepared at a dilution of 1:1000 from the stock.

   (b) **Filling the Wells:** Approximately 4 µL of the prepared antibody solution was added to each well of the spotting device. Each well can contain a different antibody, but for the proof of concept, Anti-IgG PE was used in each well.

4. **Assembly and Spotting:**

   (a) **Device Assembly:** Assemble the spotting device to ensure that the filled well chambers align correctly with the membrane below.

   (b) **Spotting:** Leave the device to deposit spots of the antibody solution onto the membrane.

5. **Incubation:**

   (a) **Duration:** The membrane was incubated with the spotted antibodies for varying durations: one hour, two hours, overnight, and up to 24 hours to assess different binding dynamics and staining intensities.

6. **Washing:**

   (a) **Post-Incubation Washing:** After incubation, the spotting device was removed, and the membrane was thoroughly washed with PBS to remove any unbound antibodies.

7. **Visualization and Storage:**

   (a) **Immediate Visualization:** The membrane could be visualized immediately using the VyCAP system to analyze the spots.

   (b) **Storage:** Alternatively, the membrane was stored in Milli-Q water until ready for visualization to preserve the integrity of the antibody spots.

Appendix D

Identification and sorting of cells in different cell cycle phases

The ability to identify and sort cells based on their cell cycle phase is crucial for numerous biological investigations. This was achieved using Fluorescence-Activated Cell Sorting (FACS), incorporating Hoechst 33342 staining to differentiate cells in various phases of the cell cycle.

FACS Staining Protocol:

1. **Cell Preparation:**
   (a) Cells were harvested when they reached approximately 80% confluency to ensure a high viability and representative population distribution.
   (b) The cells were then counted and centrifuged at 3000 G for 5 minutes to pellet them.
2. **Resuspension and Staining:**
   (a) The supernatant was carefully removed, and the cells were resuspended in a solution of 2% FBS in PBS to a concentration aimed at reaching 300,000 cells per 200 µL in each FACS tube.
   (b) Hoechst 33342 was added to each sample at a concentration of 1 µL per 100 µL of cell suspension. The cells were incubated with the dye for 30 minutes on ice to allow adequate staining while minimizing cell stress and dye toxicity.
3. **Washing:**
   (a) After staining, the cells were washed by adding an additional 300 µL of 2% FBS in PBS to bring the total volume to 500 µL. The cells were then centrifuged to remove excess dye, and the supernatant was discarded.

FACS Analysis and Sorting:

1. **Setup and Calibration:**
   (a) The flow cytometer was set up and calibrated for UV excitation (340 to 380 nm) and detection of Hoechst 33342 fluorescence at blue wavelengths. Adjustments were made to accurately gate single cells and exclude doublets using pulse-width/pulse-area analysis.

(b) A negative control (non-stained cells) was used to set the baseline fluorescence and adjust the sensitivity of the flow cytometer.

2. **Measurement and Data Collection:**

   (a) The stained cells were analyzed by flow cytometry. Hoechst 33342 fluorescence was measured to determine the DNA content of the cells, allowing the identification of cells in G1, and G2/M phases.

   (b) Settings were adjusted as necessary based on the intensity of cell fluorescence and resolution of cells in different cell cycle phases.

3. **Sorting:**

   (a) Cells were sorted based on their DNA content into different collection tubes for further experiments.

   (b) Parameters such as Forward Scatter (FSC) and Side Scatter (SSC) were used alongside Hoechst fluorescence to refine the sorting accuracy.

4. **Post-Sorting Processing:**

   (a) Sorted cells were collected and could be cultured further or used immediately for downstream analyses.

Considerations and Precautions:

1. The viability and cell cycle progression of sorted cells could be influenced by the staining procedure due to the potential light sensitivity induced by Hoechst 33342.

2. Appropriate controls and replicates were included to ensure the reliability of the sorting process.

Appendix E

Membranes and secretion detection

To investigate the secretion dynamics of Prostate-Specific Antigen (PSA) across different cell cycle phases, a detailed analysis was performed using PVDF membranes and the VyCAP imaging system. This method allowed for the quantitative assessment of PSA secretion from cells sorted into G1, and G2/M phases.

Protocol for PSA and GAPDH Detection on PVDF Membranes:

1. **Membrane Preparation:**
    - Follow the protocol for preparing and activating PVDF membranes as described in "Staining PVDF Membranes to Visualize PSA Secretion." This ensures that the membranes are properly conditioned for cell seeding and subsequent protein detection.
2. **Cell Seeding on Membranes:**
    - Cells sorted into different cell cycle phases (G1, G2/M) using FACS were seeded onto the prepared PVDF membranes. Seeding sorted cells enables the investigation of phase-specific PSA secretion.
3. **Overnight Incubation:**
    - The seeded membranes were incubated overnight under optimal cell culture conditions to facilitate cell attachment and secretion. Overnight incubation is crucial as it allows sufficient time for cells to recover from the sorting process and begin secreting PSA.
4. **Washing of Membranes:**
    - Post-incubation, the membranes were washed with PBS containing 0.1% Tween-20 to remove and reduce background staining in subsequent steps. This step is crucial for removing cellular debris and any unattached cells, ensuring that subsequent antibody staining reflects PSA secreted from the cells.
5. **Antibody Staining for PSA and GAPDH:**
    - PSA Detection: Follow the antibody staining steps detailed in "Staining PVDF Membranes to Visualize PSA Secretion." Apply a primary antibody specific to PSA, followed by a compatible secondary antibody to visualize the protein.

- GAPDH Detection: Concurrently, GAPDH is detected using a specific antibody. As a housekeeping protein, GAPDH serves to normalize the data, providing a baseline that compensates for variations in cell density and antibody application across the membrane.

6. **Imaging Using the VyCAP System:**

   - After staining, the membranes were imaged using the VyCAP imaging system. This technology allows for detailed quantification of the fluorescent or chemiluminescent signals emitted by the labeled antibodies, enabling accurate measurement of both PSA and GAPDH levels.

7. **Data Analysis and Normalization:**

   - The intensity of the signals from both PSA and GAPDH was quantified using image analysis software. Normalizing PSA signal intensity against GAPDH is critical as it ensures that the measured differences in PSA secretion are due to biological factors rather than technical variables like cell number or uneven distribution on the membrane.

Appendix F

Poly-L-Lysine synthesis

To prepare PLL derivatives, including PLL-OEG and PLL-OEG-Biotin, a series of synthesis, dialysis, and freeze-drying steps were performed. The specific steps involved are outlined below.

Synthesis of PLL-OEG and PLL-OEG-Biotin:

1. **Preparation:** Materials were taken out of the freezer (-30°C) at least 30 minutes before starting. The necessary materials included micropipettes, 1X PBS (filtered, pH 7.4), dry DMSO for stock solutions, and clean, dry vials.
2. **Stock Solutions:**
   (a) **PLL:** 10 mg/mL PLL solution was prepared by dissolving 100 mg of PLL in 10 mL of PBS (pH 7.4, filtered).
   (b) **OEG NHS Ester:** 0.25 M solution prepared by dissolving 100 mg of OEG NHS ester in 1.2 mL of DMSO.
   (c) **Biotin-OEG NHS Ester:** 0.25 M solution prepared by dissolving 50 mg of Biotin-OEG NHS ester in 339.7 µL of DMSO.
3. **Mixture Preparation:** In a clean and dry vial, 1 mL of PLL.HBr (10 mg/mL), 1 mL of PBS (pH 7.4), and the appropriate amounts of OEG NHS ester and Biotin-OEG NHS ester solutions were mixed, depending on the desired final product:
   (a) **For PLL-OEG:** 30% OEG, requiring 57.4 µL of OEG NHS solution.
   (b) **For PLL-OEG-Biotin:** 4% Biotin, requiring 9.6 µL of Biotin-OEG NHS solution.
4. **Stirring:** The mixture was stirred vigorously for 4 hours at a shaker to ensure complete reaction.
5. **Dialysis:** The synthesized solution was dialyzed using SpectraPor dialysis tubing with a 6-8 kDa MWCO, diameter 6.4 mm:
   (a) **Against 70% PBS, 50% PBS, 30% PBS, and MQ water:** Two to three rounds for each solution.
   (b) The dialysis solution was changed twice a day to ensure thorough purification.
6. **Freeze-Drying:** The dialyzed product was freeze-dried to obtain a powdered form of the final compounds.

7. **Storage:** The resulting product was stored in the freezer for further use.

Appendix G

Nuclear Magnetic Resonance spectroscopy

To characterize the molecular structures of the synthesized compounds, Nuclear Magnetic Resonance (NMR) spectroscopy was employed. This section outlines the preparation and procedure used for structural analysis.

Preparation of Sample for NMR:

1. **Dissolution:** The freeze-dried product was dissolved in D_2O at a concentration of 10 mg/mL, ensuring complete dissolution by thorough mixing.

2. **Transfer to NMR Tube:** The dissolved sample was transferred to an NMR tube, ensuring no air bubbles were present. The tube was sealed securely with a cap to prevent contamination or evaporation.

NMR Procedure:

1. **Spectrometer Setup:** The NMR spectrometer was calibrated using standard compound with known chemical shifts, ensuring accuracy in the recorded spectra.

2. **Sample Insertion:** The prepared NMR tube was carefully inserted into the spectrometer, ensuring proper alignment and secure placement.

3. **Data Acquisition:** The spectrometer was set to acquire spectra at a frequency of 400 MHz for ^{1}H NMR. Data acquisition parameters, including pulse sequence, relaxation delay, and acquisition time, were configured to optimize signal-to-noise ratio and spectral resolution.

4. **Data Processing:** The acquired data was processed using appropriate software, applying Fourier transformation to convert time-domain signals into frequency-domain spectra. Phase correction, baseline adjustment, and peak integration were performed as needed.

5. **Spectral Analysis:** The resulting spectra were analyzed to identify chemical shifts, coupling constants, and integration values, allowing for structural elucidation of the synthesized molecules. During the analysis, the integral of the alpha proton peak was set to 1, and a linear fit integration was performed to ensure accurate measurements.

6. **Reporting:** The spectral data was documented, including key chemical shifts, coupling patterns, and other relevant information, to provide a comprehensive structural characterization of the synthesized molecules.

Appendix H

Quartz Crystal Microbalance

The Quartz Crystal Microbalance with Dissipation Monitoring (QCM-D) technique was employed to validate the functionalization of synthesized products described in Section 2.6 on Pt-plated electrodes. This method allows for precise measurement of changes in mass at the surface of the chip due to adsorption or binding of molecules.

QCM-D Setup and Chip Preparation:

1. **Chip Cleaning:**
   (a) **Piranha Solution Preparation:** A cleaning solution was prepared using a mixture of Milli-Q water, ammonia (25%), and hydrogen peroxide (30%). The ratio used was 50:10:10 respectively. It's important to note that piranha solution should be handled with extreme care, as it is highly reactive and corrosive.
   (b) **Heating:** The cleaning mixture was preheated on a hotplate set to 300°C to quickly reach an operational temperature of 75°C. The appearance of bubbles around 65°C indicates the evolution of oxygen from the hydrogen peroxide.
   (c) **Chip Immersion:** Once the solution reached 75°C, the Pt-plated QCM chips were immersed using a Teflon holder. The temperature was monitored and maintained at 75°C.
   (d) **Duration:** After maintaining the chips in the solution for 5 minutes at 75°C, the heating was turned off, and the chips were allowed to cool beside the hotplate.
2. **Rinsing and Drying:**
   (a) **Chemical Disposal:** The piranha solution was carefully disposed of following safety protocols.
   (b) **Rinsing:** The chips were rinsed 2-3 times with Milli-Q water to remove any residual cleaning chemicals.
   (c) **Ethanol Rinse and Sonication:** Chips were then rinsed with 99% ethanol and sonicated for 5 minutes to ensure complete cleaning.
   (d) **Drying:** Finally, the chips were dried using nitrogen air to remove any moisture or residual solvents, making them ready for functionalization.

Preparation of Sample for QCM-D:

1. **QCM-D Setup:**

(a) The QCM device was set up according to the manufacturer's instructions. This included attaching the tubing and ensuring all connections were secure.

(b) The cleaned and dried chips were loaded into the device.

2. **Stabilization and Baseline Establishment:**

   (a) Pumps were set to a flow rate of 300 µL/min to rinse the chips with PBS.

   (b) The system was allowed to stabilize, and measurements were continuously monitored until the frequency signals overlapped and stabilized.

3. **Sample Application and Measurement:**

   (a) **Initial PLL Derivative Flow:** After stabilization, the flow rate was reduced to 100 µL/min. PLL derivatives at a concentration of 0.5 mg/mL were prepared by diluting the 10 mg/mL stock solution to 0.5 mL. This solution was flowed over the chips for 10 minutes to allow attachment.

   (b) **Rinsing:** Pumps were stopped, sample tubes were carefully switched to PBS, and pumps were restarted at 300 µL/min for rinsing. This step was continued for 10-15 minutes until the signal stabilized again.

4. **Subsequent Binding Steps:**

   (a) **Streptavidin Application:** The sample tubes were switched to freshly prepared streptavidin (0.2 mM in PBS) at a reduced flow rate of 50 µL/min, flowed for about 30 minutes to bind to any biotinylated sites.

   (b) **Second Rinsing:** After streptavidin application, the system was rinsed again with PBS for 10 minutes to remove unbound streptavidin.

   (c) **Anti-EpCAM Antibody Application:** Biotinylated anti-EpCAM antibody solution at a concentration of 10 µg/mL was prepared by diluting the 1.59 mg/mL stock solution to 2 mL. This solution was then flowed through the chips.

   (d) **Proof of Concept with EpCAM Protein:** Finally, a solution containing EpCAM protein was flowed through to test the system's ability to detect the attachment of this target protein.

5. **Device Cleaning:**

   (a) After all experiments, the QCM device was cleaned with Hellmanex solution as per manufacturer's instructions to ensure no residues interfered with future analyses.

6. **Data Analysis:**

   (a) **Interpretation:** The frequency shifts recorded by the QCM were analyzed to determine the mass of the adsorbed layer, confirming the successful functionalization of the chips.

   (b) **Validation:** The experiment was performed with various PLL derivatives to observe if changes in frequency are occurring where not attachment is expected.

Appendix I

Cyclic Voltammetry

Cyclic Voltammetry (CV) is a widely used electrochemical technique that allows for the examination of the electrochemical properties of substances based on their oxidation and reduction behaviors. In this study, CV was utilized to measure real-time concentrations of the EpCAM protein using Methylene Blue as a redox mediator.

CV Setup and Protocol:

1. **Flow Cell Setup:**
   (a) The flow cell was set up with functionalized Pt-plated electrodes, which had been cleaned with 0.5 M sulfuric acid to ensure that all surfaces were free from organic contaminants and ready for functionalization.
2. **Validation of Methylene Blue:**
   (a) **Bare Electrode Testing:** Initially, bare electrodes (not functionalized) were tested with Methylene Blue to establish a baseline electrochemical response. This step confirms that the redox mediator behaves as expected on the clean electrode surface.
   (b) **Principle of CV with Redox Mediator:** Methylene Blue acts as a redox mediator by facilitating electron transfer between the electrode and the proteins bound to the surface. The more the electrode surface is blocked or occupied (e.g., by bound proteins), the less accessible it is for Methylene Blue to reach the electrode, resulting in a lower current signal. This decrease in current is proportional to the amount of surface coverage, allowing for quantification of the bound protein.
3. **Functionalization and Protein Measurement:**
   (a) **Electrode Functionalization:** After cleaning, the electrodes were functionalized with PLL-OEG-Biotin, Streptavidin, and biotinylated Anti-EpCAM to ensure selective binding of the target protein, EpCAM.
   (b) **Protein and Methylene Blue Preparation:** Various concentrations of the EpCAM protein were prepared alongside solutions of Methylene Blue. This setup was used to evaluate how different protein concentrations affect the electrochemical response.

(c) **Real-Time Measurement:** The CV was performed by flowing the solutions over the functionalized electrodes. Changes in the current were recorded as the potential was cycled, allowing for the detection of different levels of protein binding based on the changes in current due to the presence of Methylene Blue.

4. **Data Acquisition and Analysis:**

   (a) **Signal Acquisition:** The cyclic voltammograms were analyzed to observe peaks corresponding to the oxidation and reduction of Methylene Blue. The presence and intensity of these peaks were directly influenced by the interaction between Methylene Blue and the electrode surface.

   (b) **Quantification:** By comparing the cyclic voltammograms obtained from different protein concentrations, a relationship between the EpCAM concentration and the signal intensity was established, allowing for the quantification of protein levels based on electrochemical response.

Appendix J

Protein Analyzer Software

This appendix describes the workings of the Protein Analyzer Software developed by Jan Pieter de Rie, an MSc student in Robotics and Embedded Systems at the University of Twente. The tool was developed to analyze protein secretions by examining pixel intensity of each spot, which corresponds to a specific biomarker. The following sections explain the workings of the written code. The code is designed around an image of four membranes used in the protein array assay. For clarity, the focus will be on the process of analyzing a single array assay, as depicted in Figure J.1.

FIGURE J.1: Picture of a single to-be-analyzed protein array membrane.

Initially, a reference image of the assay's array, as shown in Figure J.2a, is loaded to establish the relative pixel positions of the proteins within the array. This facilitates the creation of a reference matrix containing the pixel coordinates of each protein within the array, depicted in Figure J.2b. This matrix will be fitted over the to-be-analyzed protein array's. From this matrix, we determine the relative positions of the upper-right, upper-left, and lower-left points. These will be later used for the fitting process.

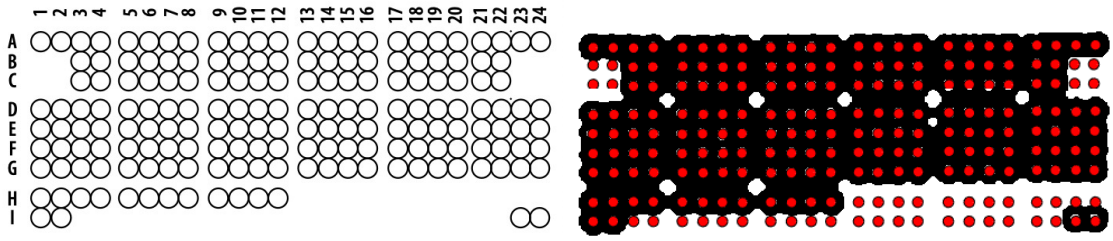

(A) (B)

FIGURE J.2: Schematic structure conversion to digital array overlay. A) This schematic provides an overview of the structure of the protein array. It serves as a reference for computing the reference matrix, a crucial step in the analysis process. B) This is the computed reference matrix. The red dots represent all positions ranging from [A..I] and [1..24]. The algorithm includes all points within the matrix for simplicity. However, it's important to note that in the final analysis, only the red dots within the black area are pertinent and contribute to the intended analysis.

Next, the image of the protein array membrane undergoes analysis. To align the reference matrix with the array's membrane image, the upper-right, upper-left, and lower-left points must be identified. This involves utilizing image processing techniques to isolate the spots, shown in Figure J.3, focusing on the reference spots. After detecting these spots, sorting algorithms are applied to determine the reference positions, such as the upper right. These are marked with a green circle in Figure J.4a.

FIGURE J.3: Image processing result for detecting the reference spots within the to-be-analyzed protein array membrane (Left). Found possible reference spots marked with a red circle (Right)

Following this, a bounding box is applied to the reference points to facilitate their exclusion when identifying reference points on multiple protein array membranes.

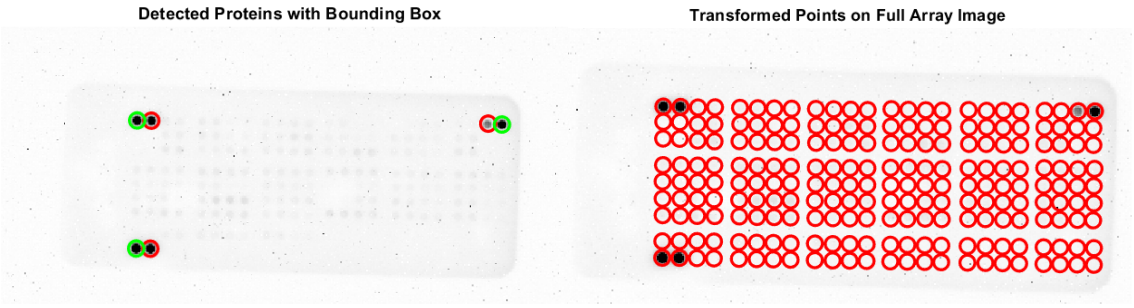

(A) (B)

FIGURE J.4: Schematic structure conversion to digital array overlay. A) Detected reference spots marked with a green circle. B) The to-be-analyzed protein array membrane with the reference matrix fitted over.

With the reference points established for both the reference matrix and the to-be-analyzed protein array membrane, the geometrical difference between the two can be determined using MATLAB's fitgeotrans function and stored in a transformation matrix. This transformation matrix is then applied to the reference matrix to fit it over the protein array membrane, as shown in Figure J.4b, enabling the identification of pixel coordinates for each spot in the assay's array membrane. Finally, with the pixel coordinates of all spots within the assay's array determined, the intensity of each protein is computed. This involves calculating the average pixel intensity within a 5-pixel radius around each point, resulting in a matrix corresponding to the assay's array, see Figure J.5.

LnCAPs

	1	2	3	4	5	6	7	8	9	10	11	12	13	14	15	16	17	18	19	20	21	22	23	24
A	182	190	240	247	246	246	247	247	245	245	244	244	244	245	247	247	248	246	245	246	246	244	206	180
B			242	245	245	245	244	244	239	241	244	245	246	246	247	246	246	245	245	246	243	243		
C			243	243	246	246	244	244	245	244	240	242	245	245	242	242	244	244	245	246	242	242		
D	245	245	246	246	243	243	244	245	245	244	246	246	246	246	246	248	245	245	245	245	243	243	245	244
E	246	244	245	246	218	215	244	246	246	246	248	247	248	248	248	248	245	245	246	246	243	243	244	243
F	247	243	239	246	237	236	241	243	246	246	246	246	247	247	246	246	244	244	245	245	242	242	244	243
G	246	245	243	244	240	240	244	245	246	246	247	248	244	244	245	246	244	242	244	244	241	242	244	243
H	238	241	245	245	247	246	246	247	245	245	248	247												
I	183	180																					246	244

(A)

PC-3

	1	2	3	4	5	6	7	8	9	10	11	12	13	14	15	16	17	18	19	20	21	22	23	24
A	170	176	236	244	238	240	244	244	241	241	242	243	241	242	245	245	244	244	244	244	244	243	221	208
B			241	243	243	244	242	242	229	230	242	243	242	243	244	245	240	240	243	244	243	241		
C			241	242	241	242	242	242	243	241	243	242	243	244	242	241	242	242	244	244	242	241		
D	242	241	244	244	241	241	237	238	245	245	241	241	243	243	244	244	245	244	244	244	244	242	241	241
E	216	215	242	244	243	243	244	244	245	246	245	244	246	244	244	245	243	243	244	245	243	242	242	241
F	239	236	242	243	237	236	238	240	245	245	244	244	244	244	243	243	242	241	243	244	242	242	243	242
G	243	240	240	243	212	211	240	243	244	244	244	244	241	239	232	231	241	242	242	242	243	242	242	241
H	233	236	242	244	238	237	243	245	244	242	241	241												
I	176	173																					245	244

(B)

22Rv1

	1	2	3	4	5	6	7	8	9	10	11	12	13	14	15	16	17	18	19	20	21	22	23	24
A	178	178	239	245	244	245	246	247	245	245	244	245	244	245	244	247	247	246	245	245	245	242	211	205
B			243	244	245	244	241	242	229	230	242	243	245	245	245	245	245	244	246	246	242	242		
C			243	243	246	244	233	235	242	242	237	240	246	245	242	243	241	241	246	247	242	242		
D	246	245	245	245	243	242	243	243	244	244	246	246	246	245	245	245	245	245	246	246	245	245	246	246
E	245	245	245	245	241	241	245	246	245	245	246	246	247	247	247	246	245	245	246	247	245	245	245	244
F	246	246	244	244	237	236	238	240	245	246	244	244	246	247	247	245	242	241	243	244	241	241	245	244
G	245	244	243	243	227	228	241	243	245	245	245	245	242	241	243	243	241	240	242	243	241	242	245	244
H	238	238	244	245	245	245	246	245	244	243	245	245												
I	185	185																					247	245

(C)

Medium control

	1	2	3	4	5	6	7	8	9	10	11	12	13	14	15	16	17	18	19	20	21	22	23	24
A	185	187	240	245	246	246	247	247	246	246	245	245	246	245	246	246	246	246	245	244	245	244	221	192
B			245	245	245	246	247	248	246	246	244	244	246	245	245	246	245	245	245	246	245	244		
C			245	245	246	246	245	246	246	246	246	245	246	245	243	244	246	245	245	246	244	244		
D	246	246	246	246	245	245	245	246	246	245	245	245	246	246	245	245	246	246	245	246	245	245	244	243
E	247	247	247	248	246	245	246	247	246	246	246	246	249	250	247	246	246	246	246	246	245	245	245	243
F	247	247	248	250	247	244	243	244	247	246	246	245	249	248	246	245	245	245	246	246	244	244	245	243
G	246	246	246	247	246	244	245	245	247	246	247	246	245	245	244	244	245	244	245	245	244	245	245	243
H	232	234	244	245	245	245	245	247	246	246	247	246												
I	173	178																					245	242

(D)

FIGURE J.5: Intensity matrix resulted from the Protein Analyzer Software. Here the intensity values are converted into color-codes to improve the visualization of the values mapped from 0 to 255.

Appendix K

QCM-D experiments

Table K.1: Complete set of results for QCM-D experiments.

For PLLs				
Test	PLL-OEG Biotin 4%	OEG-Biotin 1%	PLL-OEG	PLL
1		21	22	
2		22	22	
3		23	23	
4		20		
5		15		
6		18		
AVG		19.8	22.3	
STD		2.9	0.6	
For SAv				
Test	PLL-OEG Biotin 4%	OEG-Biotin 1%	PLL-OEG	PLL
1	30	18	3	3
2	30	19	1	3
3	28	23	1	
4	28	21		
5	32	21		
6	32	22		
AVG	30.0	20.7	1.7	3.0
STD	1.8	1.9	1.2	0.0
For anti-EpCAM				
Test	PLL-OEG Biotin 4%	OEG-Biotin 1%	PLL-OEG	PLL
1	10	24	5	1
2	13	20	5	2
3	18	14	3	
4	20	20		
5	11	24		
6	11	25		
AVG	13.8	21.2	4.3	1.5
STD	4.2	4.1	1.2	0.7
For EpCAM				
Test	PLL-OEG Biotin 4%	OEG-Biotin 1%	PLL-OEG	PLL
1		7	2	
2		6	5	
3		8	2	
4		8		
5		7		
6		8		
AVG		7.3	3.0	
STD		0.8	1.7	